

***Synthesis of organic pillar molecules and
their application after intercalation into
synthetic layered silicates***

DISSERTATION

zur Erlangung des akademischen Grades eines
Doktors der Naturwissenschaften (Dr. rer. nat.)
an der Fakultät für Biologie, Chemie und Geowissenschaften
der Universität Bayreuth
am Lehrstuhl für Organische Chemie I
bei Herrn Prof. Dr. Rainer Schobert

vorgelegt von

Mathias Schwedes

aus Dachau

Bayreuth, 2018

Die vorliegende Arbeit wurde in der Zeit von 10/2013 bis 08/2018 in Bayreuth am Lehrstuhl Organische Chemie I unter Betreuung von Herrn Professor Dr. Rainer Schobert angefertigt.

Vollständiger Abdruck der von der Fakultät für Biologie, Chemie und Geowissenschaften der Universität Bayreuth genehmigten Dissertation zur Erlangung des akademischen Grades eines Doktors der Naturwissenschaften (Dr. rer. nat.).

Dissertation eingereicht am: 03.09.2018

Zulassung durch die Promotionskommission: 12.09.2018

Wissenschaftliches Kolloquium: 29.03.2019

Amtierender Dekan: Prof. Dr. Stefan Peiffer

Prüfungsausschuss:

Prof. Dr. Rainer Schobert (Gutachter)

Prof. Dr. Josef Breu (Gutachter)

Prof. Dr. Matthias Breuning (Vorsitz)

JProf. Dr. Mirijam Zobel

„It's not who I am underneath, but what I do that defines me!”

Batman

Abbreviations

MOPS	microporous organic pillared silicate
PILC	pillared interlayered clays
MOF	metal organic framework
PCP	porous coordination polymer
bdc	benzene dicarboxylate
CV	coefficient of variation
phen	phenanthroline
diNOsaur	1,8-dinitro-3,6,10,13,16,19-hexaazabicyclo[6.6.6]-eicosane
diAMsar	1,8-diamino-3,6,10,13,16,19-hexaazabicyclo[6.6.6]-eicosane
en	ethylenediamine
bpy	2,2'-bipyridine

Table of contents

A Introduction	1
1 Microporous materials	1
2 Definition of Pillaring.....	3
3 Characteristics of Microporous Organic Pillared Silicates (MOPS)	4
4 A timeline of PILCs/MOPs.....	8
5 Aim of the thesis.....	12
6 References.....	13
A Main Part.....	16
1 Synthesis of pillaring agents.....	16
1.1 Attempted synthesis of the cage compound 7 based on ninhydrin and 1,4-piperidinone	16
1.2 Synthesis of the cytosine based pillar	22
1.3 Synthesis of the cobaltocenium based pillar.....	28
1.4 Synthesis of the paracyclophan based pillar	36
2 Application of the microporous organic pillared silicates.....	43
2.1 Intercalation of pillar 9 into stevensite $[\text{Na}_{0.47(3)}]^{inter}[\text{Mg}_{2.59(5)}\text{Li}_{0.17(3)}]^{oct}[\text{Si}_4]^{tet}\text{O}_{10}\text{F}_2$ and its application in the adsorption of but-3-yn-2-ol and 2-methyl-but-3-yn-2-ol.....	43
2.2 Intercalation of pillar 10 into hectorite $[\text{K}_{0.48(2)}]^{inter}[\text{Mg}_{2.54(8)}\text{Li}_{0.43}]^{oct}[\text{Si}_4]^{tet}\text{O}_{10}\text{F}_2$ and its application in the adsorption of but-3-yn-2-ol and 2-methyl-but-3-yn-2-ol.....	46
3 References.....	49
C Summary	51
1 Conclusion	51
2 Zusammenfassung.....	54
D Experimental.....	58
1 General Information.....	58
2 Synthesis of the organic compounds	60
2.1 Synthesis of (-)-Methyl-(1R,9R)-6-oxo-7,11-diazatricyclo[7.3.1.0]tridecane [22] ⁶	60
2.2 Synthesis of (+)-(1R,2S,9S)-11-Methyl-7,11-diazatricyclo[7..3.1.0]tridecane [24] ⁶	60
2.3 Synthesis of (+)-(1R,2S,9S)-11-Methyl-7,11-diazatricyclo[7.3.1.0]tridecane-(1R,5S,11aS)-3,3,7-trimethyldodecahydro-1,5-methanopyrido[1,2-a][1,5]diazocine-3,7-dium [6]	62
2.4 Synthesis of 4,13-Hydroxymethylen-[2.2]paracyclophan [52] ⁶¹	62
2.5 Synthesis of pseudo-meta-bis(5,12-(N-Methylaminomethylen))- [2.2]paracyclophan [54] ⁶⁶ .	63
2.6 Synthesis of pseudo- <i>meta</i> -bis(5,12-brommethylen)-[2.2]paracyclophan [53] ^{61,67}	64
2.7 Synthesis of pseudo-meta-bis(5,12-(N,N,N-trimethylmethylenaminium))- [2.2]paracyclophan dibromide [10] ⁶¹	64
2.8 Synthesis of pseudo-meta-bis(5,12-(N,N,N-Triethylmethylenaminium)) [2.2]paracyclophan dibromide [55a] ⁶¹	65

2.9 Synthesis of pseudo-meta-bis(5,12-(N,N,N-dimethylphenylmethylenaminium))- [2.2]paracyclophan dibromide [55b] ⁶¹	66
2.10 Synthesis of (L)-alanine methylester hydrochloride [30] ⁴⁶	67
2.11 Synthesis of (L)-alanine methylamide [31] ⁴⁶	67
2.12 Synthesis of (S)-N ¹ -methylpropane-1,2-diamine [32] ⁴⁶	68
2.13 Synthesis of (4S)-1,4-dimethyl-2-phenylimidazolidine [57]	68
2.14 Synthesis of (n ⁵ -Cyclopentadienyl)[n ⁴ -(exo)-1,3-cyclopentadiene]cobalt(I) and (Trimethylsilyl) ethynyl)-cobaltocenium Hexafluorophosphate [35] ⁵⁰	69
2.15 Synthesis of Cobaltocenium carboxylic acid hexafluorophosphate [36] ⁵⁰	70
2.16 Synthesis of Ethynylcobaltocenium Hexafluorophosphate [39] ⁵⁰	71
2.17 Synthesis of Cobaltocenium carboxylic acid methyl ester hexafluorophosphate [37] ⁶⁸	72
2.18 Synthesis of 1,5-(Ferrocen-1,10-diyl)pentan-1,5-dione [58] ^{43e}	72
2.19 Synthesis of (3E,3E)-3,5-dibenzylidenpiperidin-4-on [16] ³⁷	73
2.20 Synthesis of 2-Hydroxy-11-methyl-13-phenyl-16-[(E)-phenyl-methylidene]-1,11- diazapentacyclo[12.3.1.0 ^{2,10} .0 ^{3,8} .0 ^{10,14}]octadeca-3(8),4,6-triene-9,15-dione [19] ³⁷	74
3 Adsorption experiments	75
3.1 Synthesis of the MOPS	75
3.2 Adsorption of a mixture of 2-methyl-but-3-yn-2-ol and rac-but-3-yn-2-ol	76
3.3 Adsorption of rac-but-3-yn-2-ol	77
4 References	79
E Acknowledgment	80

A Introduction

1 Microporous materials

Microporous inorganic materials have drawn a lot of attention during the past decades. They offer size- and shape-selectivity in adsorptivity and are also able to control reaction pathways by reactant or transition state selectivity. Especially aluminosilicate zeolites and aluminophosphates are well-known for their catalysis of fuel cracking and synthesis of a variety of commodity chemicals. Despite of their narrow pore size distribution and large surface area, the advantages of zeolites clearly lies in their stability according to temperature, hydrolysis and low pH. Therefore, plenty of framework-topologies could be realized by adjusting synthetic parameters and diversifying molecular templates.¹

The Metal Organic Frameworks (MOFs), also known as porous coordination polymers (PCPs), attracted a lot of attention since the early 90's when they were established as a new class of microporous hybrid material with both organic and inorganic components. Thereby, the inorganic metal fits the role of a tie bar for the organic linker molecules. This opens up an almost indefinitely amount of variations by combining transition-metal ions with nearly any organic linker molecule. Using this pool of components, the size, shape and chemical nature of the micropores from the MOF can be regulated. As a coordination polymer the number of possible linkers depends on the oxidation state of the transition metal. It can range from 2 to 7, making many different geometries possible, for example linear, T- or Y-shaped, tetrahedral, square-planar, square-pyramidal, trigonal-pyramidal, octahedral, trigonal-prismatic, pentagonal-bipyramidal and their corresponding distorted forms. Within one metal, for instance Ag^I and Cu^I with d¹⁰- configuration, different coordination numbers and geometries can be achieved by varying reaction conditions, solvents, counteranions and ligands. The lanthanide ion with its large coordination numbers from 7 to 10 and the polyhedral coordination geometry suites very well for the realization of unusual coordination topologies. Additionally, if a coordinated solvent is removed a coordinatively unsaturated site is generated which can be used in chemical adsorption, heterogeneous catalysis and sensors.² Utilizing a metal-complex instead of a naked metal ion, coordination sites can be blocked by a chelating or macrocyclic ligand leaving specific sites open for organic linkers. For instance, the polymer $\{[\text{Ni}(\text{C}_{12}\text{H}_{30}\text{N}_6\text{O}_2)(1,4\text{-bdc})]\cdot 4\text{H}_2\text{O}\}_n$ ($\text{C}_{12}\text{H}_{30}\text{N}_6\text{O}_2$ = macrocyclic ligand; bdc = benzene

dicarboxylate) forms 1D chains, where the Ni-macrocylic units are linked by the 1,4-bdc ligand. A 3D network is built up by the hydrogen-bonds between the 1D chains.³

Although MOFs are inferior to zeolites regarding their thermal and chemical stability, their modular character allows to shift the attention from high temperature reactions towards the improvement of separation and purification of gases and stereodiscrimination.⁴

Kitagawa et al. suggested in 1998 to classify the MOFs into three generations. Materials of the first generation do not have permanent porosity due to the porosity collapsing after removal of the solvent. Materials porosity of the second generation are the most similar compared to zeolites showing an interesting adsorption behavior. The third generation materials can be regarded as the most flexible ones possessing a reversibly dynamic, porous framework. Those MOFs, in difference to the inflexible framework of zeolites, owning such a gate opening effect have pulled the attention of many material researchers.⁵

Solids undergo dense packings and a thermodynamic equilibrium is not represented by microporous materials. Using strong covalent (sub-) structures the metastability of those non-dense solids can be assured. Thereby, the synthesis can be done in two ways: 1. Filling the micropores with guest templates which are then removed subsequently, 2. Applying topotactic reactions to generate an inflexible (sub-) structure.

Another independent way to produce microporous materials is to pillar layered materials, especially 2 : 1 layered silicates. This unique route has been disregarded by the zeolite and MOF communities since the early 50's. Compared to MOFs and zeolites, there exists no rigid covalent linkage between the two-dimensional layer structure and the pillars for Microporous Organic Pillared Silicates (MOPS). They are held in place only via non-directional electrostatic interactions. Subsequently, post-synthesis changes are possible by contrast to zeolites and MOFs where it is not. Consequently, the porosity of the MOPS is only dependent on the homogeneity and magnitude of the negative layer charge of the silicate and on the nature of the pillar (size, shape, charge). Those two properties can now be fully controlled as recently discovered by *Breu* et al. Also, via an expeditious melt synthesis layered silicates with a homogeneous charge density are now available on large scale.⁶ Using organic cations for the intercalation process then results in MOPSs, which are characterized by narrow pore size distribution and a high degree of long-range order of the pillar arrays. Now, for the first time functional MOPS with continuously adjustable microporosity are now available in large

quantities.⁷ The possibility to tune the interlayer cavities by changing the shape of the pillar is a unique feature only accessible to MOPs, not to MOFs.

2 Definition of Pillaring

As stated by the IUPAC in 1999 pillaring is defined as “a process by which a layered compound is transformed in a thermally stable micro- and/or mesoporous material with retention of the layer structure. ... A pillared compound has the following characteristics: (i) the layers are propped apart vertically and do not collapse upon removal of the solvent; (ii) the minimum increase in basal spacing is the diameter of the N₂ molecule, commonly used to measure surface areas and pore volumes: 0.315-0.353 nm; (iii) the pillaring agent has molecular dimensions and is laterally spaced in the interlamellar space on a molecular length scale; (iv) the interlamellar space is porous and at least accessible to molecules as large as N₂; there is no upper limit to the size of the pores. ... There is no restriction on the nature of the intercalating agent or on the mechanism of intercalation.”⁸

The definition classifies the MOPs as porous subgroup of intercalation compounds and that the microporosity needs to be in the interlayer space. The regular stacking of host layers and mono-sized pillars in the interlayer space have to result in a layer spacing. Although mentioning that “the XRD pattern must show clearly the d_{001} line” the report does not insist on an ideal one-dimensional crystallinity (“but a rational series of d_{001} lines is not required”). The fact that the $00l$ -series is of non-Bragg-nature gives space for a lot of speculation and different interpretations, but this problem has to be discussed elsewhere. Nevertheless, a host material pillared by guest molecules must be regarded a single phase. For instance, to prove the single phase of an amorphous sophisticated nanocomposite, solid state NMR techniques using double quantum excitation could be the method of choice. Another requirement from the IUPAC definition that is not clearly stated is the question of thermal stability. Compared to earlier definitions where a minimum thermal stability of 200 °C is required, this report only asked tangentially for thermal stability: “... After removal of the solvent, e.g. heating at 120 °C in air or N₂ (Ar, He) for the removal of water.”⁹

3 Characteristics of Microporous Organic Pillared Silicates (MOPS)

Micropores in 2:1-layered silicates (Figure 1) are generated post-synthesis via a topotactic reaction by incorporating the pillaring agent into between two layers using a cation exchange reaction. The charge neutrality condition defines the amount of pillar molecules that can be incorporated. From this follows that the number of pillars is defined by the valency of it and also by the charge density of the host silicate. The driving force of the incorporation reaction is the electrostatic attraction between the positively charged pillar molecules and the negatively charged silicate layers, the basal spacing between the layers is therefore minimized by this fact.¹⁰ So, if the guest molecules are not perfectly spherical and show more of an elliptical shape they will always arrange themselves with their longer principal axis oriented in the plane of the interlamellar space. Consequently, the design of the micropores is dependent on three facts: the size and shape of the intercalated pillar, the charge of the pillar, charge homogeneity and layer charge of the silicate host.

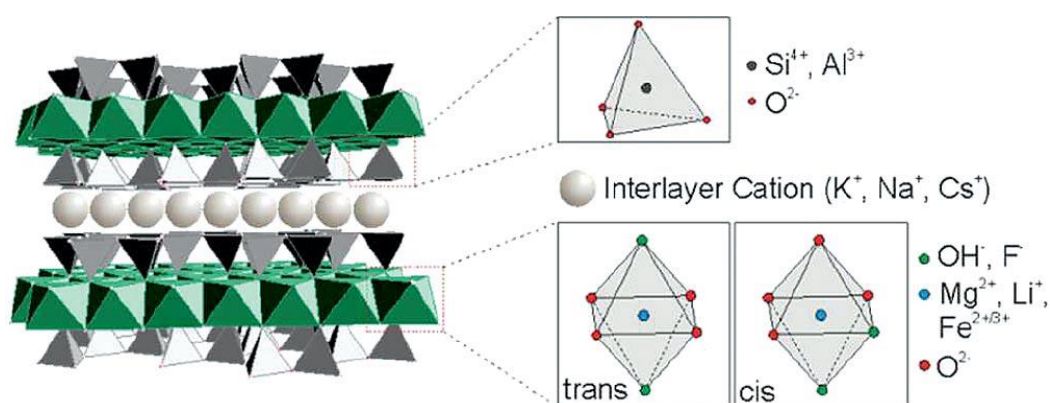


Figure 1: Structure of 2:1 layered silicates.

The Micropores are of slot nature. The height is defined by the shorter principal axis of the pillar and has to be larger than 3.2 Å to fulfill the definition of the IUPAC to be accessible for N₂. So lower limit of the basal spacing, which is the sum of pore height and the thickness of the layer (9.6 Å), to make this access possible is at least 12.8 Å. But it has to be larger than this value, because it is known that the kinetic diameter of N₂ is larger than 3.2 Å.^{6e} The distance between two pillars is much harder to estimate. But it can be assumed that the electrostatic forces between the pillar molecules makes them to arrange in a hexagonal lattice. In a 2:1 silicate the distance between two pillars is going to be greater than 5.3 Å (the *a*-axis of the host silicate lattice). Therefore, the pillar lattice must be regarded as a superlattice being

incommensurate to the host lattice. The Value of the a -axis from the pillar superlattice is dictated by the charge density of the layered silicate and the valency of the pillar. Then the diameter of the pillar must be subtracted from the a -axis the pillar lattice to receive the distance between two molecules. Since 3.2 Å is the minimum for the pore width to ensure access of N₂, there is always existing a limit of the charge density of the host silicate for any pillar that might be used, because a higher charge density will allow more molecules to be intercalated. The pore width might also fall below the limit of 3.2 Å when the equivalent area of the pillars (room of the interlayer space plane occupied by the pillar divided by its valency). This is either possible by increasing the lateral dimension (e.g. longer side-chains, bigger substituents) or decreasing the valency of the pillar.¹¹

All those assumptions are only valid if the charge density of the layered silicate is strictly homogeneous. The charge density of 2:1 silicates can be influenced by isomorphous substitutions in the octahedral and/or tetrahedral layers. This isomorphous substitution has to be strictly statistical, so a homogeneous charge density can be obtained. Monte Carlo simulations of the order-disorder behavior of octahedral sheets of phyllosilicate layers propose a segregation of the octahedral cations for the most compositions, what means that the layers show charge inhomogeneities at low temperatures. The cation itself plays naturally an important role on the degree of segregation, but high temperatures over 1000 K have also shown that they are necessary to gain a disordered solid solution with a homogeneous charge density. If lower temperatures are applied different cations start to cluster in domains of lower and higher charge density. For example, the genesis of the clay mineral montmorillonite takes place at temperatures below 400 K. The charge density, determined by the alkylammonium method broad, thereby shows sometimes bi-modal, charge density distributions.¹²

With the coulomb interaction between the host and the pillar being responsible for the structure and the pillar packing densely between host domains or layers of higher charge density, the micropore volume is going to be very uneven. So again, a homogeneous charge density is required for the pillaring concept to succeed. The concept also needs an ongoing interlayer micropore volume. The pore size is not fixed inevitable as already pointed out by *Barrer*.¹³ Like PCPs of the third generation, the basal spacing of MOPs can be temporarily increased by inclusion of certain sorbate molecules into micropores. This effect, called breathing of the micropores, is accompanied by a reorientation of the pillar molecules. Using this effect, a sort of a 'swelling mechanism', non-porous compounds can also intercalate guest

molecules. This stands for a thermodynamically favored solvation of interlayer cations and lacks selectivity. Physisorption is compared to X-ray diffraction the method of choice because its capable to differ between sorption into permanent but breathing micropores and swelling. To gain further information on MOPs or the intercalated compounds in general, is innately complicated because the anisotropic bonding situation makes them vulnerable to two distinct type of disorder. The statistical interstratification of different basal spacings along the stacking direction and stacking faults, which means that the relative orientation and/or position of close layers is not exactly defined.

If adjacent layers throughout the silicate have different charge densities, the interlayer cations will fluctuate in their interlayer domains and result in a different intracrystalline reactivity. Parallel stacked layers are commonly considered as tactoid, not crystal. An easy hydration experiment, "swelling with water", can examine the intracrystalline reactivity of layered compounds with their interlayer cations like Na^+ . With a homogeneous charge density all layers would have exact hydration states of zero, one and two layer hydrate as a function of increasing humidity with a gradual change of hydration at well-defined levels. The rational $00l$ series are observed for all hydration states. This means that along the stacking direction the symmetry is strictly obeyed resulting in a one-dimensional Bragg-type diffraction. Layered silicates produced at temperatures >1000 °C show little to none interstratifications of differently hydrated interlayers within the same tactoid. This uncommon intracrystalline reactivity proves again an excellent homogeneous charge density.¹⁴ In contrast to this, for silicates produced at lower temperatures at any intermediate relative humidity, smectite (group name for 2:1 phyllosilicates, di- or trioctahedral, with hydrated exchangeable cations and a layer charge $x = 0.2-0.6$ ¹⁵) for instance, random interstratifications are observed.¹⁶ Weak absolute intensities of the basal reflections and large full widths at half maximum with a dependency diverging from the usual 2θ -dependency are definite signs of interstratification. But the clearest sign is that the $00l$ -series becomes irrational, indicating that the calculated basal spacing from different $00l$ reflections alters according to *Mering's* principles.¹⁷ However, when a material with a heterogenous charge density is used and the pillar density is varied, a rational $00l$ -series is realized as long as the pillars have an equal orientation within the interlayer region. For instance, a natural montmorillonite in its hydrated state has a strongly irrational $00l$ -series. After pillaring with $\text{Me}_2\text{DABCO}^{2+}$ (N,N-dimethyl-1,4-diazabicyclo [2.2.2]octane-dication) the $00l$ -series is more rational. The much lower coefficient of variation

(CV)¹⁸ of the *00l*-series of the intercalated montmorillonite in comparison to the hydrated one indicates that translational symmetry along the stacking direction will be realized as long as the size of the pillar is explicit and the charge neutrality condition in a monolayer is fulfilled. So irrational *00l*-series should not be accepted for MOPs when the *00l*-series of Me₂DABCO²⁺ pillared tainiolite shows a perfect translational symmetry, suggesting by CV of 0.06.¹⁹

The other type of disorder beside of interstratifications are stacking faults. Looking at the surface of 2:1 layered silicates it shows corrugation and a high hexagonal pseudo-symmetry to interlayer species. A pseudo-hexagonal pattern is formed by the hexagonal cavities. With this pseudo-symmetry, rotational faults and/or polytypes occur cavities in micas (2:1 phyllosilicates, di- or trioctahedral, with non-hydrated monovalent cations and a layer charge $x = 0.6-1.0$ ¹⁵) even when all cavities are occupied. This is because the first coordination sphere for the interlayer cations is equal and in a first approximation the rotational faults are energetically degenerate. Reduction of the charge density might still cause the lower number of interlayer cations to match to a not ordinary rotated symmetry. Additionally, if the size of interlayer cations is decreased the repulsion from the oxygen atoms, forming the tetrahedral layer, of adjacent layers can occur. This can cause a slippage of those layers. Slippages along the longer axis direction are energetically degenerate and stacking faults are created in a statistical manner. Slippages can also arise by hydration of the interlayer causing the loss of the phase relationship between adjacent layers.²⁰

These stacking fault must be considered when the layer charge is decreased. But with larger interlayer cations like Cs⁺, three-dimensionally ordered 2:1 layered silicates with a layer charge of $x = 0.5$ are approachable using melt synthesis. They still show adequate intracrystalline activity making the silicates appropriate for the whole pillaring process. Silicates occupying a three-dimensional order can maintain their stacking order although the interlayer space is expanded drastically. On the other way around, existing stacking faults cannot be healed through pillaring the material. This would require an organized movement of all layers of the tactoid, which is extremely improbable.²⁰

Another point to consider are the formed microstructures caused by the anisotropic particle shape in combination with the small particle size. Those microstructures, containing wedge-like pores, are build when two tactoids meet at a pointed angle. These external pores disguise the interlayer micropores, produced by pillaring, and are able to falsify stereodiscrimination and enantioselective autocatalysis experiments. The technical UIPAC report recommends

measurements of N₂ adsorption-desorption isotherms but also mentioned that “Care must be taken to ensure that the observed porosity is the result of pillaring and not simply a consequence of interparticle texture.” Therefore, physisorption measurements are mandatory to ensure microporosity generated by pillaring is stated in the interlayer.¹⁹

4 A timeline of PILCs/MOPs

In the 1950's the upcoming concept of pillaring was first dealt with by *Barrer*. His work described the intercalation of simple organic cations like tetramethylammonium [N(CH₃)₄]⁺ and tetraethylammonium [N(C₂H₅)₄]⁺ in natural montmorillonites. The intercalation caused a permanent increase of the interlamellar space allowing paraffins and aromatic hydrocarbons but with the new organophilic material also polar organic species like methanol, ethanol, water, ammonia and pyridine. *Barrer* and *MacLeod* also observed an expected decrease of micropore volume when changing to a larger pillar with constant charge density.²¹ However, some of the sorption was probably caused by mesoporosity, but this sorption of external surface was corrected later by *Barrer* through inclusion isotherms of type I.²² In his follow up work, *Barrer* published papers using new pillars like different alkylammonium and alkyldiammonium cations and Cobalt(III)-ethylenediamine.²³ There he investigated adsorption capacities and micropore volumes and deduced from his work that the results are dependent on the equivalent area of the pillars and the charge density of the layered silicate.²⁴ He also calculated the interlayer pore volume from the basal spacing, pillar shapes and densities.²⁵ Unfortunately, this great new concept was not followed up for around two decades. Synthetic Zeolites gained all the attention at that time on the topic of microporous materials. Their characteristic of thermal stability seemed to be just too important at that time.

When people were asking for increased pore diameters, the concept was finally picked up again by *Brindley* et al. However, he only used no organic pillars like polyhydroxyaluminum in order to be able to keep up with zeolites in terms of thermal stability.²⁶ Interests in the topic of pillared silicates showing thermal stability however have not decreased since then, and there have been a lot of publications reviews on this topic, even recently.²⁷

In 1976 *Mortland* and *Berkheiser* were able to intercalate H₂DABCO²⁺ into smectite and vermiculite. Thus, they achieved larger pore volumes giving access to interlayer space for gas

with his pillars. If we consider the equivalent area of the utilized metal complex cations it is very improbable that the silicates were truly porous. *Breu et al.* again intercalated $[\text{Ru}(\text{bpy})_3]^{2+}$ into a synthetic hectorite but did not find remarkable microporosity. Decreasing the equivalent area of the pillar by changing the metal complex just from ruthenium(II) to ruthenium(III) lead to interlayer microporosity. This indicates that the chiral discrimination is probably caused by the external surface area instead of the interlayer porosity.¹⁹

In 1994 *Chen et al.* intercalated cobalt(III) and chrome(III) metal complexes into vermiculite fluorohectorite and montmorillonite. He was also able to customize the pore size in the interlayer space to examine adsorption and diffusion of the pillared material.³⁴

Thomas et al. used trinuclear cobalt complexes like $[\text{Co}(\text{OC}_2\text{H}_4\text{NH}_2)_6]^{3+}$ as pillar and intercalated them into montmorillonite in order to make those PILCs/MOPSS as catalysts available for applications under temperatures of 200 °C. Thermogravimetric analyses of PILCs/MOPSS showed ligand decomposition at higher temperatures and thus a structure collapse and loss of the pillar structure. Here again, no N_2 -physisorption was measured to prove the microporosity of the material, so it can only be regarded as intercalation compound.³⁵

In 2001, *Meier et al.* choose smectite out of the variety of layered silicates and modified it with several organic cations. As pillaring agent he used ammonium cations with long flexible side-chains, but also ammonium cation with a rigid structure, for example Bis(α ; α' -oxylylene)ammonium dibromide or Bis(2,2'-dimethylen-biphenylylen). The structural more complex cation, for example the xylylene compound was synthesized by providing a mixture of α , α' -dibromo-*o*-xylylene and 25% solution of ammonia. While stirring the reaction was refluxed overnight. After workup of the solution, recrystallisation gave the pure salt. *Meier et al.* then examined the adsorption of 2-Chlorophenol showing better results for the cations owning a rigid structure than the flexible ones.³⁶ Unfortunately, the authors missed out proving the microporosity of their compounds by measuring N_2 -physisorption and so, despite calling them pillared, they can only be regarded as intercalation compounds. It is known that organoclays like to swell with 2-Chlorophenol.

In 2012, *Breu et al.* intercalated hectorite with $\text{Me}_2\text{DABCO}^{2+}$ and $[\text{Ru}(\text{bpy})_3]^{3+}$ (Figure3). $\text{Me}_2\text{DABCO}^{2+}$ has been synthesized by refluxing a mixture of 1,1-diazabicyclo[2.2.2]octane and MeI for 4 h with subsequently recrystallisation. By controlling the layer charge post synthesis through layer charge reduction, they were able to tailor the size of micropores. This

fine tuning allows to generate the perfect layer charge for every pillaring agent to maximize the pore volume. They did not fail to report physisorption measurements, so their materials can be regarded as truly microporous.^{7e}

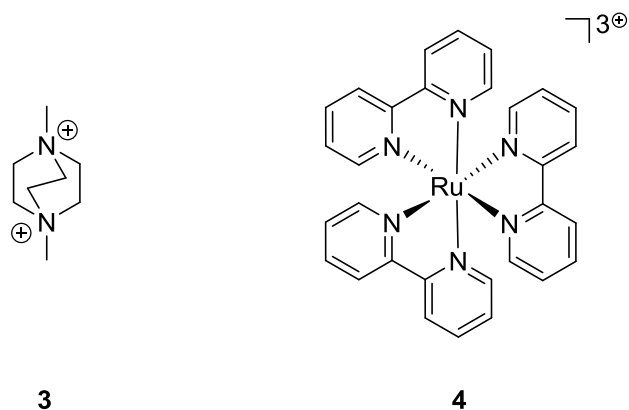


Figure 3: Molecular Structure of $\text{Me}_2\text{DABCO}^{2+}$ **3** and $[\text{Ru}(\text{bpy})_3]^{3+}$ **4**.

Most of research spend on pillared interlayer clay systems first of all concerns pure inorganic compounds due to their thermal stability in order to compete with other porous materials. Less effort has been spent on systems containing organometallic or pure organic pillars. The great advantage of metal complexes compared to organic molecules is of course the property of being able to reach high oxidation states which results in high charges of the metal complex. This on the other hand increases the pore size in the interlayer space, granting access for larger molecules without decreasing the charge density of the host layers. Also, a lot of research must be invested into the application of pure organic molecules as pillaring agent. This goes along with some difficulties. The molecule needs to contain either nitrogen or phosphor so at least one positive charge can be introduced by quaternizing one of them. A molecule with more hetero atoms is even better cause everyone is potential charge carrier. In addition, the organic pillar should be spherical, otherwise the pillar does not create any relevant interlayer height. The planar the molecule is the more space from the micropore is occupied by the pillar. A lot of issues should be considered when choosing the right pillar.

5 Aim of the thesis

The goal of this thesis is to synthesize pillaring agents. Thereby different approaches should be pursued. Starting from natural products, pillars could be obtained through derivatization with adjacent quaternization of at least two hetero atoms. Also, non-natural spherical molecules gained through organic synthesis is another possibility to achieve this goal. Furthermore, the synthesis of organometallic complexes is another choice. Each of the possibilities has pros and cons which are discussed later. Some promising options can be seen in Figure 4.

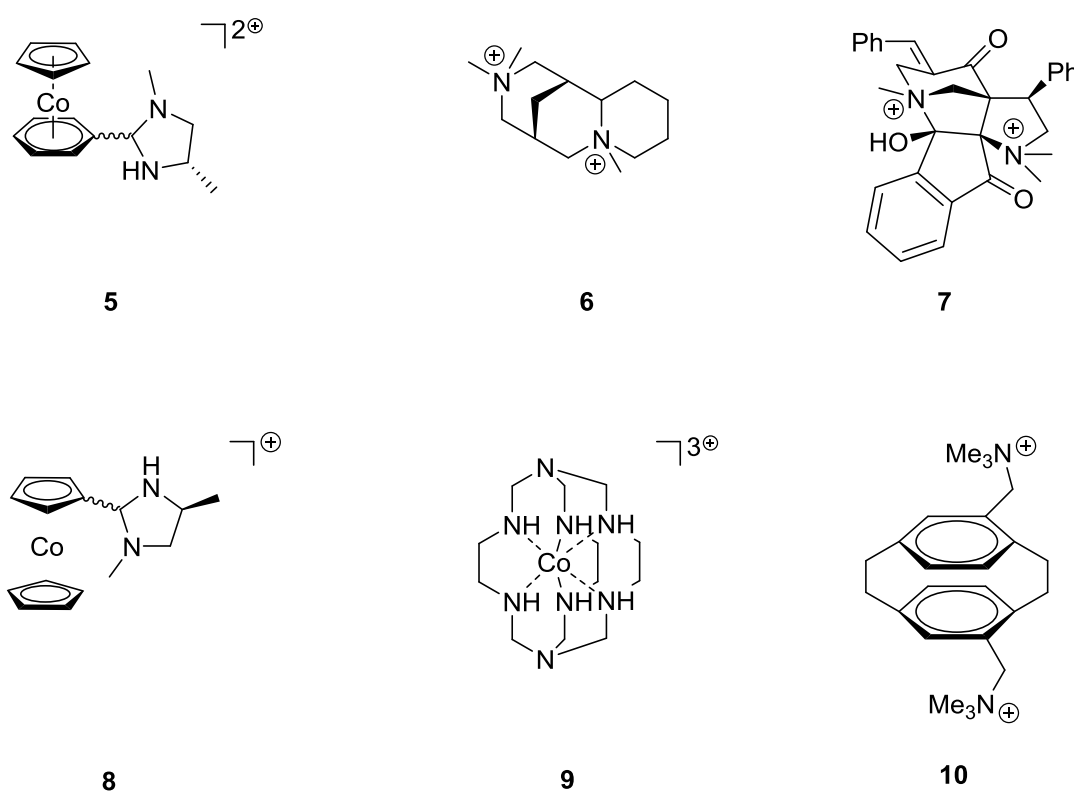


Figure 4: Molecular structure of possible pillar cations **5 + 8** (cobaltocenium derivatives), **6** (cytosine derivative), **7** (heterocyclic cage compound), **9** (cobalt(III)sepulchrate), **10** ([2.2]paracyclophane derivative).

Those pillars should be applied for intercalation into silicates with subsequent application in adsorption and catalysis experiments.

6 References

- ¹ a) J. Weitkamp, *Solid State Ionics* **2000**, *131*, 175–188; b) A. Corma, *J. Catal.* **2003**, *216*, 298–312; c) F. Schüth, *Annu. Rev. Mater. Res.* **2005**, *35*, 209–238; d) W. Schmidt, *ChemCatChem* **2009**, *1*, 53–67; e) S. I. Zones, *Microporous Mesoporous Mater.* **2011**, *144*, 1–8.
- ² S. Kitagawa, R. Kitaura, S. Noro, *Angew. Chem. Int. Ed.* **2004**, *43*, 2334–2375.
- ³ H. J. Choi, M. P. Suh, *Inorg. Chem.* **1999**, *38*, 6309 – 6312.
- ⁴ a) O. M. Yaghi, M. O’Keeffe, N. W. Ockwig, H. K. Chae, M. Eddaoudi, J. Kim, *Nature* **2003**, *423*, 705–714; b) J. R. Li, R. J. Kuppler, H. C. Zhou, *Chem. Soc. Rev.* **2009**, *38*, 1477–1504; c) A. U. Czaja, N. Trukhan, U. Muller, *Chem. Soc. Rev.* **2009**, *38*, 1284–1293; d) L. Ma, C. Abney, W. Lin, *Chem. Soc. Rev.* **2009**, *38*, 1248–1256; Y. Liu, W. M. Xuan, Y. Cui, *Adv. Mater.* **2010**, *22*, 4112–4135.
- ⁵ S. Kitagawa, M. Kondo, *Bull. Chem. Soc. Jpn.* **1998**, *71*, 1739–1753.
- ⁶ a) J. Breu, W. Seidl, A. J. Stoll, K. G. Lange, T. U. Probst, *Chem. Mater.* **2001**, *13*, 4213–4220; b) H. Kalo, M. W. Möller, M. Ziadeh, D. Dolejs, J. Breu, *Appl. Clay Sci.* **2010**, *48*, 39–45; c) H. Kalo, M. W. Möller, D. A. Kunz, J. Breu, *Nanoscale* **2012**, *4*, 5633–5639; d) M. Stöter, D. A. Kunz, M. Schmidt, D. Hirsemann, H. Kalo, B. Putz, J. Senker, J. Breu, *Langmuir* **2013**, *29*, 1280–1285.
- ⁷ a) M. Stöcker, W. Seidl, L. Seyfarth, J. Senker, J. Breu, *Chem. Commun.* **2008**, 629–631; b) A. Baumgartner, K. Sattler, J. Thun, J. Breu, *Angew. Chem. Int. Ed.* **2008**, *47*, 1640–1644; c) A. Baumgartner, F. E. Wagner, M. Herling, J. Breu, *Microporous Mesoporous Mater.* **2009**, *123*, 253–259; d) M. Stöcker, L. Seyfarth, D. Hirsemann, J. Senker, J. Breu, *Appl. Clay Sci.* **2010**, *48*, 146–153; e) M. Herling, H. Kalo, S. Seibt, R. Schobert, J. Breu, *Langmuir* **2012**, *28*, 14713–14719; f) C. D. Keenan, M. Herling, R. Siegel, N. Petzold, C. R. Bowers, E. A. Rössler, J. Breu, J. Senker, *Langmuir* **2013**, *29*, 643–652.
- ⁸ R. A. Schoonheydt, T. Pinnavaia, G. Lagaly, N. Gangas, *Pure Appl. Chem.* **1999**, *71*, 2367–2371.
- ⁹ a) F. Bergaya, *Concerted European Action – Pillared Layered Structures* **1995**, Newsletter 7, 11–12; b) D. H. Brouwer, R. J. Darton, R. E. Morris, M. H. Levitt, *J. Am. Chem. Soc.* **2005**, *127*, 10365–10370.
- ¹⁰ J. Breu, C. R. A. Catlow, *Inorg. Chem.* **1995**, *34*, 4504–4510.
- ¹¹ G. Lagaly, *Clay Miner.* **1981**, *16*, 1–21.
- ¹² a) E. J. Palin, M. T. Dove, A. Hernandez-Laguna, C. I. Sainz-Diaz, *Am. Mineral.* **2004**, *89*, 164–175; b) A. R. Mermut, G. Lagaly, *Clays Clay Miner.* **2001**, *49*, 393–397.
- ¹³ R. M. Barrer, *Pure Appl. Chem.* **1989**, *61*, 1903–1912.

- ¹⁴ a) E. Ferrage, B. Lanson, N. Malikova, A. Plancon, B. A. Sakharov, V. A. Drits, *Chem. Mater.* **2005**, *17*, 3499–3512; b) N. Malikova, A. Cadene, E. Dubois, V. Marry, S. Durand-Vidal, P. Turq, J. Breu, S. Longeville, J. M. Zanotti, *J. Phys. Chem. C* **2007**, *111*, 17603–17611; c) V. Marry, N. Malikova, A. Cadene, E. Dubois, S. Durand-Vidal, P. Turq, J. Breu, S. Longeville, J. M. Zanotti, *J. Phys.: Condens. Matter* **2008**, *20*, 104205–104215; d) M. W. Möller, U. A. Handge, D. A. Kunz, T. Lunkenbein, V. Altstadt, J. Breu, *ACS Nano* **2010**, *4*, 717–724; e) M. W. Möller, D. Hirsemann, F. Haarmann, J. Senker, J. Breu, *Chem. Mater.* **2010**, *22*, 186–196; f) V. Marry, E. Dubois, N. Malikova, S. Durand-Vidal, S. Longeville, J. Breu, *Environ. Sci. Technol.* **2011**, *45*, 2850–2855; g) V. Marry, E. Dubois, N. Malikova, J. Breu, W. Haussler, *J. Phys. Chem. C* **2013**, *117*, 15106–15115.
- ¹⁵ R. T. Martin, S. W. Bailey, D. D. Eberl, D. S. Fanning, S. Guggenheim, H. Kodama, D. R. Pevear, J. Srodon, F. J. Wicks, *Clays Clay Miner.* **1991**, *39*, 333–335.
- ¹⁶ a) E. Ferrage, B. Lanson, B. A. Sakharov, N. Geoffroy, E. Jacquot, V. A. Drits, *Am. Mineral.* **2007**, *92*, 1731–1743; b) E. Ferrage, B. A. Sakharov, L. J. Michot, A. Delville, A. Bauer, B. Lanson, S. Grangeon, G. Frapper, M. Jimenez-Ruiz, G. J. Cuello, *J. Phys. Chem. C* **2011**, *115*, 1867–1881.
- ¹⁷ D. M. Moore, R. C. Reynolds, in *X-ray Diffraction and the Identification and Analysis of Clay Minerals*, Oxford University Press, Oxford **1997**, pp. 263.
- ¹⁸ Coefficient of Variation (CV): standard abbreviation/mean value x 100.
- ¹⁹ M. M. Herling, J. Breu, *Z. Anorg. Allg. Chem.* **2014**, *640*, 547–560.
- ²⁰ a) D. M. Moore, R. C. Reynolds, in *X-ray Diffraction and the Identification and Analysis of Clay Minerals*, Oxford University Press, Oxford **1997**, pp. 330; b) J. Breu, W. Seidl, A. Stoll, *Z. Anorg. Allg. Chem.* **2003**, *629*, 503–515.
- ²¹ R. M. Barrer, D. M. Macleod, *Trans. Faraday Soc.* **1955**, *51*, 1290–1300.
- ²² R. M. Barrer, *Pure Appl. Chem.* **1989**, *61*, 1903–1912.
- ²³ R. M. Barrer, D. L. Jones, *J. Chem. Soc. A* **1971**, 2594–2603.
- ²⁴ R. M. Barrer, *Clays Clay Miner.* **1989**, *37*, 385–395.
- ²⁵ R. M. Barrer, A. D. Millington, *J. Colloid Interface Sci.* **1967**, *25*, 359–372.
- ²⁶ G. W. Brindley, R. E. Sempels, *Clay Miner.* **1977**, *12*, 229–237.
- ²⁷ a) J. T. Kloprogge, *J. Porous Mater.* **1998**, *5*, 5–41; b) A. Gil, L. M. Gandia, M. A. Vicente, *Catal. Rev. Sci. Eng.* **2000**, *42*, 145–212; c) Z. Ding, J. T. Kloprogge, R. L. Frost, G. Q. Lu, H. Y. Zhu, *J. Porous Mater.* **2001**, *8*, 273–293; d) A. Gil, S. A. Korili, M. A. Vicente, *Catal. Rev. Sci. Eng.* **2008**, *50*, 153–221; e) A. Gil, S. A. Korili, R. Trujillano, M. A. Vicente, *Pillared Clays and Related*

Catalysts, Springer, New York **2010**; f) M. A. Vicente, A. Gil, F. Bergaya, in *Developments in Clay Science Handbook of Clay Science Fundamentals* (Eds.: F. Bergaya, G. Lagaly), Elsevier, Amsterdam, **2013**, vol. 2, pp. 523–557.

²⁸ M. M. Mortland, V. Berkheiser, *Clays Clay Miner.* **1976**, *24*, 60–63.

²⁹ A. Yamagishi, *J. Coord. Chem.* **1987**, *16*, 131–211.

³⁰ M. Kaneyoshi, A. Yamagishi, M. Tanaguchi, A. Aramata, *Clays Clay Miner.* **1993**, *41*, 1–6.

³¹ A. Yamagishi, M. Taniguchi, Y. Imamura, H. Sato, *Appl. Clay Sci.* **1996**, *11*, 1–10.

³² N. Kakegawa, A. Yamagishi, *Chem. Mater.* **2005**, *17*, 2997–3003.

³³ T. Kawasaki, T. Omine, K. Suzuki, S. Hisako, A. Yamagishi, K. Soai, *Org. Biomol. Chem.* **2009**, *7*, 1073–1075.

³⁴ B. Y. Chen, H. Kim, S. D. Mahanti, T. J. Pinnavaia, Z. X. Cai, *J. Chem. Phys.* **1994**, *100*, 3872–3880.

³⁵ S. M. Thomas, J. A. Bertrand, M. L. Ocelli, J. M. Stencel, S. A. C. Gould, *Chem. Mater.* **1999**, *11*, 1153–1164.

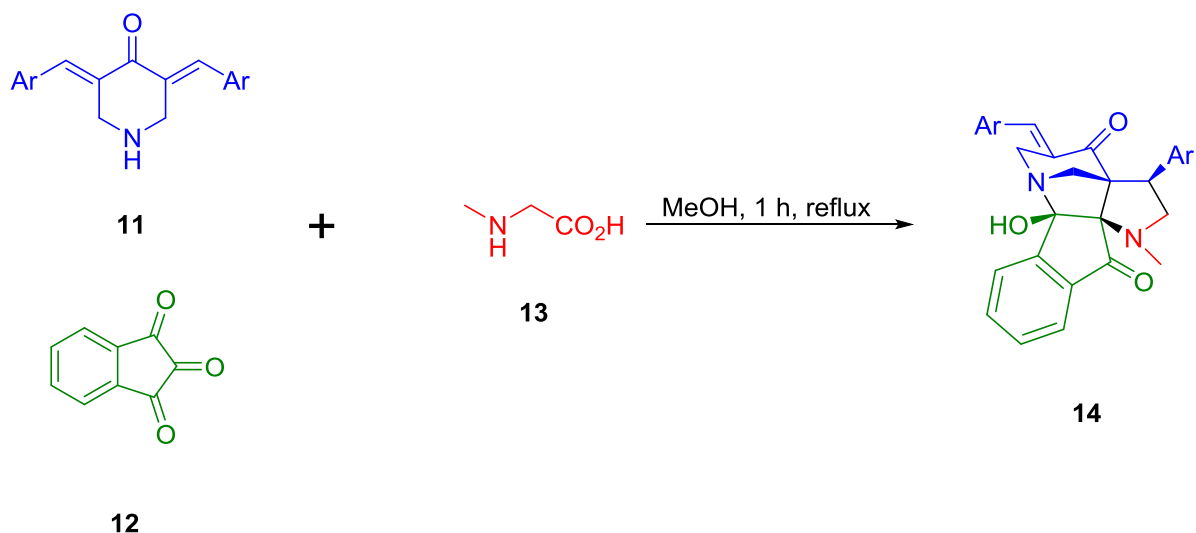
³⁶ L. P. Meier, R. Nüesch, F. T. Madsen, *J. Colloid Interface Sci.* **2001**, *238*, 24–32.

A Main Part

1 Synthesis of pillaring agents

1.1 Attempted synthesis of the cage compound 7 based on ninhydrin and 1,4-piperidinone

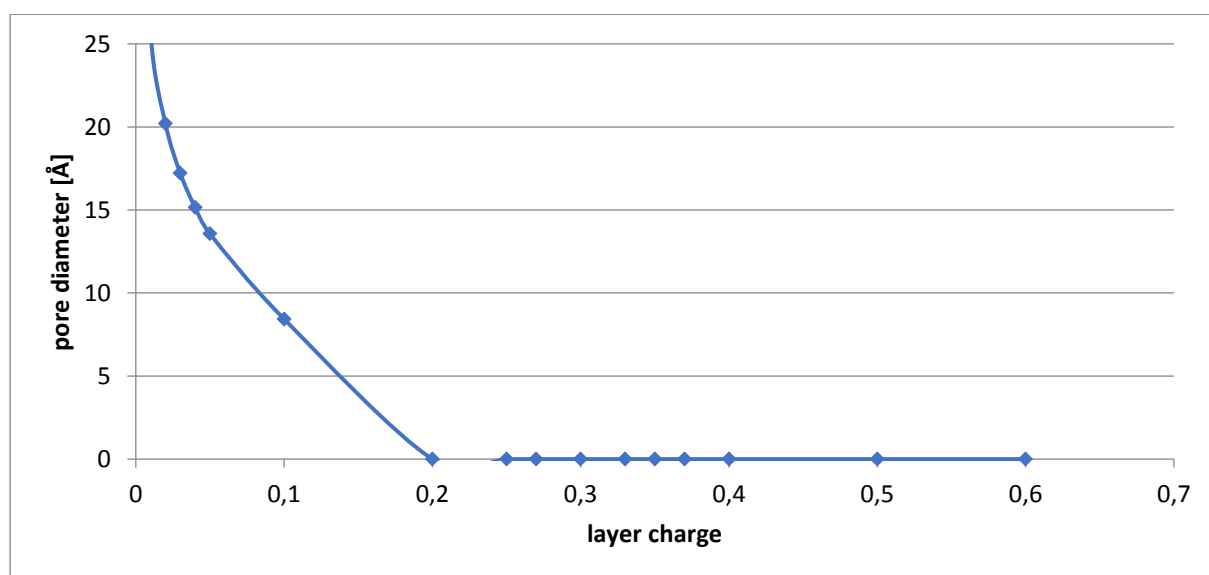
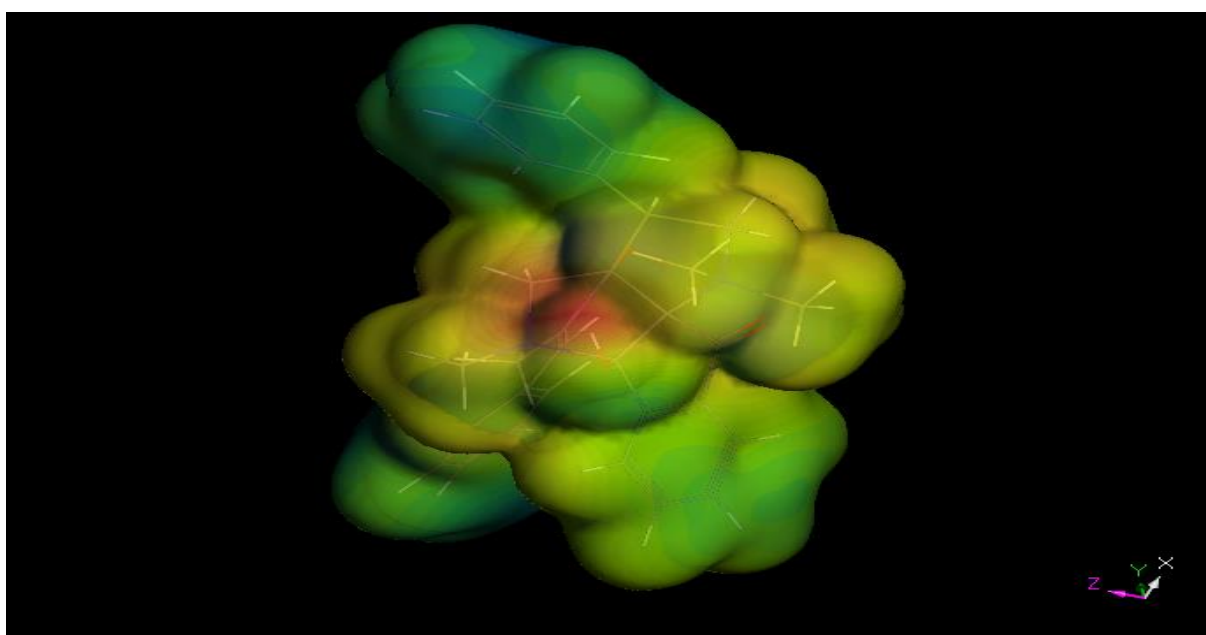
One type of substance that seems to suite very well for the usage as pillaring agent in the beginning is the cage compound 7. It is synthesized by a three-component [3+2]-cycloaddition/annulation out of 3,5-bis[(*E*)-arylmethylidene]tetrahydro-4(1*H*)-pyridinones, sarcosine and ninhydrine³⁷ (Figure 5). A simple methylation of the nitrogen atoms in the cage system should easily introduce the positive charge, making it possible to intercalate the cation. One of the many advantages is its spherical shape. Even if the molecule positions itself with their longer axis planar into the interlayer space, it should create enough height between the layers to enable access to the interlayer space for small molecules.



Scheme 1: Three-component [3+2]-cycloaddition.

The set of starting materials allows for fine tuning of the micropores. If we consider the number of different amino acids and different substituted aryl compounds in addition to the before mentioned adjustment of the layer charge density, an almost indefinite amount of variations is accessible. It should be possible to generate the perfect shaped micropore for many applications. The smooth conditions of the reaction, the cheap solvent, the low reaction time and the availability of the starting materials, with amino acids as a natural product, make this compound even more attractive. Some problems might occur though when it comes to the final dimethylation of the cage-like molecule, because the ring structure might not be stable enough to carry two positive charges. But this will be discussed later.

Computer simulations for the electron density distribution of **7** (Figure 6) allowed calculations for the micropore volume of the layered silicate after the intercalation of the di-cation. The simulations revealed values of 9.1 and 17.4 Å for the dimensions of the pillar to calculate the pore diameter. The middle diagram shows the pore diameter calculation of **7** dependent of the layer charge, using 17.4 Å as parameter for the *ab*-layer of the silicate, while 9.1 Å is used as parameter for the bottom diagram. Currently, a layer charge of -0,33 can be generated. Since no pore volume would be generated if the longer axis lies planar in the interlayer space its strongly dependent on the intercalation angle of pillar **7**. The availability of the starting materials for this type of pillar are good reasons to synthesize the pillar and make use of it.



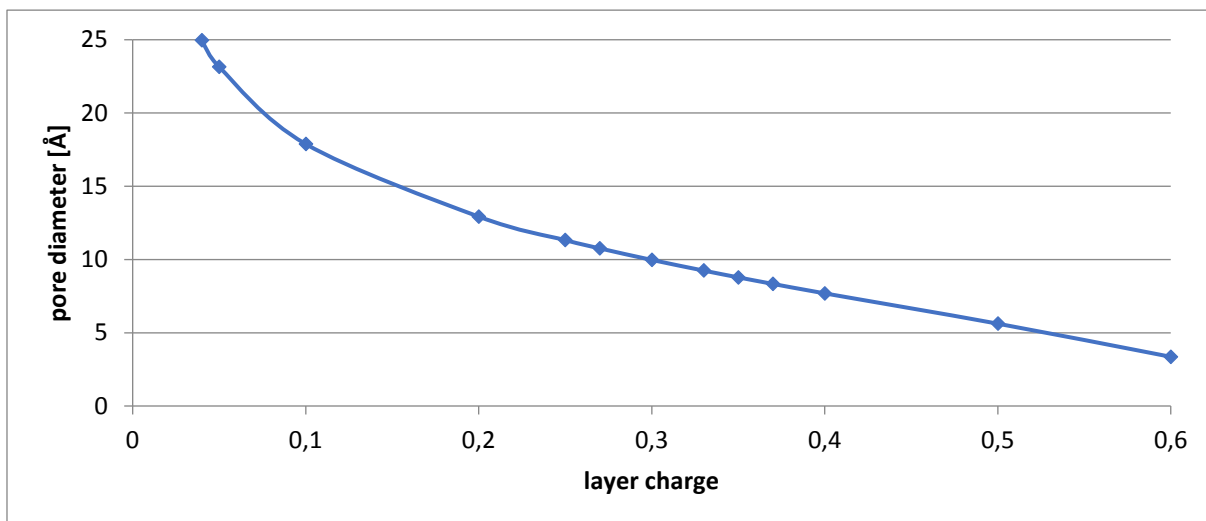
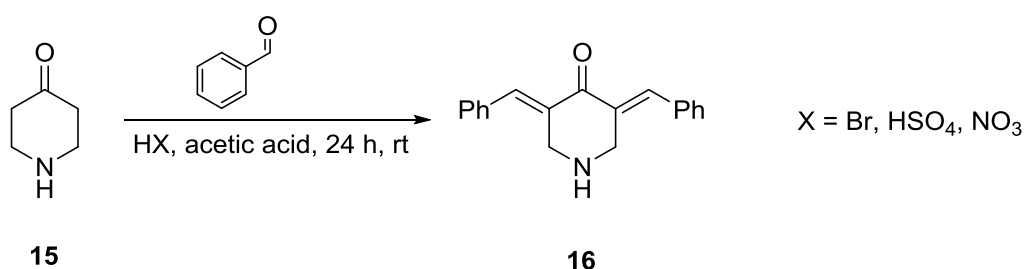


Figure 6: top) electron density distribution simulation for **7**, revealing 9.1 and 17.4 as values for the pore diameter calculation; middle) pore diameter calculation with 17.4 Å for the ab-layer; bottom) pore diameter calculation with 9.1 Å for the ab-layer.

1.1.1 Synthesis of the diaryl compound

Since two of the starting materials are commercially available (ninhydrin, sarcosine), only the diaryl compound has to be synthesized. For the condensation of benzaldehyde with 4-piperidinone hydrochloride *Choon* et al. used acetic acid as solvent in the presence of *insitu* generated HCl gas.³⁸ Despite of the good yields, which could be reproduced, achieved with *insitu* generated HCl gas in the condensation reaction, it is always risk factor to work with gaseous HCl. In order to minimize this risk, one could think of other possibilities for the condensation reaction.



Scheme 2: Condensation of 4-piperidinone with benzaldehyde.

HCl as a strong halogenic acid can be replaced by other strong acids. Therefore, different easy available, common acids were tested in this reaction, like bromic-, sulfuric- and nitric acid. The great advantage compared to HCl is that at room temperature these acids are in the fluid state and can be handled much easier.

15 and glacial acetic acid were provided in round flask. HX was then added dropwise until all of the starting material has been dissolved. Subsequently, benzaldehyde was dropped into the solution. After 24 h stirring at room temperature the precipitate was filtered and dried. The Salt was then treated with K_2CO_3 to obtain the pure organic compound **16**. As it can be seen in Table 1, bromic acid showed with a yield of 91% the best result and nitric acid with only 26% the lowest value. So, the value from the original literature could be slightly improved by 4%.

entry	HX	Yield [%]
1	NO_3	25
2	HSO_4	75
3	Br	91
4	Cl	87 ²

Table 1: Condensation of benzaldehyde (1.75 mmol) with **15** (0.88 mmol), 4 mL acetic acid as solvent, HX, 24 h, rt.

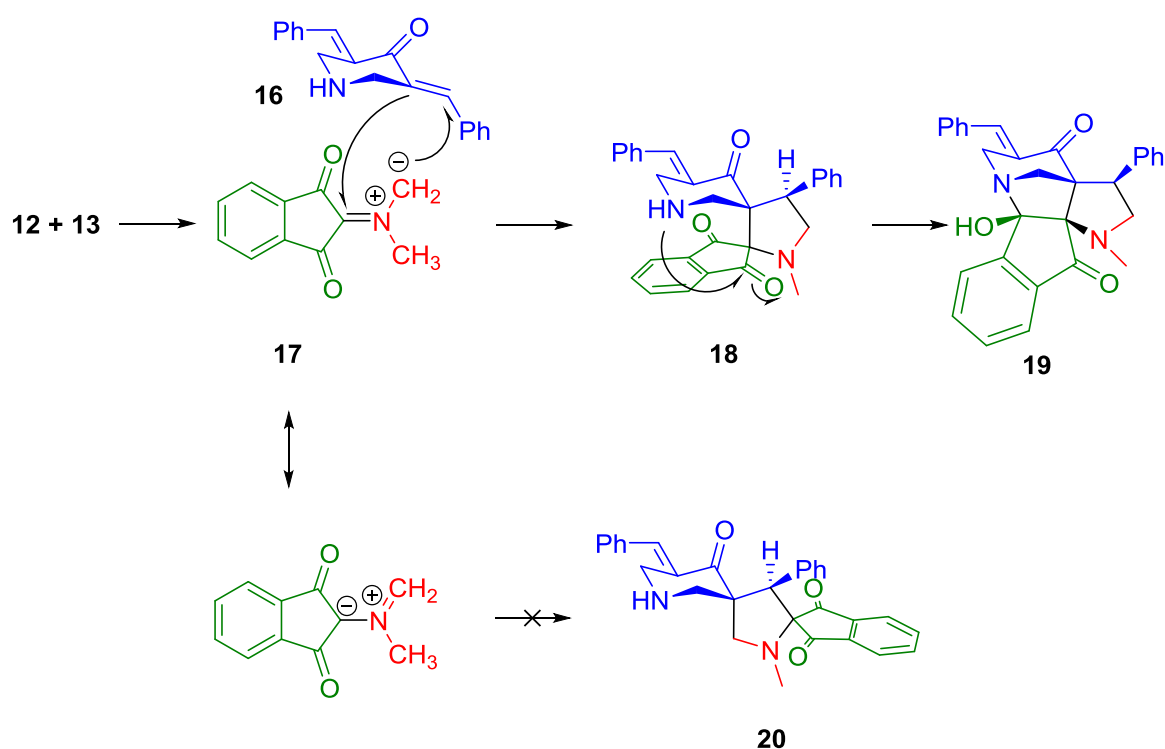
1.1.2 The three-component reaction

This reaction resulting in a pentacyclic diazapentacyclo[12.3.1.0^{2,10}.0^{3,8}.0^{10,14}]octadeca-3(8),4,6-triene-9,15-dione has already been investigated by *Choon* et al.³⁷ Nevertheless, I want to highlight some details of the mechanism since this cycloaddition works stereoselective without any auxiliaries or catalysts.

As it can be seen in Scheme 3, sarcosine and ninhydrin are forming the azomethine adduct **17**. Afterwards it is added to the carbon double bond of **16** resulting in the cycloadduct **18**. The remaining amino function then attacks the neighboring carbonyl group to form a hemiaminal and final product **19**. This hemiaminal is also stabilized by intramolecular hydrogen-bonding. The complicated stereochemistry is decided through the azomethine formation by the activity of the carbonyl groups of compounds **12** and **16**. The sterically hindrance of **16** with its two phenyl groups and the ring structure is much bigger than the one of ninhydrin. Another reason for the less active carbonyl group of **16** is its conjugated system of π -electrons which creates far lower partial positive charges. The next stereo determining step is the 1,3-dipolar cycloaddition of **17** to **16**. **17** has two possible mesomeric structures which can undergo this cycloaddition. The nucleophilic carbon of the ylide **17** then adds to the end of the enone

system of piperidinone fragment **16**. This results in the intermediate **18** instead of **20**, as it is the expected outcome of the reaction.³⁹ Although it is the unusual outcome it can be explained by steric reasons, but also by the fact that the interaction of the nitrogen lone pair with the carbonyl function can happen during the cycloaddition. That is decreasing the energy of activation for the cycloaddition.

The mild reaction parameters (reflux in MeOH) allowed *Choon* et al. to finish the reaction after only one hour. He could achieve yields from 72-87% using this conventional heating method, changing to microwave heating he could improve the max. yield to 96% for one of his compounds. The yields generated with the conventional method could not be reproduced in



Scheme 3: Mechanism of the cycloaddition/annulation.³⁷

this work, 67% at maximum, although no time was wasted on finding the perfect crystallization conditions since the focus lies clearly on the methylation of **19**.

1.1.3 Methylation of cage compound **19**

There are three ways how **19** can be methylated and a positive charge is generated. Either one of both nitrogen atoms is in its methylated form or both are quarternized. Methyl as a substituent was chosen to minimize the steric impact on the size of the micropores to

guarantee access to the interlayer space for small molecules, because **19** itself has a pretty big equivalent area.

Many different reaction conditions (Table 2, selection) and methylation reagents were applied but none of them lead to the desired product **7**. Analysis of the reaction revealed plenty of decomposition products. Unfortunately, none of them could be clearly identified. Column chromatography or crystallization did not result in a complete separation. The analyzed spectra did not give a lot of elucidation. What we can assume is an opening of the hemiaminal structure formed in the last step of the multi-component-reaction. Hemiaminals are known to be intermediates, unless they are stabilized by other substituents.^{40,41}

Entry	methylation reagent	equivalents	solvent	t [h]	yield [%]
1	MeI	2.0	MeOH	24	0, decomposition
2	MeI	10.0	MeOH	72	0, decomposition
3	MeI	2.0	CH ₂ Cl ₂	24	0, decomposition
4	MeI	4.0	CH ₂ Cl ₂	24	0, decomposition
5	MeI	10.0	CH ₂ Cl ₂	24	0, decomposition
6	MeI	10.0	CH ₂ Cl ₂	24*	0, decomposition
7	-	-	MeI	24	0, decomposition
8	-	-	MeI	24*	0, decomposition
9	-	-	MeI	72	0, decomposition
10	MeOTf	4.0	THF	2	0, decomposition
11	MeOTf	4.0	THF	4	0, decomposition
12	MeOTf	4.0	O(CH ₃) ₂	2	0, decomposition
13	MeOTf	4.0	CH ₂ Cl ₂	0.5	0, decomposition
14	MeOTf	4.0	CH ₂ Cl ₂	2	0, decomposition
15	MeOTf	4.0	CH ₂ Cl ₂	24	0, decomposition

Table 2: Methylation of compound **19** (0.11 mmol), refluxing solvent. Reactions at rt have been examined too. *Reaction was executed in a bomb tube at 90°C.

The ring structure might have opened and somehow an aldehyde function has been created. The hemiaminal could have also reacted back to the tertiary amine and the carbonyl function. The NMR did not show any additional peaks for the required methyl-group, so, a partial methylation can be excluded.

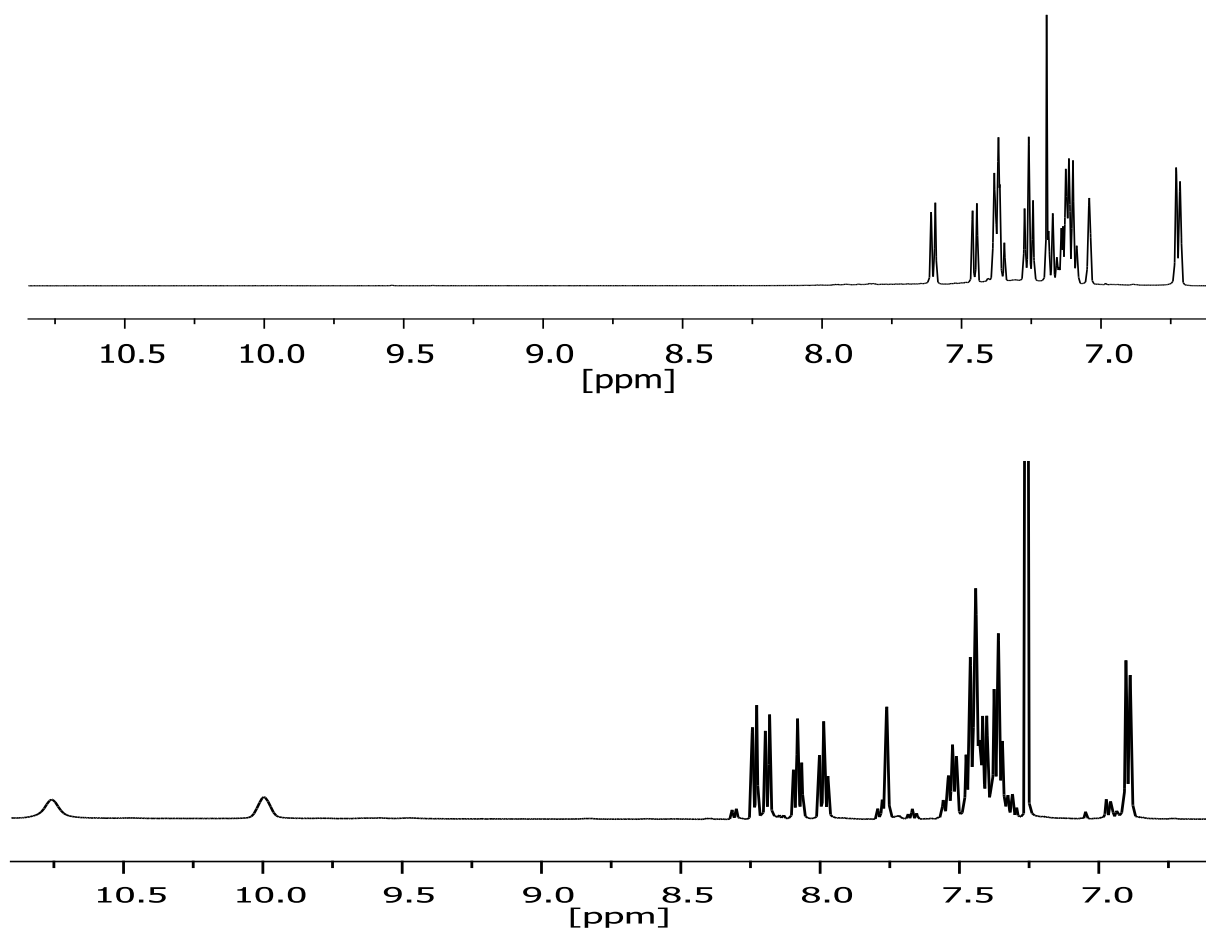
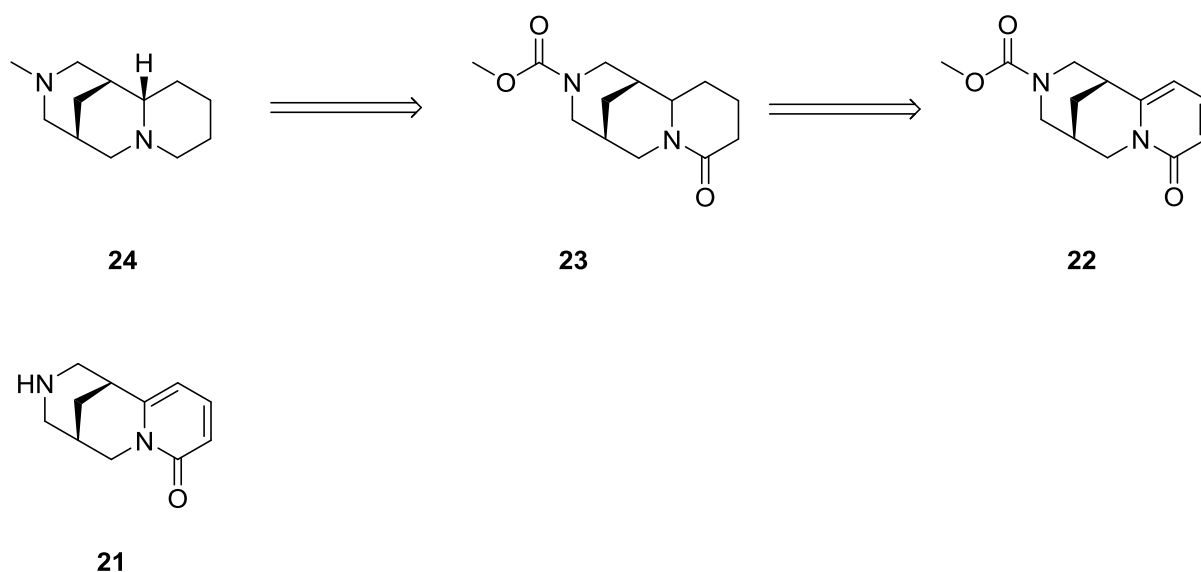


Figure 7: NMR spectra of compound **19** before (top) and after (bottom) methylation, indicating a ring opening.

1.2 Synthesis of the cytosine based pillar

Another class of substances that can possibly be used as intercalation compounds are natural products. Many of them own a spherical structure while there is at least one nitrogen atom that is capable of carrying a positive charge after alkylation. Only some can be used straight away for methylation experiments, but the majority of products has to be derivatized before they are appropriate for methylation reactions and subsequently for intercalation experiments.

One possible natural product that has all the requirements for a pillar molecule is cytosine which is obtained from *Laburnum anagyroides* seeds.⁴² After extraction and derivatization of (-)-cytosine (Scheme 4) methylation can be approached.



Scheme 4: Retrosynthesis overview for the derivatization of (-)-cytisine.

Advantages for this type of pillar are of 6666 that it can be derived from natural resources and also their existing chirality before and consequently after derivatization. The molecule rather small than other natural products in addition to its spherical shape. The two nitrogen atoms that can carry a positive charge make it even more attractive for the application in intercalation, since the equivalent area for the pillar in the interlayer space decreases for every additional charge.

Computer simulations for the electron density distribution of **6** (Figure 8) allowed calculations for the micropore volume of the layered silicate after the intercalation of the di-cation. The simulations revealed values of 7.8 and 11.4 Å for the dimensions of the pillar to calculate the pore diameter. The middle diagram shows the pore diameter calculation of **6** dependent from the layer charge, using 11.4 Å as parameter for the *ab*-layer of the silicate, while 7.8 Å is used as parameter for the *c*-axis. The bottom diagram shows the calculation with switch values. Currently, a layer charge of -0,33 can be generated. In both cases a micropore volume would be generated. If it is large enough to grant access for small molecules depend on the angle of intercalation which cannot be predicted, but it can be assumed generated pore volume would be more likely than none.

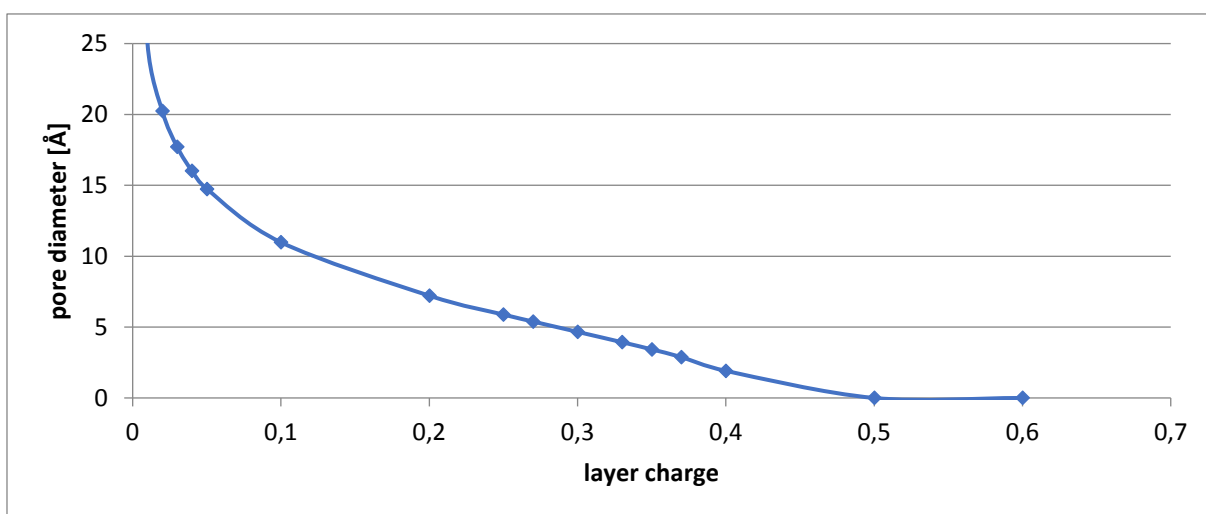
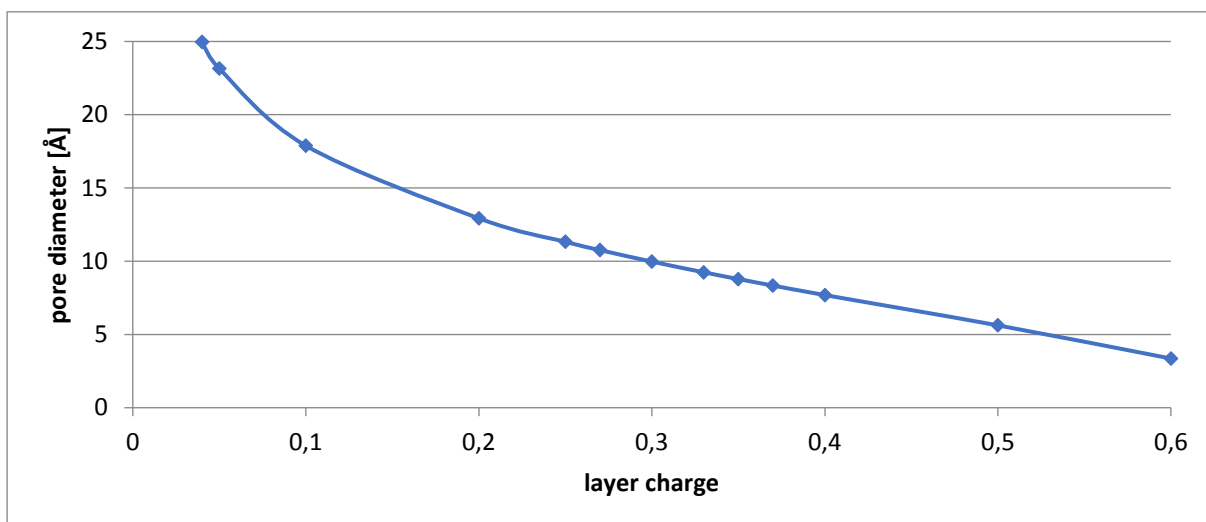
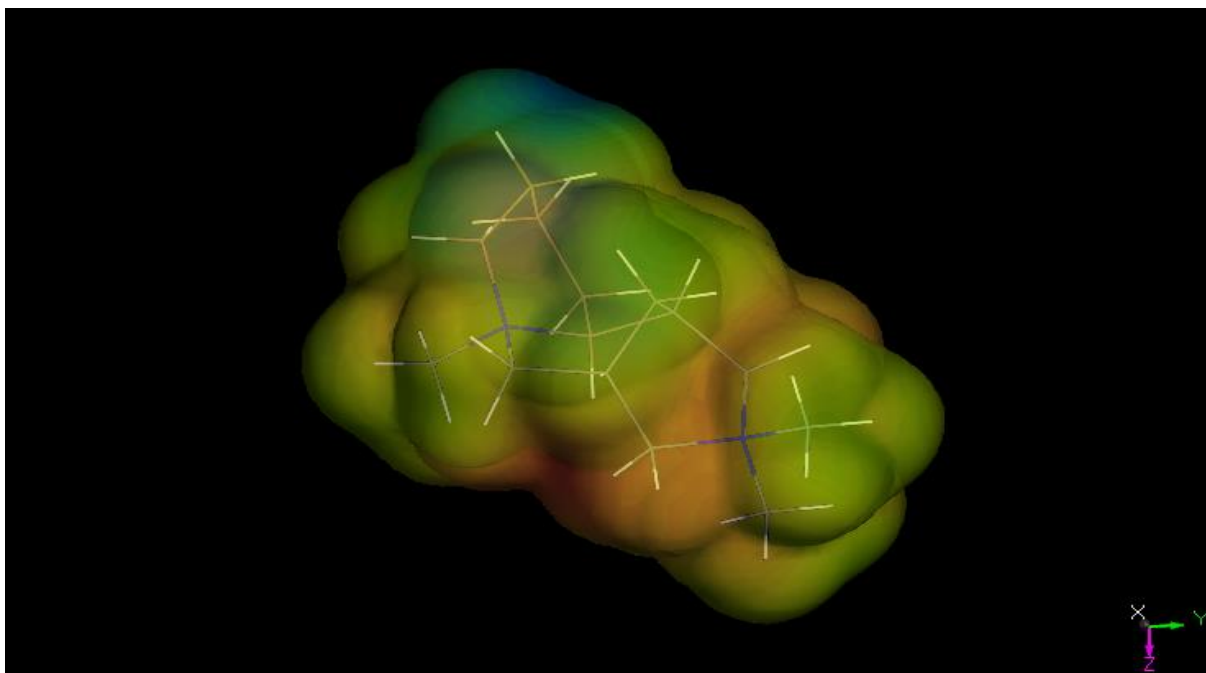
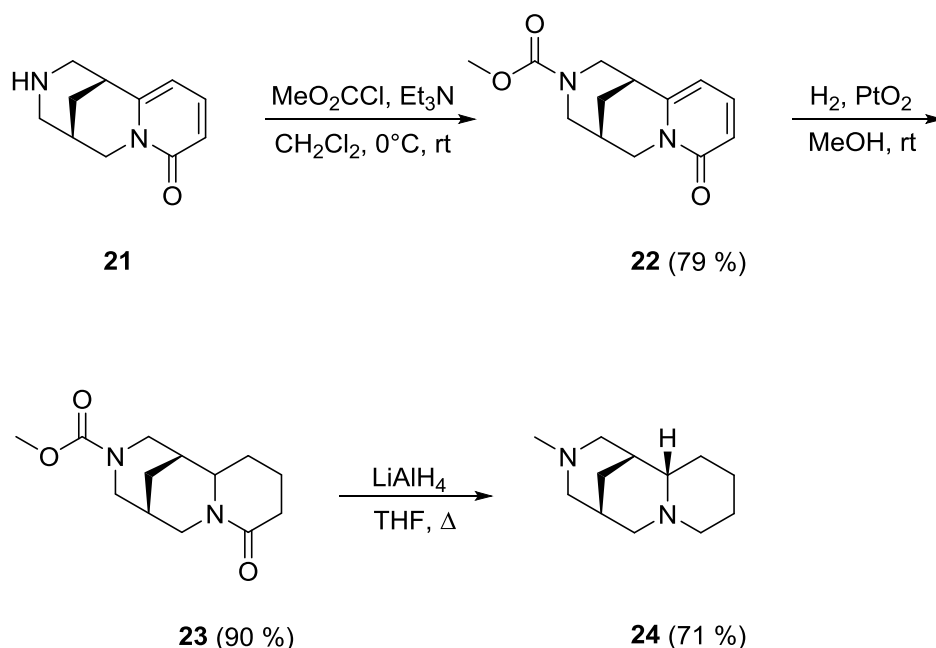


Figure 8: up) electron density distribution simulation for **6**, revealing 7.8 and 11.4 as values for the pore diameter calculation; middle) pore diameter calculation with 11.4 Å for the *ab*-layer; bottom) pore diameter calculation with 7.8 Å for the *ab*-layer.

1.2.1 Derivatization of (-)-cytisine

Enantiomeric pure (-)-cytisine had to be extracted from *Laburnum anagyroides* seeds first. This happened by a long and exhausting extraction procedure, gaining (-)-cytisine as a yellow-brown solid. As shown in Scheme 5 **21** then reacted with methyl chloroformate to form **22** with the carboxy protected amino function using CH_2Cl_2 as solvent at moderate temperatures.



Scheme 5: Derivatization of (-)-cytisine.

The conjugated π -system was then hydrogenated to compound **23** using platinum(IV)oxide as catalyst, whereby a variation of hydrogenation time from 5-12 h could be observed. After the successful hydrogenation, reduction of the carbonyl groups has been the next step. This happened via a simple reduction using LiAlH_4 in THF with refluxing conditions. All results from *Dixon et al.* were reproduced with similar yields.⁴²

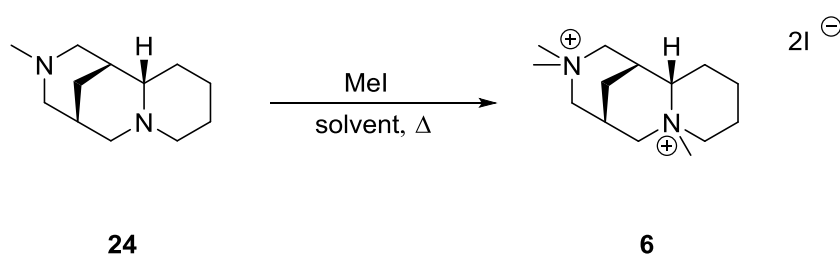
1.2.2 Methylation of compound 24

Having compound **24** in hand, methylation of the two nitrogen atoms should follow to form the di-cationic molecule with the respective anion (Scheme 6). Many different reaction conditions were approached (Table 3), from low to high temperatures, different amounts of equivalents, various solvents. All common methylation reagents were used. MeI showed the best results for the methylation of **24**. Nevertheless, a complete methylation of both nitrogen

atoms has been achieved only once using 10 equivalents of MeI and MeOH as solvent. The mixture was heated in a bomb tube up to 95°C for 24 h. All other attempts resulted in a partly

Entry	methylation reagent	equivalents	solvent	t [h]	T [°C]	ratio [mono-/dication]
1 ⁱ	MeOTf	2	O(CH ₃) ₂	2	rt	no yield
2 ⁱⁱ	Me ₃ OBF ₄	2	CH ₂ Cl ₂	2	rt	no yield
3 ⁱⁱⁱ	Me ₂ SO ₄	2	THF	2	rt	no yield
4	MeI	2	THF	2	rt	10/90
5	MeI	2	EtOH	2	rt	10/90
6	MeI	2	MeOH	2	95	20/80
7	MeI	10	MeOH	12	95	40/60
8	MeI	10	MeOH	24	95	40/60
9	MeI	10	MeOH	48	95	40/60
10	MeI	10	MeOH	72	95	40/60

Table 3: Reaction conditions for a methylation of 0.26 mmol of compound **24**. i-iii) various solvents and temperatures were approached without success; ratios are rough estimations from NMR-integrals.



Scheme 6: Methylation of **24**.

or no methylation of **24**. The more polar the solvent has been the better has been the methylation. The monomethylated compound still has to be solvable so that the second methylation can happen. A reaction where MeI has been used as solvent resulted in an immediate precipitation of the monomethylated compound. Except of the attempt with full conversion, a maximum of methylation was obtained at a reaction time of 24 h. The attempts of separating the mono-cation and di-cation via recrystallization did not end in a positive

result. Unfortunately, the only attempt where a full conversion was realized could not have been reproduced. Other attempts to obtain the di-cation **6** failed too. The amount of **6** produced in the full conversion of **24** was barely enough to record NMR spectra which can be seen in Figure 7. Analyzing the ^1H -NMR spectra of compound **6**, one immediately notices the three singlets at 3.28, 3.33 and 3.35 ppm. Each one of the signals is integrated to 3, although

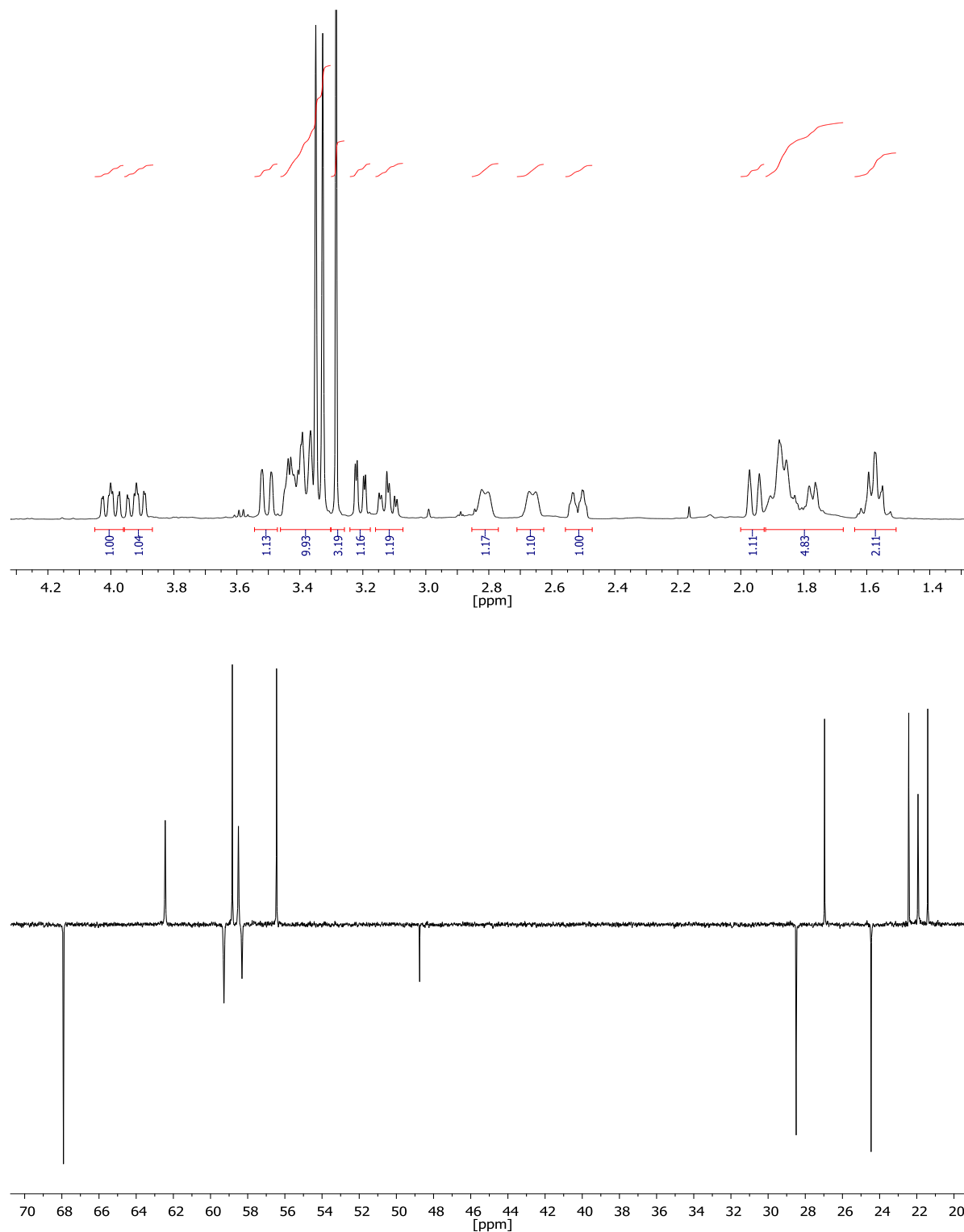


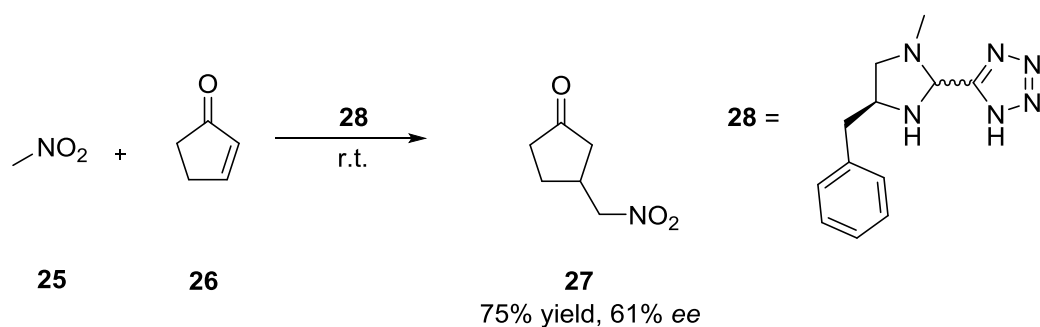
Figure 9: Recorded ^1H -NMR and ^{13}C -NMR spectra of **6** in D_2O .

one of them is slightly overlapped with another multiplet. After the experiments with no pure di-cation **6**, the singlet at 3.28 ppm is not integrated to 3, indicating a mixture of mono- and di-cation. If we study the ^{13}C -NMR 135dept spectra all 14 signals are detected. The 8 peaks with a positive intensity belong to the $-\text{CH}_2-$ groups. 3 of the other signals with the lower negative intensity belong to the $-\text{CH}-$ groups. The other 3 small peaks belong to the $-\text{CH}_3$ groups. The intensity of the signal at 48.8 ppm varies from attempt to attempt. This was a second evidence for the incomplete methylation of **24**. Unfortunately, no pure di-cation could be obtained and the experiment with working reaction conditions could not be reproduced.

1.3 Synthesis of the cobaltocenium based pillar

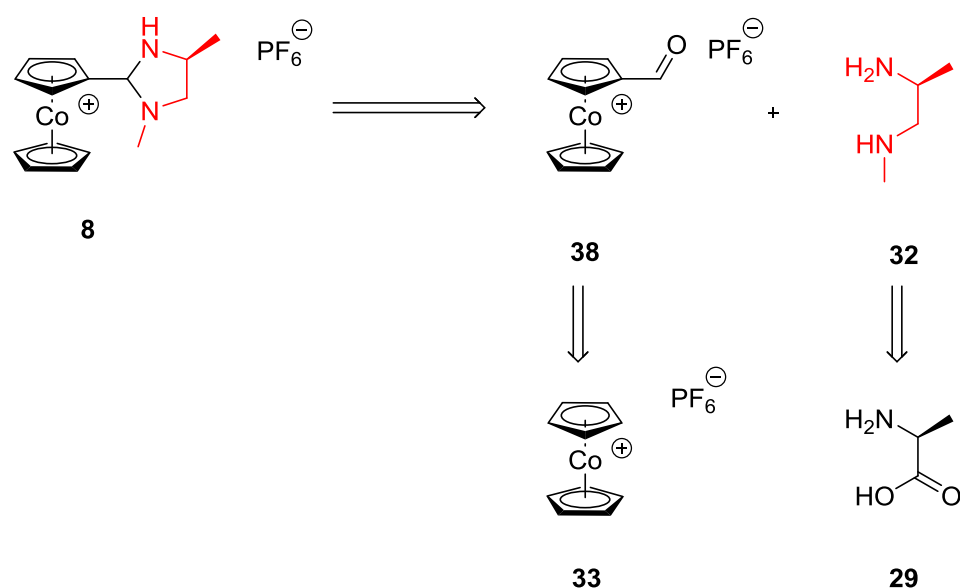
As mentioned above, metal complexes are attractive for the use as intercalation compounds. Reasons for this are that, dependent on the metal ion and its ligands, many of them are positively charged and own a spherical structure, for instance tetrahedral, trigonal bipyramidal and octahedral. E.g. ruthenium(III)(bypy) $_3^{3+}$ **4** and cobalt(III)(sep) $^{3+}$ **9** possess an octahedral conformation. Another advantage is the introduction of higher positively charged complexes is pretty easy. This reduces the equivalent area of the complex, which increases the micropore volume. A possible class of metal complexes that fits very well for the usage as pillar are the metallocenes. Despite of their linear configuration with two ligands, the bulkiness of the ligands allows them to be used. Additionally, the chemistry of metallocenes is well investigated.⁴³

Most attention has been paid on ferrocenes⁴⁴, but the complex is not appropriate for usage as pillar due to its charge neutrality. Another sandwich complex that fits to the requirements is cobaltocenium, which attracted some attention too.⁴⁵ The cyclopentadienyl ligand can be further modified by chemical reactions to attach organic side chains or organo catalysts in order for fine tuning of the micropores or to make catalysis in the interlayer space possible. There are of course certain requirements to consider, for instance the organo catalyst cannot be too big or micropore volume will not be created after intercalation. The substances of the catalytic reaction must have a vapor pressure that is large enough to ensure presence of the starting materials in the gaseous phase. A reaction that fulfills all precondition is the asymmetric addition of nitroalkanes which has been investigated by *Prieto* et al. previously.⁴⁶ He also approached a new imidazolidine-tetrazole organo catalyst (Scheme 7).



Scheme 7: Addition of nitromethane to cyclopentenone using **28** as organo catalyst.⁴⁶

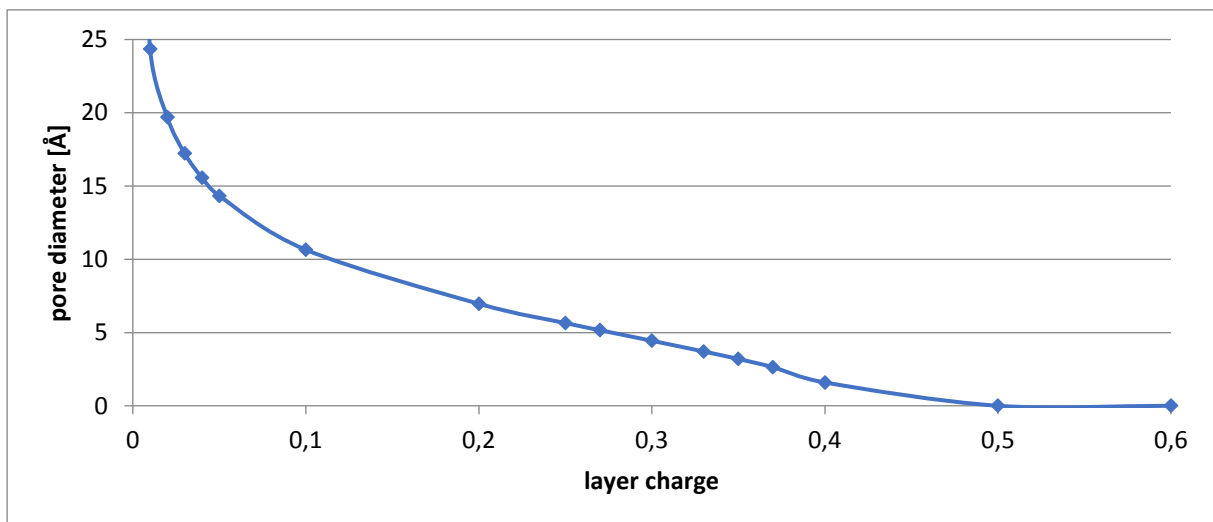
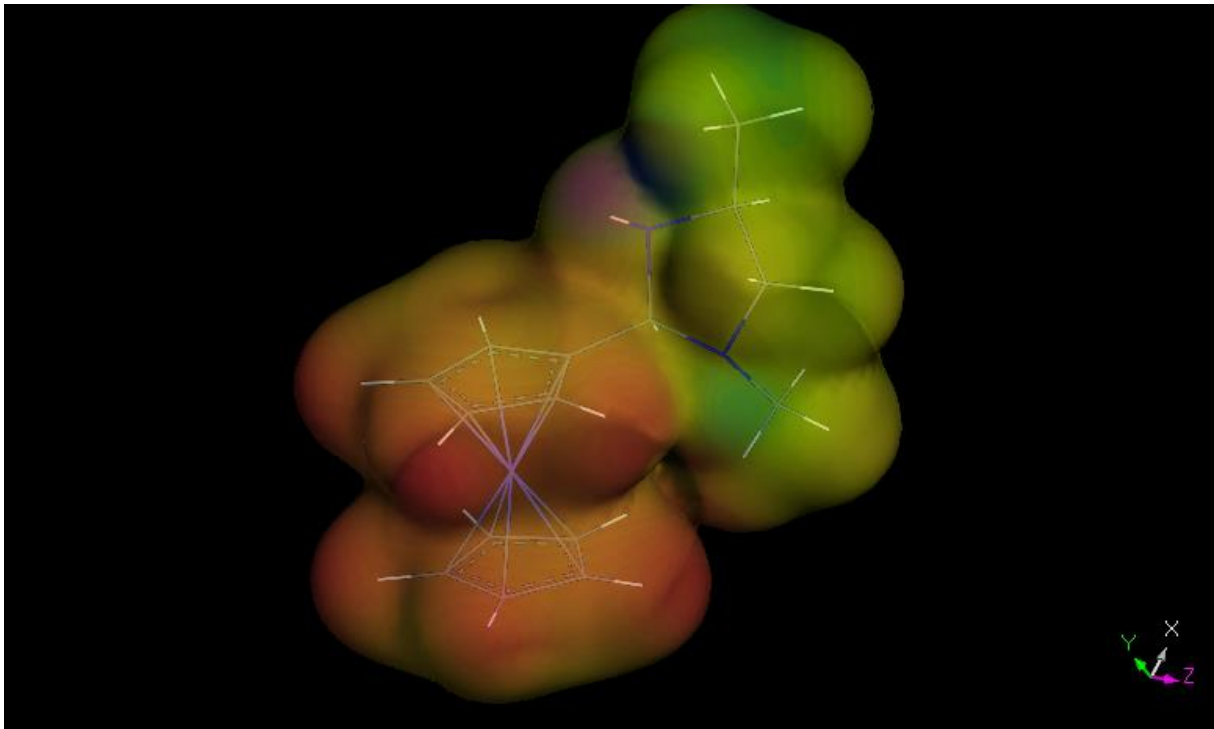
Transferring this organo catalyst onto the cobaltocenium complex, the tetrazole motif must be replaced by the sandwich complex. The catalytic part of the catalyst should stay the same although a decrease in size would be better for reasons mentioned before. A formyl group has to be attached to one of the cyclopentadienyl rings which should then react with a 1,2-diamine, which is derived from the amino acid alanine, to form the final pillar (Scheme 8). In principle, this type of catalyst should even improve the enantiomeric excess of the reaction, because the steric impact delivered by the cobaltocenium part from **8** should be much bigger than the tetrazole part from **28**, plus rigid position of the pillar, because it cannot rotate uncontrolled.



Scheme 8: Retrosynthesis of pillar **8**.

To prove the eligibility of the cobaltocenium compound as pillar, computer simulations were made for the molecular structure and the electron density distribution (Figure 10). 7.4 and 11.5 Å were obtained as parameters for calculation of the pore volume dependent on the layer charge. The middle diagram of Figure 8 shows the pore diameter calculation of **8**

dependent on the layer charge, using 11.5 Å as parameter for the *ab*-layer of the silicate, while 7.4 Å is used as parameter for c-axis. The bottom diagram shows the calculation with switched values. Currently, a layer charge of -0,33 can be generated. In both cases a micropore volume would be generated. The size of the micropores is now dependent in which angle θ intercalates into the silicate layers.



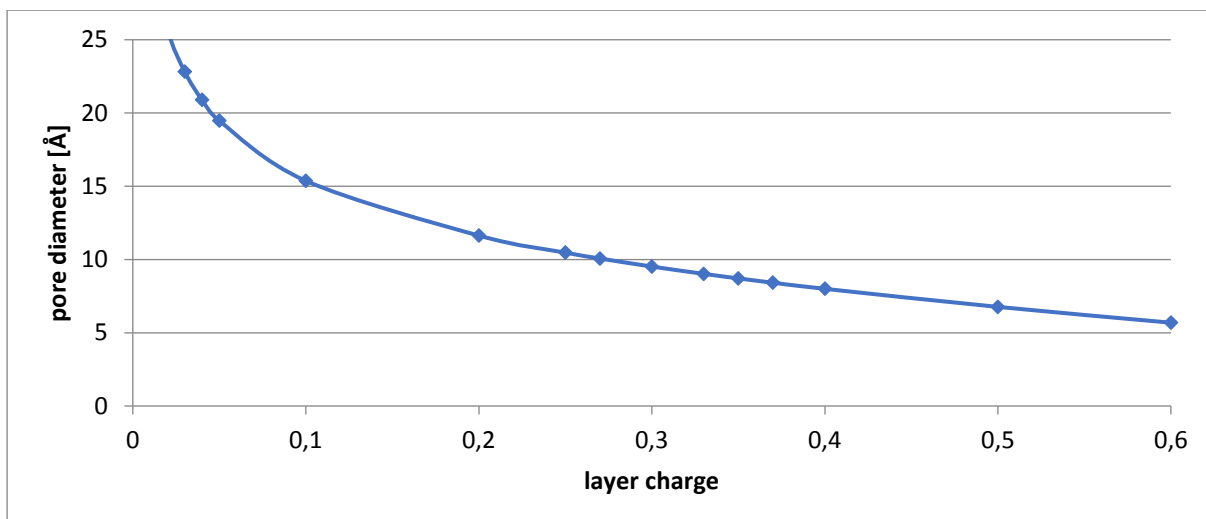
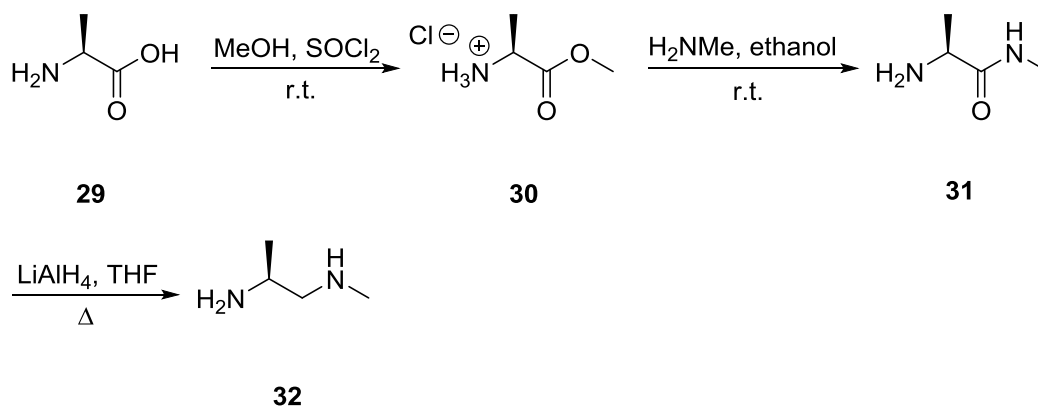


Figure 10: top) electron density distribution simulation for **8**, revealing 7.4 and 11.5 as values for the pore diameter calculation; middle) pore diameter calculation with 11.5 Å for the *ab*-layer; bottom) pore diameter calculation with 7.4 Å for the *ab*-layer.

1.3.1 Synthesis of the diamine compound **32**

With alanine being the starting material for the precursor **32**, another great advantage of this type of pillar and reaction is revealed. Beginning with an amino acid, modification of the reaction and subsequently fine-tuning of the micropores can be achieved easily by just exchanging the amino acid. Chemistry of amino acids is well investigated and no problems should be expected on synthesizing the diamine compound **32**.

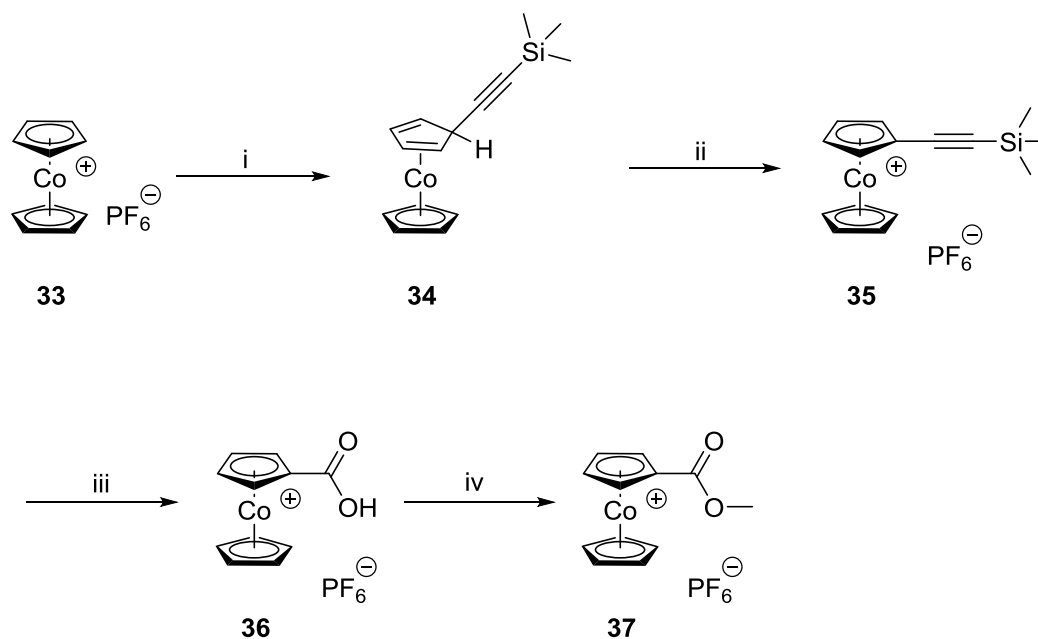
In the first reaction *L*-alanine **29** was esterified with methanol as reagent and solvent plus SOCl_2 quantitatively. The resulting *L*-alanine methyl ester hydrochloride **30** was then converted into the methyl amide hydrochloride using an ethanolic methylamine solution. After the reaction with K_2CO_3 to obtain the free amine **31**, the carbonyl group was reduced with LiAlH_4 in THF resulting in *N*-methylpropan-1,2-diamine **32** with an overall yield of 55% (Scheme 9).⁴⁷



Scheme 9: Synthesis of N-methylpropane-1,2-diamine **32**.

1.3.2 Synthesis of the cobaltocenium based part **37** of the pillar **8**

Cobaltocenium hexafluorophosphate **33**, which was used as starting material, has been purchased commercially. The synthesis of **33** has already been developed by *Wilkinson* in 1952, transferring cobalt(II)-acetylacetonate and cyclopentadienyl magnesium bromide into the sandwich complex.⁴⁸ Nowadays it synthesized by the reaction of NaCp and CoCl₂.⁴⁹ Beginning with the sandwich complex, it is transferred into the cobalt(I) specie **34** almost quantitatively via a nucleophilic addition of the organolithium reagent of trimethylsilylacetylide. **34** is then oxidized to the substituted cobalt(III) derivative **35** by a chemoselective endo-hydride abstraction, using triphenylcarbenium hexafluorophosphate as reagent. The next step is oxidative cleavage of the alkyne. This happens equally to synthesis of carboxylic acids from alkynes. Potassium permanganate served as oxidizing reagent, resulting in cobaltocenium carboxylic acid hexafluorophosphate **36**.⁵⁰ Again equally to a normal esterification the carboxy group was converted into the methyl ester **37**, using SOCl₂ and methanol as reagent and solvent. The conversion happened quantitatively at room temperature overnight (Scheme 10).

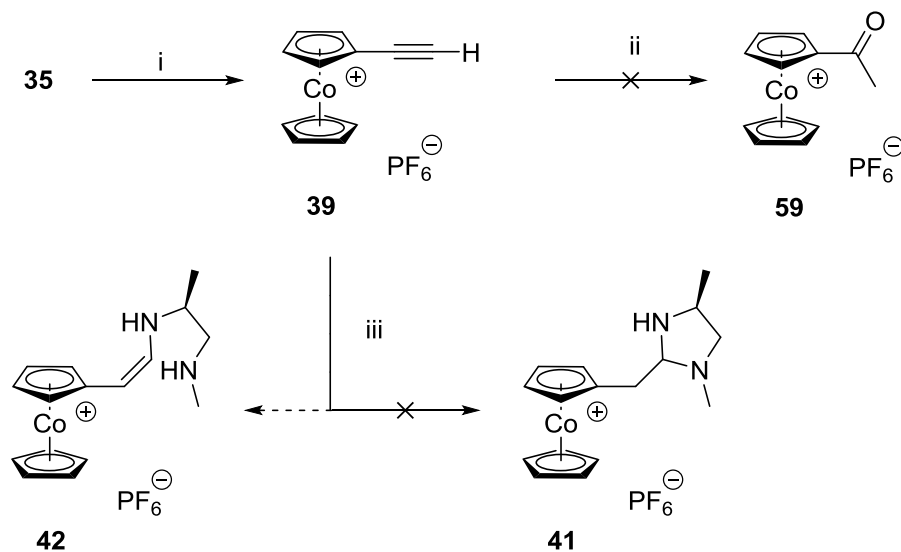


Scheme 10: Synthesis of cobaltocenium carboxylic methyl ester (**37**); i) $(\text{H}_3\text{C})_3\text{SiC}\equiv\text{CLi}$, THF, 95%; ii) $(\text{H}_5\text{C}_6)_3\text{C}^+\text{PF}_6^-$, CH_2Cl_2 , n-hexane, 69%; iii) NaF, CH_3CN , KMnO_4 , $\text{H}_2\text{O}/\text{HPF}_6$, 85%; iv) MeOH, SOCl_2 , 75%.

The last step in order to reach the final precursor **38** is a chemoselective reduction of the ester to the corresponding aldehyde. DIBAL-H is the reagent of choice for such a reaction. But all approached reaction conditions (low and high temperature, reaction time, solvent) failed to generate the formylcobaltocenium hexafluorophosphate. The *in situ* generation of the cobaltocenium carboxy chloride cation, using pure SOCl_2 , with a subsequently reduction using $\text{LiAlH}(\text{O}t\text{-Bu})_3$ as reagent did not end in a positive result⁵². The carboxy chloride species was verified via $^1\text{H-NMR}$. In all reduction experiments an aldehyde species could not be detected. A direct formylation of one Cp-ring, similar to the formylation of ferrocene, has not been successful, too. The formyl group seems to destabilize the sandwich complex and decompose it.⁵¹ No aldehyde function could have been detected in any of the experiments. A strategy switch has been necessary, since a reduction to the alcohol was not possible either.

Instead of synthesizing the carboxylic acid **36** and consequently the ester **37**, **35** was converted into ethynyl cobaltocenium hexafluorophosphate **39**. The conversion to the methyl cobaltocenium ketone **40** failed too, approaching different reagents, solvents and reaction conditions (time, temperature), and no product could be isolated or identified. Reasons for this might be, that the carbon neighbored to the Cp-ring is less reactive than the second ethynyl carbon or that the keto group is destabilizing the Cp-ring and the sandwich complex was decomposed. Oxidative hydroboration of **39** did not lead to a positive result, this time resulting in a complete recovery of the educt.⁵³ A conversion of **39** and the diamine **32**

according to *Wang* did not generate the desired product **41**, whereby only adducts of the amine could be isolated without a ring closure.⁵⁰



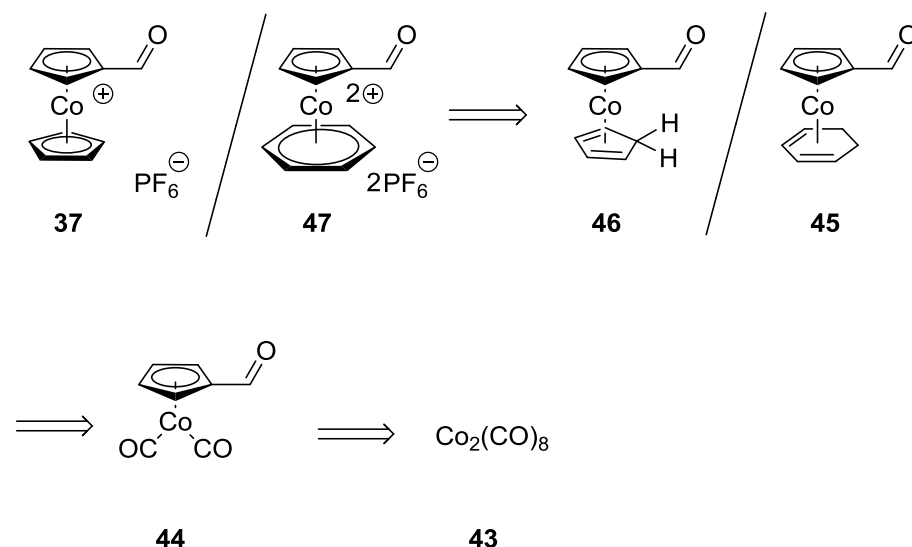
Scheme 11: Synthetic path to **40** and **41**; i) 1) K_2CO_3 , CH_3OH 2) $(\text{H}_3\text{C})_3\text{C}^+\text{PF}_6^-$, CH_2Cl_2 , *n*-hexane⁴⁹; ii) various conditions according to *Basset*⁵⁴; iii) various conditions according to *Wang*⁵⁰.

1.3.3 Synthesis of **8** starting from $\text{Co}_2(\text{CO})_8$

As determined in chapter 1.3.2, the synthesis of **38** is not possible by introducing the formyl group through reduction of the carboxy group after formation of the sandwich complex. So, another possibility to reach the target compound is to first produce a cobalt-formylcyclopentadienyl complex with other additional ligands. Such a complex is reported in literature.⁵⁵ Starting from cobalt carbon monoxide complex **43**, **44** should be synthesized via a ligand exchange reaction using formylcyclopentadienyl lithium in the presence of iodine. The remaining carbon monoxide ligands should then be further exchanged by cyclic diene, either cyclopentadiene or 1,3-cyclohexadiene, to gain the intermediates **45** and **46**. In a subsequent β -H abstraction using one or two equivalents of triphenylcarbenium hexafluorophosphate as reagent, the final precursors **47** and **37** should be synthesized (Scheme 12).

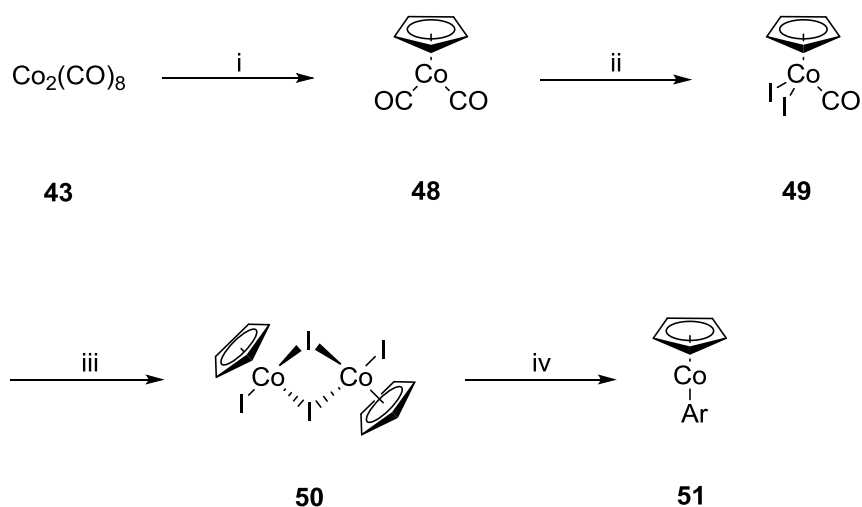
Before the first ligand exchange reaction, formylcyclopentadienyl lithium was synthesized from cyclopentadienyl lithium using ethyl formiate as reagent with similar yields compared to literature.⁵⁶ Unfortunately, this route had to be buried very fast because the yields achieved in the ligand exchange reaction are not worth mentioning.⁵⁷ Reasons for this might be, as

mentioned earlier, the missing electron density on the formylcyclopentadienyl ring of the sandwich compound. The possibly air sensitive product might also be decomposed, although provisions have been made to prevent it.



Scheme 12: Retrosynthesis of **37** and **47** starting from $\text{Co}_2(\text{CO})_8$.

Another synthesis route for the target compound is shown in scheme 13. The starting compound is **43** like in the previous route. But instead of using the formylcyclopentadienyl **44**,



Scheme 13: Synthesis of cobalt sandwich compounds; i) NaCp, I_2/THF ; ii) I_2 , diethylether; iii) petrol ether (100-140); iv) AgPF_6 , different solvents and aryl compounds.

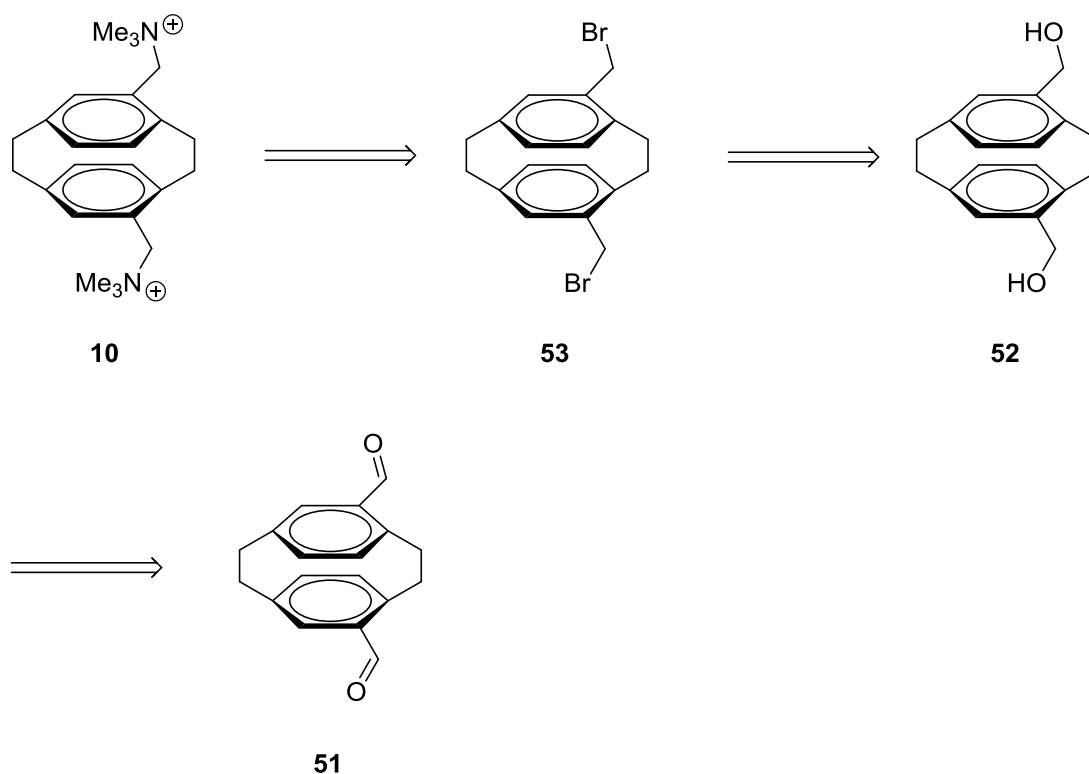
unsubstituted cyclopentadienyl is used in the ligand exchange reaction. Yields were obtained as high as expected from literature. The same counts for the next two reaction steps. **48** was converted into **49** using pure iodine in dry diethylether stirring at room temperature until no gas evolution could be observed. **49** was further heated in petrolether (100-140) to gain **50**. **50** was then used as starting material for a series of exchange reactions in order to obtain a

cobalt sandwich complex substituted with a formyl group like *Plitzko* et al. or *Loginov* et al. did in their work.^{58,59} Unfortunately, no complex could be prepared. The lack of electron density in the aryl ring of the formyl substituted benzylic rings must be the reason for the instability and or immediate decomposition of the desired cobalt sandwich complexes. Preparing the catalytic part onto the aryl ligand with the following ligand exchange reaction did not result in a positive result either. *Plitzko* and *Loginov* used aryl compounds that were higher substituted with methyl groups and even the cyclopentadienyl ring was fully substituted with methyl groups in the majority of their experiments. The use of mesitylaldehyde, as a highly substituted aryl ring, did not end in a positive result, neither did the use of stabilizing solvents like THF, acetonitrile and diethylether, although the acetonitrile complex $\text{CpCo}(\text{CN})_3$ was isolated. This complex could not be successfully converted into the desired type of complex **51** either. A higher substitution of the cyclopentadienyl part was not examined due to the much higher steric requirement that is determined marginally, which is counterproductive for the micropores, which should be generated after an intercalation into the layered silicate. Computer simulations have shown steric requirement that is too high, and it would be very unlikely for the micropores to be created. In literature, BF_4^- was mostly used as counter ion. In this study the experiments were executed with PF_6^- as counter ion which should even improve the stability of the complex due to steric reasons. Additionally, we made only positive experiences working with PF_6^- during the preparation of the cobaltocenium carboxylic methyl ester **37**.

Although the idea and concept of this type of pillar, with the metal carrying the positive charge while the catalytic part is attached to the ligand, looked very promising in the beginning. Unfortunately, such cobalt complexes seemed to be very unstable and or too air sensitive to be handled.

1.4 Synthesis of the paracyclophan based pillar

Another possible class of pillar molecules are the ones owning a spherical skeletal structure of [2.2]paracyclophanes. They are offering a huge variety of accessible pillars. The combination of the cyclophanes substitution pattern plus the variation of substituents in addition to the adjustment of the layer charge density allows for fine-tuning of the micropores. Scheme 14 shows the retro synthesis of a possible pillar starting from dialdehyde **51**.



Scheme 14: Short retro synthesis of **10** starting from dialdehyde **51**.

Compared to other pillars, this time the positive charge is not introduced by a methylation reaction, because nitrogen is already existent in the molecular structure, or by using a positively charged metal complex. Now, the charge is introduced by a nucleophilic attack of a tertiary amine on a bromoalkane. Again, a simulation has been made to see if the pillar creates any micropore volume. The limit for the layer charge reduction that can be realized is currently at -0.33. The parameters for the pillar were calculated as 8.4 and 15.9 Å. The two diagrams in Figure 9 (up: 8.4 Å for the ab-layer; down: 15.9 Å for the ab-layer) show the calculation for the pore diameter dependent on the layer charge. So, the angle of the pillar between the two layers decides if micropores are going to be created that grant access to the interlayer space.

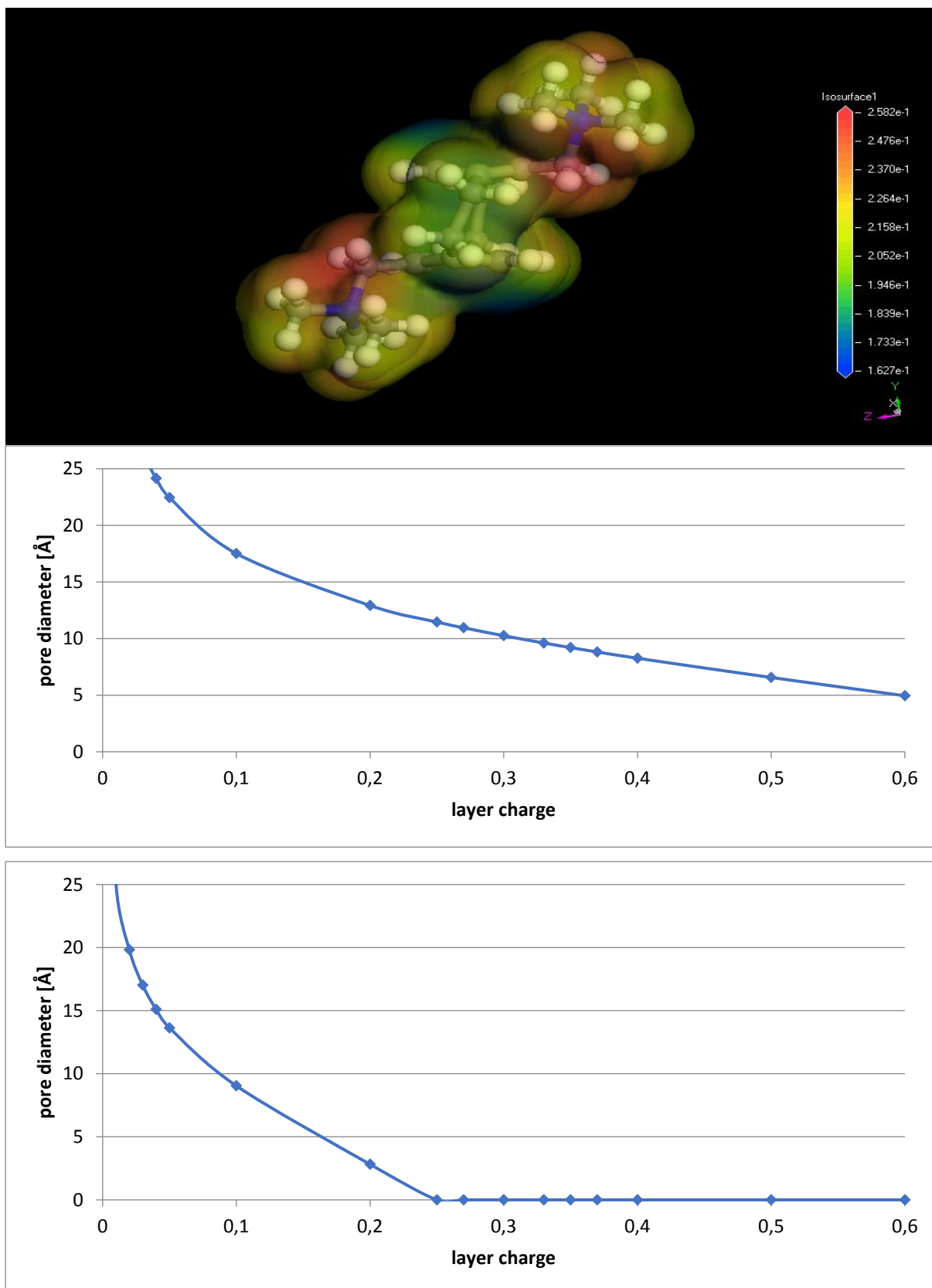
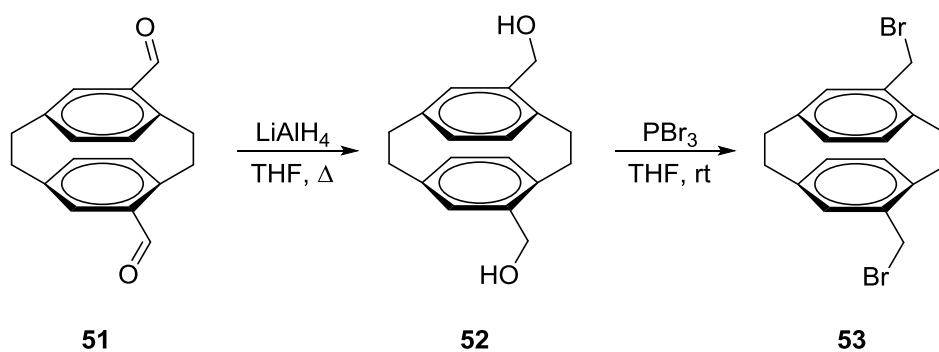


Figure 11: up) electron density distribution simulation for **10**, revealing 8.4 and 15.9 as values for the pore diameter calculation; middle) pore diameter calculation with 15.9 Å for the *ab*-layer; bottom) pore diameter calculation with 8.4 Å for the *ab*-layer.

The electron density distribution indicates, that the pillar positions itself not fully horizontal in the interlayer space. So, the synthesis and intercalation of **10** is worth a try.

1.4.1 Synthesis of the [2.2]paracyclophan precursor

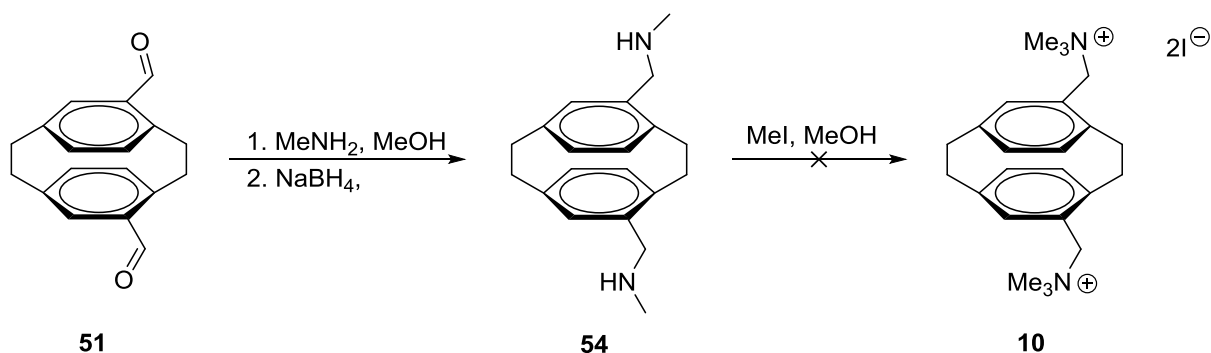
The starting material, 4,13-diformyl[2.2]paracyclophan **51**, was kindly provided by the group of Greiner *et al.* and no further material had to be purchased. In general, **51** is synthesized by a cycloaddition of 1,2,4,5-hexatetraene and propiolic aldehyde⁶⁰ followed by an extensive purification process.⁶¹ **51** was transferred into the corresponding alcohol **52** by a reduction using LiAlH₄, THF as solvent and refluxing conditions for 3 h yielding in moderate 70% of the final product **52**. After column chromatography, **52** was further treated with PBr₃ to form the dibromo compound **53** with a yield of 60% after purification. (Scheme 15)



Scheme 15: Reduction of **51**, reaction of **52** with PBr₃ to **53**.

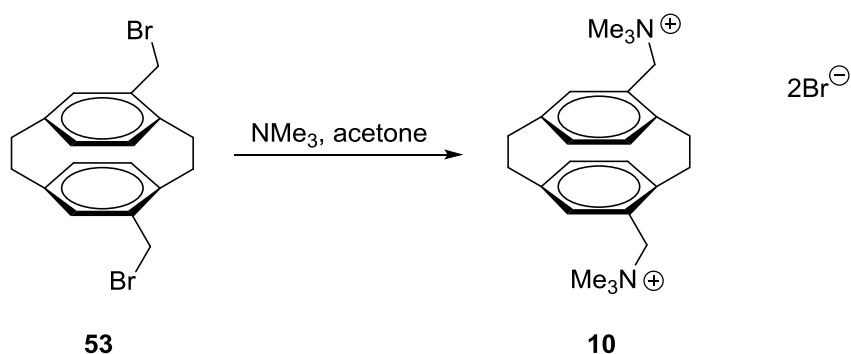
1.4.2 Synthesis of pillar **10**

The next step would be to introduce the amino function on the side chain of the paracyclophan ring structure. This was easily achieved through the reaction of methylamine with the dialdehyde **51**, before the route, illustrated in scheme 15, has been developed. The schiff'sche base was formed and through the following reduction with NaBH₄ the secondary amine **54** was generated in a yield of 78%. Unfortunately, in the next step no yields of the desired molecule could be obtained and pillar **10** could not be synthesized this way (Scheme 16).



Scheme 16: synthesis route for pillar **10** with the amino function being introduced at the start.

That is the reason why the route described in 1.4.1 was approached. Despite the fact that this route lead to a dead end, the other one has great advantages anyway. Starting off from the dibromo compound **53**, a series off pillars could be easily generated through its reaction with a tertiary amine.⁶² Pillar **10** was synthesized by a simple nucleophilic addition of trimethylamine to **53** at room temperature overnight using acetone as solvent, whereby the product started to precipitate. After removal of the solvent the salt was purified by crystallization and obtained as a white solid of 70% yield (Scheme 17).



Scheme 17: Synthesis of pillar **10**.

The whole synthesis can be followed beautifully via NMR-spectra as it is shown in Figure 10.

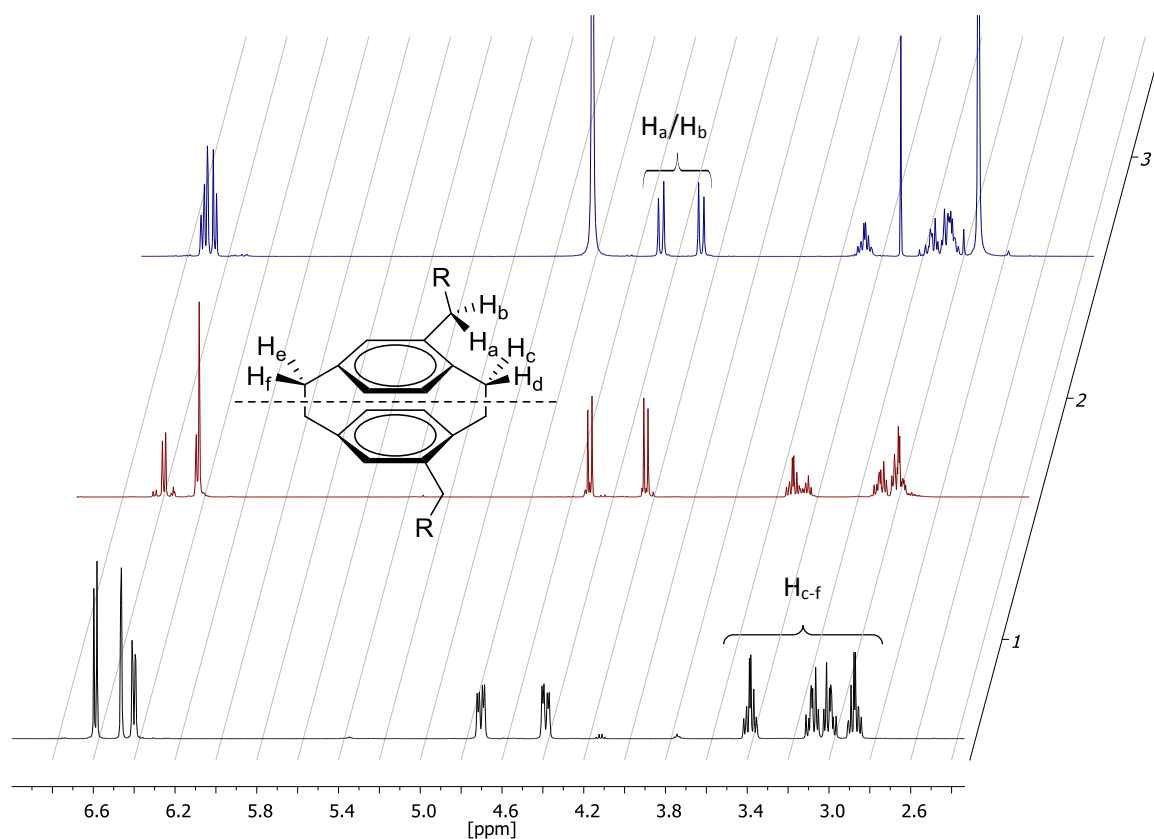


Figure 12: Stacked NMR-spectra of **52** (1), **53** (2) and **10** (3) in the range of 2.4-6.8 ppm.

The pattern of the aromatic protons stays always the same, one singlet with two paired doublets at a chemical shift of 6.6-6.9 ppm, which might overlap sometimes. The protons $H_{a/b}$ appear after the reduction of the dialdehyde **51**. Because they are always next to a hetero atom during the synthesis, their chemical shift ranges from 4.2-4.8 ppm. As expected the chemical shift is more downfield for oxygen as a direct neighbor as for nitrogen or bromine. Each of the protons of the ethylene bridge H_{c-f} forms a multiplet as splitting pattern at a chemical shift of 2.8-3.6 ppm. The type of multiplet changes from step to step and sometimes the multiplets are overlapping. 3 shows the spectra of the final pillar **10**. Since methyl groups are the only residues of the quaternized nitrogen only one additional singlet appears in the spectra with a chemical shift of 2.9 ppm. The more complex the residues are, the higher is the probability of overlapping for the signals and the reaction cannot be followed that beautiful anymore.

Using the same synthesis route, except of exchanging the tertiary amine (ethylamine, N,N-dimethylbenzylamine) in the last step, other pillar molecules have been synthesized with

yields of 80% (**55 a**) and 96% (**55 b**) (Figure 13). Their NMR-spectra show the same pattern of signals, but as assumed not as nice to detect as before.

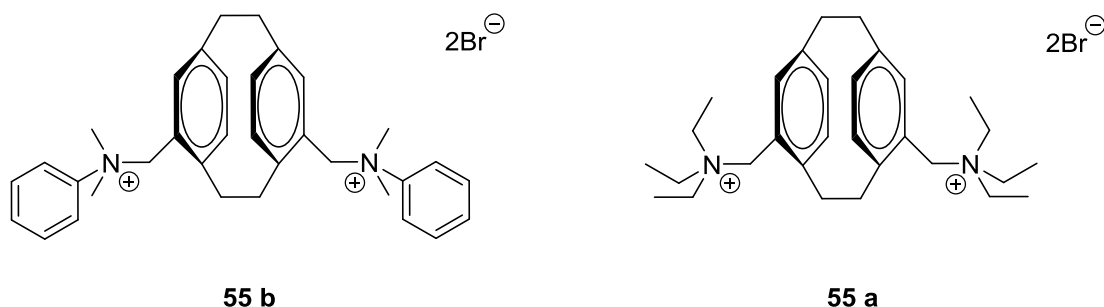
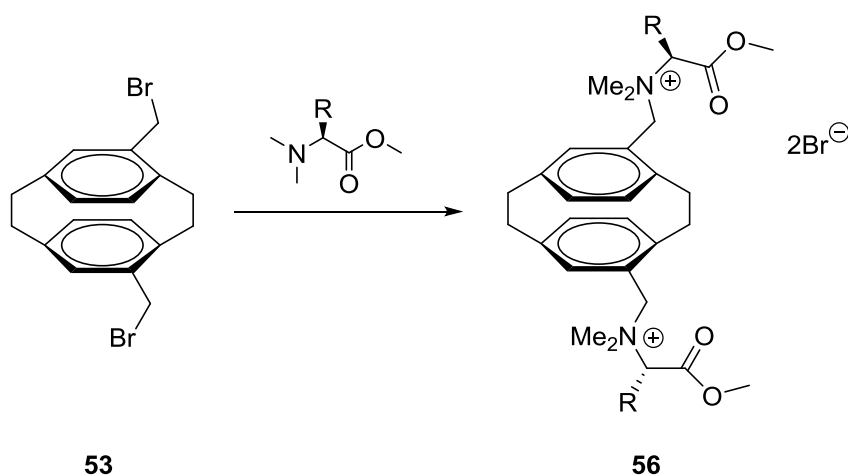


Figure 13: Molecular structure of the synthesized pillars **55 b** and **55 a**.

This route allows many different pillars to be synthesized by that simple nucleophilic addition. Almost every tertiary amine could be used in this reaction. For example, one could also easily introduce chirality into the pillar, and consequently into the micropores of the interlayer space, by using a protected amino acid as tertiary amine (Scheme 18).



Scheme 18: Possible route to a series of pillar molecules based on precursor **53**.

There is also the possibility to tag an organo catalyst to the precursor **53**. Only requirement for such a reaction has to be an amino function of the catalyst which is not involved into the catalytic process. Then it would be possible to do catalysis in the interlayer space of silicates, not to mention the opportunities in the application on chromatography.

2 Application of the microporous organic pillared silicates

2.1 Intercalation of pillar **9** into stevensite $[\text{Na}_{0.47(3)}]^{inter}[\text{Mg}_{2.59(5)}\text{Li}_{0.17(3)}]^{oct}[\text{Si}_4]^{tet}\text{O}_{10}\text{F}_2$ and its application in the adsorption of but-3-yn-2-ol and 2-methyl-but-3-yn-2-ol

As mentioned earlier the micropores in layered silicates are determined by the size, shape and charge of the pillar molecule. Another key part is the charge homogeneity of the layered silicate. The use of chiral pillars results in chiral MOPS, which, for the first time, allow the discrimination of guest molecules by size and chirality. The great advantage is its fine tunability and the modular character. For evidence, different MOPS were prepared, using $[\text{Na}_{0.47(3)}]^{inter}[\text{Mg}_{2.59(5)}\text{Li}_{0.17(3)}]^{oct}[\text{Si}_4]^{tet}\text{O}_{10}\text{F}_2$ and $\text{Co}(\text{sep})\text{Cl}_3$ (sep = $\text{C}_{12}\text{H}_{30}\text{N}_8$ = 1,3,6,8,10,13,16,19-octaazabicyclo[6.6.6]-eicosane), which is a very promising complex for the use as pillar, because of its high charge, spherical shape and chirality. Stevensite was prepared via melt synthesis.^{7e} Therefore, stoichiometric amounts of the educts weighed into a molybdenum crucible in an argon atmosphere and heated up to 1750 °C. After cooling down to room temperature the synthetic stevensite was stored in a Glovebox. Before the pillaring of **9**, MOPSs of different charge density were prepared by ion exchanging the stevensite with Mg^{2+} , using the Hofmann-Klemen effect.⁶³ It was heated for 3 h, 6 h and 12 h to receive respectively MOPS-2, MOPS-3 and MOPS-4. For the intercalation the stevensites were treated several times hydrothermally with equal amounts of (+) and (-) **9**. Integrity of the pillar after intercalation as proved by IR-spectra of the obtained MOPS. The basal spacing increases from 9.6 Å to 16.1(1) Å as determined by X-ray diffraction analysis. In addition, the *00l*-series of all MOPS were highly rational. This indicates that the whole interlayer spaces own the same gallery height.⁶⁵ The importance of physisorption measurements to prove microporosity was mentioned before. Herein, the measurements with Ar/Ar(1) were indicating a type I isotherm for all used samples without significant signs of hysteresis. This is typical for microporous materials. The increase of the median pore diameters lies in the growing interpillar distances, and thus in the reduction of the charge density. The overall increase of the median pore diameter for the measured 4-step series is 0.5 Å.

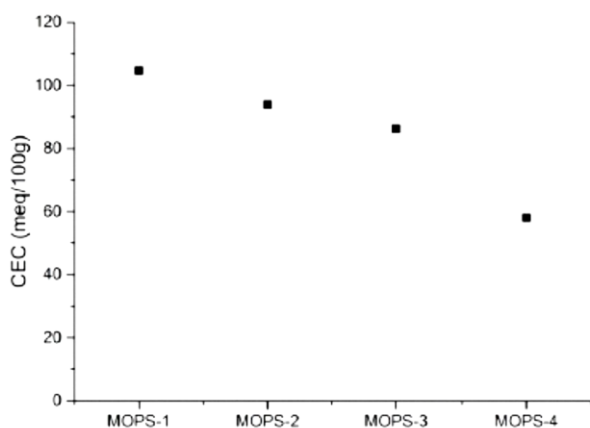


Figure 14: Cation exchange capacity as function of the charge reduction.

This tuneability of the microporosity in minute gradations by charge reduction is the enormous advantage of MOPSS. It allows for fine tuning of the accessibility to the interlayer space for organic guest molecules in contrast to their size- or enantioselective discrimination via intimate contact to the pillars. Since the basal spacing is kept constant at 16.1(1) Å for all of the MOPSS the pore size is only dependent on one variable and so it is determined in an anisotropic fashion.

To test the properties of the prepared new class of MOPS with their adjustable pore size distribution in terms of sorption, their size and shape selectivity were examined towards little organic molecules, which only differ a bit in size. Therefore, two alcohols, but-3-yn-2-ol and 2-methyl-but-3-yn-2-ol, with similar polarity, shape and vapor pressure were adsorbed from

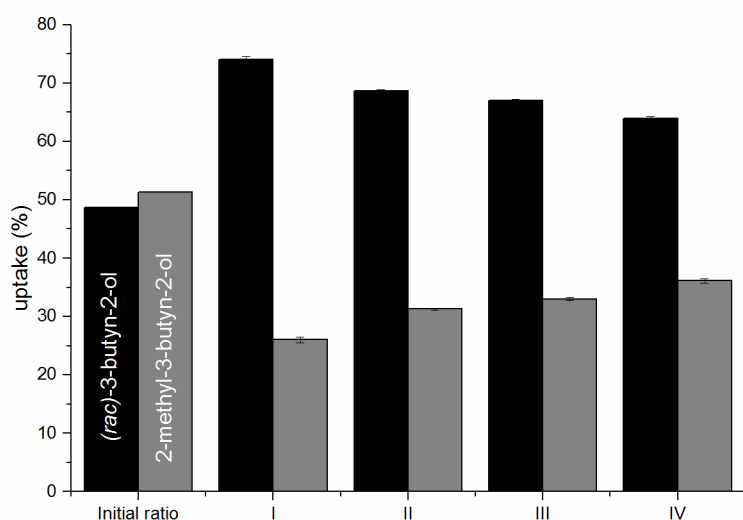


Figure 15: Size selective adsorption of a mixture of but-3-yn-2-ol for MOPS-1 to MOPS-4 at 4 °C.

their equilibrium gas phase mixture at 4 °C by dry MOPS-1 to MOPS-4 under inert conditions. This inert atmosphere was crucial to avoid the adsorption of water molecules which own a high affinity to MOPs.

The slightly smaller alcohol but-3-yn-2-ol showed a larger and increasing total uptake on the MOPS-1 to MOPS-4 from 1.58 to 1.98 mmol g⁻¹ than the 2-methyl-but-3-yn-2-ol, 0.57 to 1.01 mmol g⁻¹. The difference is in the range of about 1 mmol g⁻¹, which is remarkable. The size and shape of test molecules allows them to fit better into the micropores. They are also more amenable to small adaptations in the geometry of the micropores than the argon atoms used for the physisorption measurements. With enlarging micropores from MOPS-1 to MOPS-4 the total uptake decreases continuously from the peak at MOPS-1 for but-3-yn-2-ol, while the uptake increases for 2-methyl-but-3-yn-2-ol. The micropores probably lose contact to the smaller guest molecules and start to prefer the larger one.

So, MOPS-1(+/-) did show the maximum in adsorption capacity, but it produced the best values for the enantiomeric excess as adsorbent in the chiral discrimination of a racemic mixture of *R*- and *S*-but-3-yn-2-ol. Identification was done via high-resolution GC using a chiral column. Interestingly, MOPS-1(+) preferred *R*-but-3-yn-2-ol in the adsorption experiments and as expected MOPS-1(-) preferred the other enantiomer whereby the enantiomeric excess is the same including experimental errors. The best ee for the MOPS with the smallest micropores can be explained by the fact that chiral induction works best when there is less or no room for a variation in the configuration of the molecule. This is the case for MOPS-1 where the pillar molecules are packed the tightest. The possibility of an easy adjustment of these variables using the modular character of the MOPS can hardly be achieved by comparable MOFs. In addition, the best values for the enantiomeric excess reached in our experiments for a single equilibrium stage can be compared to values for the stereoselective adsorption of MOFs.³⁰ A complete chiral resolution should be achieved when MOPS-1 is approached as material for column chromatography (GC, HPLC,... etc) and the numbers of trays is increased

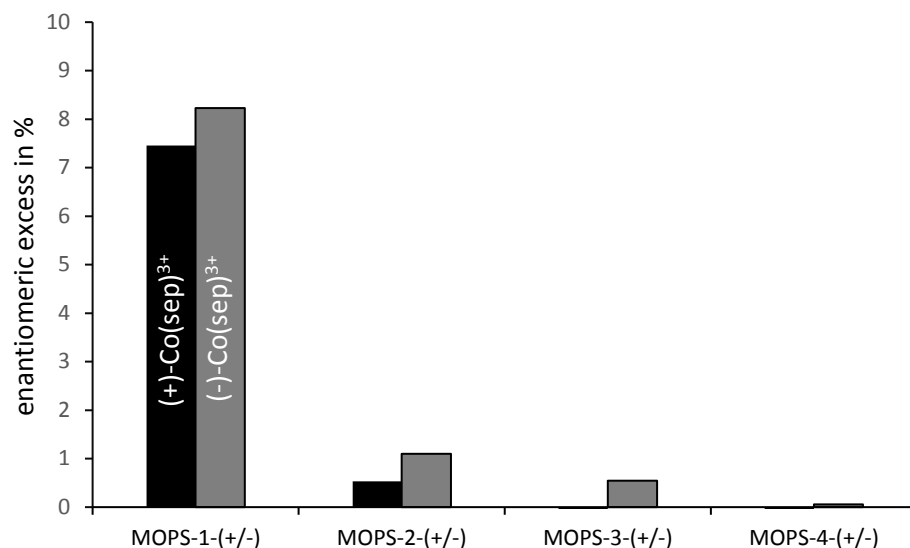


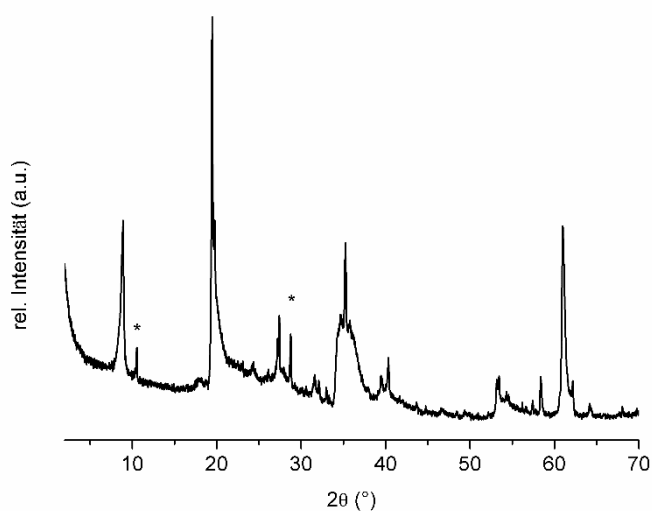
Figure 16: Enantioselective adsorption of a racemic mixture of R/S-but-3-yn-2-ol.

tremendously. Regarding the external surface area and the adsorption capacities of the MOPS its showing that stereo discrimination is a bulk phenomenon and that the diverse retention takes place in the interlayer space. The lateral dimensions, the narrow basal reflections and the full widths of half maximum are evidence of layered silicate platelet thickness of about 72 nm using the Scherrer equation to the 001-reflex. After calculation only less than 5% of the surface area are related to the external basal surface area. Supposing that but-3-yn-2-ol has the same molecular volume when it is adsorbed by MOPSs, more than 100% of the micropore volume as measured via argon adsorption is occupied. The fact of a more densely packed but-3-yn-2-ol totally matches literature precedence of similar molecules acting not like liquids but more like crystals.

2.2 Intercalation of pillar 10 into hectorite $[K_{0.48(2)}]^{inter}[Mg_{2.54(8)}Li_{0.43}]^{oct}[Si_4]^{tet}O_{10}F_2$ and its application in the adsorption of but-3-yn-2-ol and 2-methyl-but-3-yn-2-ol

The great advantage of MOPSs is their modular character. *Breu* et al. can easily provide layered silicates with different charge densities. In combination with the future pool of pillar molecules an almost indefinite number of MOPS can be generated that should be able to solve almost any separation problem. A first example has been given in 2.1, when **9** intercalated into stevensite showed a remarkable difference in its adsorption behavior towards molecules that slightly differ in their size and shape. The enantiomeric MOPS was even capable of separating a racemic mixture of but-3-yn-2-ol in very promising results.

As second pillar a pure organic, compared to the organometal complex, was chosen for intercalation into the hectorite $[K_{0.48(2)}]^{inter}[Mg_{2.54(8)}Li_{0.43}]^{oct}[Si_4]^{tet}O_{10}F_2$. Again, the silicate was synthesized via direct melt synthesis. Stoichiometric amounts of educts were provided in molybdenum crucible and the synthesis was similar to the one of stevensite. Before the intercalation of **10** into hectorite, first hectorites with different charge densities were prepared. The same procedure was approached as for stevensite and hectorites after 3 h, 6 h, and 12 h of charge reduction were prepared. Since **10** has only two charges compared to the three of **9**, it is more unlikely for it to generate micropores due to its smaller equivalent area. Therefore, it has first been intercalated into the hectorite whose layer charge has been reduced the most (12 h). The basal spacing increases from 9.6 Å to 13.4 Å as determined by X-ray diffraction analysis. In addition, the *00l*-series of the MOPS were highly rational. This **Figure**



17: Powder X-ray diffraction pattern of a hectorite intercalated with **10**.

indicates that the whole interlayer spaces have the same gallery height. For the evidence of micropores physisorption measurements were taken. The measurements indicated a type I isotherm without significant signs of hysteresis. Unfortunately, the adsorbed volume indicates that the size of the micropores created is not worth to mention. As apprehended the equivalent area was just too small to generate micropores and the packing of **10** in the interlayer space is just too tight and leaves no room even for small molecules to be adsorbed. Nevertheless, the intercalated material was tested in adsorption experiments, and since **10** is no chiral pillar, only for size-selective adsorption.

Although no micropores were generated during the process of intercalation, the material showed some interesting behavior in terms of adsorption and separation of the two alcohols.

72 % of the adsorbed alcohols from the silicate with the highest layer charge (MOPS-1) was the slightly smaller but-3-yn-2-ol. The adsorption started in a gas equilibrium at 4 °C with an initial ratio of 51.3 to 48.7 % of 2-methyl-but-3-yn-2-ol and but-3-yn-2-ol. This value cannot

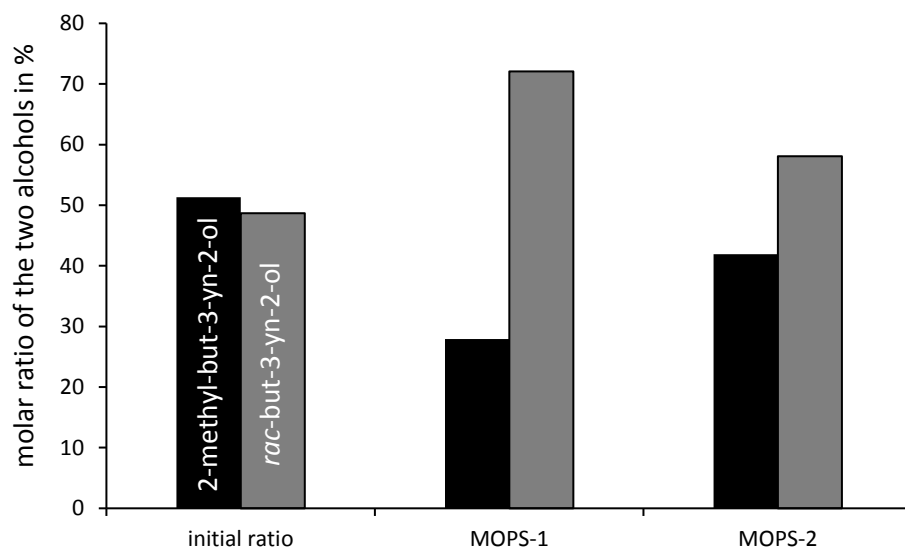


Figure 18: size-selective adsorption of 2-methyl-but-3-yn-2-ol and but-3-yn-2-ol.

quite reach the one of the silicate intercalated with **9**, but is still remarkable. The total uptake of alcohols instead is 10 to 20 times worse, which is more than comprehensible. No micropores do not adsorb substrate. The question comes up where the size-selective separation originates from. There are two possible explanations for it. One is some sort of swelling happened to the layered silicate and thus a quite good separation occurred. Otherwise should have the two alcohols been adsorbed in similar amount. So, but-3-yn-2-ol could be slightly more suited for swelling than 2-methyl-but-3-yn-2-ol. The other and more supposable possibility is that, as mentioned earlier, microstructures were formed caused by the small particle size and their anisotropic particle shape. These microstructures can contain wedge-like pores which are probably responsible for the minimal amount of uptake of the alcohols and the separation of those.

As a conclusion of physisorption measurements and the results of the adsorption experiments, the material can unfortunately only be regarded as organic pillared silicate (OPS) and not as microporous organic pillared silicate.

3 References

- ³⁷ Raju Suresh Kumar, Hasnah Osman, Subbu Perumal, J. Carlos Menéndez, Mohamed Ashraf Ali, Rusli Ismail, Tan Soo Choon, *Tetrahedron* **2011**, *67*, 3132-3139.
- ³⁸ J. R. Dimmock, M. P. Padmanilayam, R. N. Puthucode, A. J. Nazarali, N. L. Motaganahalli, G. A. Zello, J. W. Quail, E. O. Oloo, H. B. Kraatz, J. S. Prisciak, T. M. Allen, C. L. Santos, J. Balzarini, E. De Clercq, E. K. Manavathu, *J. Med. Chem.* **2001**, *44*, 586-593.
- ³⁹ a) H. Pellisier, *Tetrahedron* **2007**, *63*, 3235-3285; b) *Synthetic Applications of 1,3-Dipolar Cycloaddition Chemistry toward Heterocycles and Natural Products*, A. Padwa, W. H. Pearson, Eds.; Wiley-Interscience: **2002**.
- ⁴⁰ M. Velázquez, H. Salgado-Zamora, C. Pérez, M.E. Campos-A, P. Mendoza, H. Jiménez, R. Jiménez, *J. Mol. Struct.* **2010**, *979*, 56–61.
- ⁴¹ Md. Islam, Md. Razzak, M. Karim, A. H. Mirza, *Tetrahedron Letters* **2017**, *58*, 1429-1432.
- ⁴² A. J. Dixon, M. J. McGrath, P. O'Brien, *Organic Synthesis* **2006**, *83*, 141-154.
- ⁴³ a) A. N. Titov, Y. M. Yarmoshenko, P. Bazylewski, M. V. Yablonskikh, E. Z. Kurmaev, R. Wilks, A. Moewes, V. A. Tsurin, V. V. Fedorenko, O. N. Suvorova, S. Y. Ketkov, M. Neumann, G. S. Chang, *Chemical Physics Letters* **2010**, *497*, 187-190; b) Z.-M. Su, C.-X. Lin, Y.-T. Zhou, L.-L. Xie, Y.-F. Yuan, *Journal of Organometallic Chemistry* **2015**, *788*, 17-26; c) Y. Omote, R. Kobayashi, Y. Nakada, N. Sugiyama, *Bulletin of the Chemical Society of Japan* **1973**, *46*, 3315-3316; d) A. Almásy, K. Barta, G. Franciò, R. Šebesta, W. Leitner, S. Toma, *Tetrahedron: Asymmetry* **2007**, *18*, 1893-1898; e) A. Škvorcová, E. Rakovský, J. Kožíšek, R. Šebesta, *Journal of Organometallic Chemistry* **2011**, *696*, 2600-2606.
- ⁴⁴ a) K. P. Stahl, G. Boche, W. Massa, *Journal of Organometallic Chemistry* **1984**, *277*, 113-125; b) N. E. Murr, *Journal of Organometallic Chemistry* **1976**, *112*, 177-187; c) M. Kondo, Y. Hayakawa, M. Miyazawa, A. Oyama, K. Unoura, H. Kawaguchi, T. Naito, K. Maeda, F. Uchida, *Inorg. Chem.* **2004**, *43*, 5801-5803; d) J. E. Sheats, G. Hlatky, *Journal of Chemical Education* **1983**, *60*, 1015-1016.
- ⁴⁵ A. Prieto, N. Halland, K. A. Jørgensen, *Org. Lett.* **2005**, *7*, 3897-3900.
- ⁴⁶ a) K. A. Ahrendt, C.J. Borths, D. W. C. MacMillan, *J. Am. Chem. Soc.* **2000**, *122*, 4243-4244; b) L. Samulis, N. C. O. Tomkinson, *Tetrahedron* **2011**, *67*, 4263-4267; c) N. Halland, R. G. Hazell, K. A. Jørgensen, *J. Org. Chem.* **2002**, *67*, 8331-8338.
- ⁴⁷ G. Wilkinson, *J. Am. Chem. Soc.* **1952**, *74*, 6148–6149.

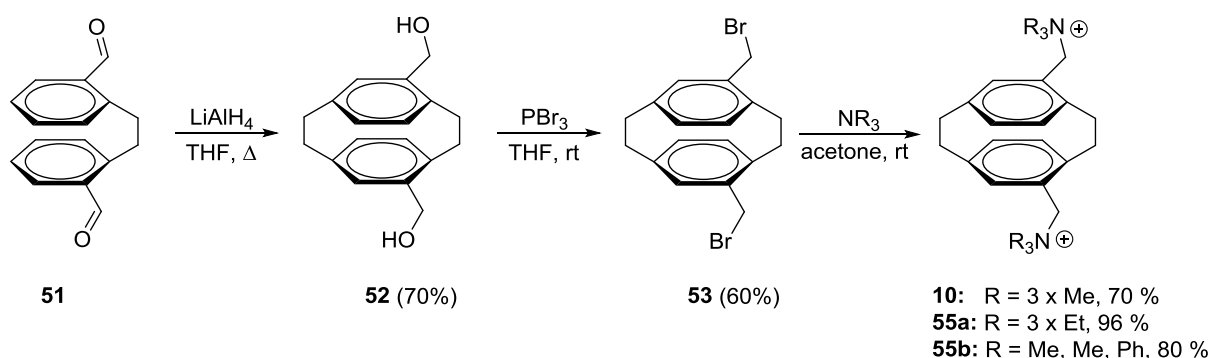
- ⁴⁸ S. Vanicek, H. Kopacka, K. Wurst, T. Müller, H. Schottenberger, B. Bildstein, *Organometallics* **2014**, *33*, 1152-1156.
- ⁴⁹ Y. Wang, A. Rapakousiou, C. Latouche, J.-C. Daran, A. Singh, I. Ledoux-Rak, J. Ruiz, J.-Y. Saillard, D. Astruc, *Chem. Commun.* **2013**, *49*, 5862.
- ⁵⁰ N. E. Murr, *Chem. Commun.* **1981**, 219-220.
- ⁵¹ H. C. Brown, B. C. Subba Rao, *Organic and Biological Chemistry* **1958**, *80*, 5377-5380.
- ⁵² L. Hintermann, A. Labonne, *Synthesis* **2007**, *8*, 1121-1150.
- ⁵³ M. Basseti, B. Floris, G. Illuminati, *Organometallics* **1985**, *4*, 617-623.
- ⁵⁴ M. D. Rausch, W. P. Hart, D. W. Macomber, *J. Macromol. Sci.-Chem.* **1981**, *A16(1)*, 243-250.
- ⁵⁵ W. P. Hart, D. W. Macomber, M. D. Rausch, *J. Am. Chem. Soc.* **1980**, *102*, 1196-1198.
- ⁵⁶ W. P. Hart, M. D. Rausch, *Journal of Organometallic Chemistry* **1988**, *355*, 455-471.
- ⁵⁷ D. A. Loginov, M. M. Vinogradov, Z. A. Starikova, P. V. Petrovskii, A. R. Kudinov, *Russian Chemical Bulletin, int. Ed.* **2004**, *53*, 1949-1953.
- ⁵⁸ K.-D. Plitzko, V. Boekelheide, *Organometallics* **1988**, *7*, 1573-1582.
- ⁵⁹ H. Hopf, F.-W. Raulfs, D. Schomburg, *Tetrahedron* **1986**, *42*, 1655-1663.
- ⁶⁰ I. Dix, H. Hopf, T. B. N. Satyanarayana, L. Ernst, *Beilstein J. Org. Chem.* **2010**, *6*, 932-937.
- ⁶¹ A.-J. Chen, I.-J. Hsu, W.-Y. Wu, Y.-T. Su, F.-Y. Tsai, C.-Y. Mou, *Langmuir* **2013**, *29*, 2580-2587.
- ⁶² T. Aida, K. Tajima, *Angew. Chem. Int. Ed.* **2001**, *40*, 3803-3806.
- ⁶³ U. Hofmann, R. Klemen, *Z. Anorg. Allg. Chem.* **1950**, *262*, 95-99.
- ⁶⁴ D. M. Moore, R. C. Reynolds, *X-Ray Diffraction and the Identification and Analysis of Clay Minerals*; Oxford University Press: Oxford, **1997**.

C Summary

1 Conclusion

In this study a new class of hybrid material has been introduced, the MOPS or microporous organic pillared silicates. They consist out of a metalorganic or organic cation that has been intercalated into a synthetic layered silicate. The organic cation is placed in the interlayer space of a silicate by the process of pillaring. The IUPAC defined pillaring as “a process by which a layered compound is transformed in a thermally stable micro- and/or mesoporous material with retention of the layered structure. ... A pillared compound has the following characteristics: (i) the layers are propped apart vertically and do not collapse upon removal of the solvent; (ii) the minimum increase in basal spacing is the diameter of the N₂ molecule, commonly used to measure surface areas and pore volumes: 0.315-0.353 nm; (iii) the pillaring agent has molecular dimensions and is laterally spaced in the interlamellar space on a molecular length scale; (iv) the interlamellar space is porous and at least accessible to molecules as large as N₂; there is no upper limit to the size of the pores. ... There is no restriction on the nature of the intercalating agent or on the mechanism of intercalation.”² By this definition MOPS are a subgroup of intercalation compounds whereby the microporosity needs to be in the interlayer space. Evidence for this must be a rational series of the d₀₀₁ lines and a physisorption measurement. Charge homogeneity is a prerequisite, so the generated micropores are homogenic too. The size and shape of the micropores are dependent on the size, shape and charge of the used pillar and on the charge density of the layered silicate. Some efforts failed to prepare an organic molecule or metal complex that fits the requirements of a highly charged cation with a spherical shape. Synthesis of cage compound **7** has not been successful. Decomposition of the starting material **19** was the only observation that could be made. The cationic hemiaminal was probably too unstable to be isolated. The pillar **6** was synthesized successfully, unfortunately the synthesis could not have been reproduced even once although the same reaction conditions have been applied. Further attempts resulted in a mixture of the mono- and dication which we were not able to separate. The synthesis of the metalorganic pillars **5** and **6** failed too. The reason for this failure was probably the lack of electron density at the cobalt ion of the sandwich complex. Therefore, the important intermediates **37** and **47**, two sandwich complexes with an aldehyde function on one ring, could not have been synthesized. Despite all disappointments, the synthesis of pseudo-meta-bis(5,12-(N,N,N-trimethylmethylenaminium))-[2.2]paracyclophan bromide **10**

and a series of other types of this class of pillar was successful. Starting from the dialdehyde **51**, **53** was synthesized via a reduction and subsequently substitution reaction. Having **53** in hand a series of molecules were synthesized by another substitution reaction using just a tertiary amine in an easy overnight reaction.



Scheme 19: Synthesis route towards pillar **10**, **55a** and **55b**.

This type of pillar is also a perfect example for the modularity of the whole system. The charge density of the layered silicate can be adjusted by layer charge reduction through cation exchange reaction using the Hofmann-Klemen-Effekt. Thus, the size of the micropores can be changed on a molecular scale. The used pillar can also be altered simply by using another tertiary amine. An almost indefinite amount of variations is available this way.

After intercalation of pillar **10** into a hectorite no micropores were created as determined by physisorption measurements. Nevertheless, the new material showed an interesting behavior in the adsorption of two very similar alcohols, but-3-yn-2-ol and 2-methyl-but-3-yn-2-ol. Starting from a molar ratio of 48.7:51.3 but-3-yn-2-ol was adsorbed better than the bigger alcohol with a molar ratio of 72.0:28.0, which is pretty remarkable for a single gas phase equilibrium adsorption. The adsorption and separation can be explained by wedge-like pores that are generated when microstructures are formed. Unfortunately, the new material can only be regarded as an intercalated compound and not as a microporous organic pillared silicate.

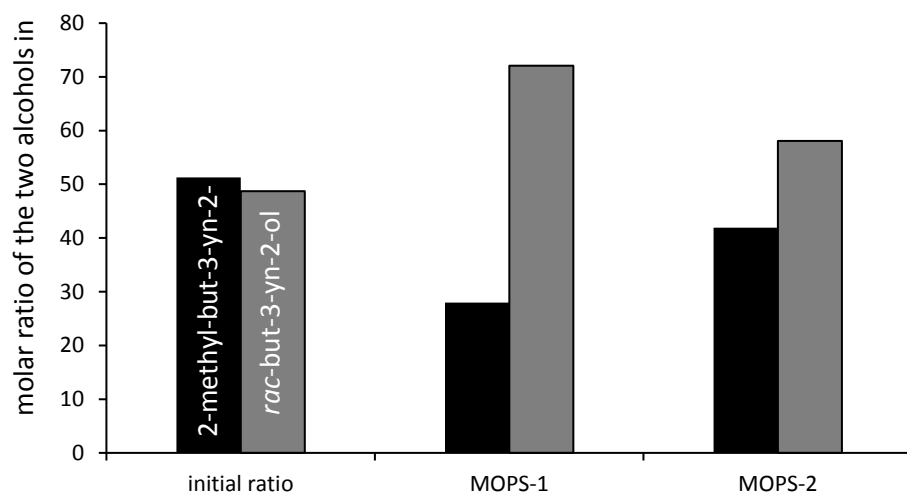


Figure 18: Size-selective adsorption of an equal mixture of 2-methyl-but-3-yn-2-ol and but-3-yn-2-ol. For the size-selective adsorption a molar ratio of 74.5:25.5 of but-3-yn-2-ol:2-methyl-but-3-yn-2-ol. For the enantioselective adsorption of a racemic mixture of R and S but-3-yn-2-ol a maximum ee of 8.2% could be achieved in the single equilibrium adsorption. (+)-Co(sep) preferred R-but-3-yn-2-ol and (-)-Co(sep) preferred the other enantiomer. This happened for pillar **9** intercalated into silicate with no layer charge reduction. The tighter the pillar is packed in the interlayer space the better seems to be the steric induction.

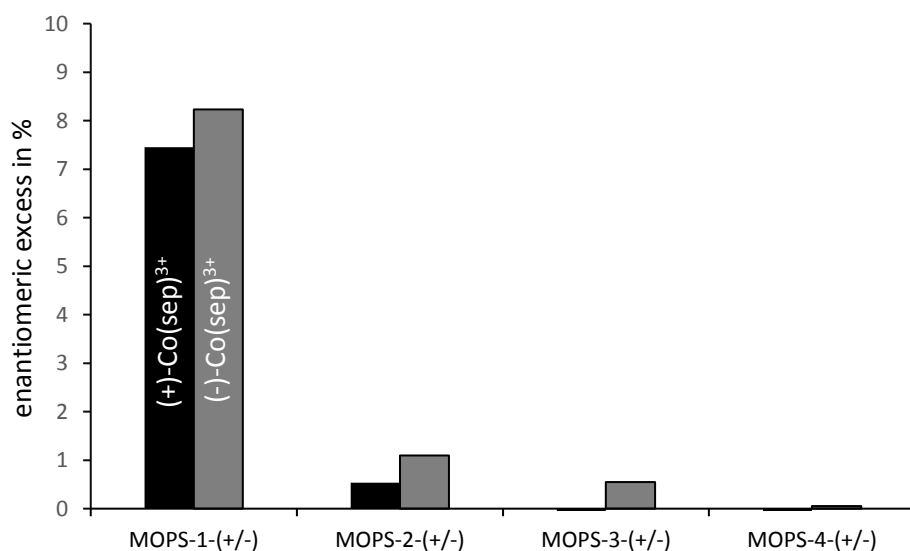


Figure 16: Enantioselective adsorption of a racemic mixture of R/S-but-3-yn-2-ol.

The whole concept looks very promising although a lot of work and effort have to be put into the research. For future work one should keep in mind that an organic cation carrying two

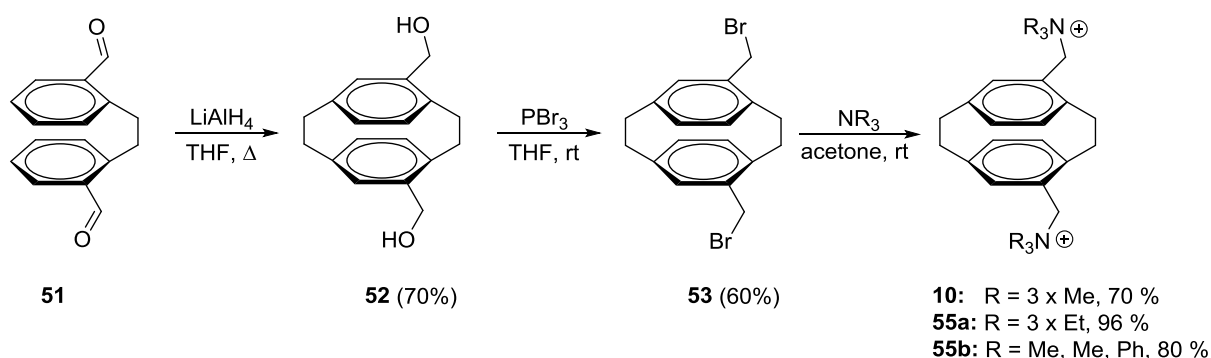
charges might not be suitable for the production of microporous organic pillared silicates, because the equivalent area of these pillar do not seemed to be small enough.

2 Zusammenfassung

In dieser Arbeit wurde eine neue Klasse der Hybridmaterialien vorgestellt, die mikroporösen organisch gepillarten Silikate oder kurz MOPS. Sie bestehen aus einem metallorganischen oder organischen Kation, welches in ein synthetisches Schichtsilikat eingelagert wurde. Das organische Kation wird durch einen Prozess, genannt "Pillaring", in dem Zwischenschichtraum des Silikats platziert. Die IUPAC definiert das Pillaring als "einen Prozess bei dem ein Schichtmaterial in thermisch stabiles, mikro- und/oder mesoporöses Material unter Beibehaltung seiner Schichtstruktur umgewandelt wird. ... Ein gepillartes Material besitzt folgende Eigenschaften: (i) Die Schichten sind vertical aufeinander abgestützt und behalten ihre Schichtstruktur nach Entfernung des Lösemittels bei; (ii) die minimale Vergrößerung des basalen Raums entspricht dem Durchmesser eines N_2 Moleküls, welches normalerweise für die Messung der Oberflächen und des Porenvolumens verwendet wird: 0.315-0.353 nm; (iii) der Pillar besitzt molekulare Dimensionen und ist lateral im Zwischenschichtraum mit molekularer Längenskala platziert; (iv) der Zwischenschichtraum ist porös und Molekülen mindestens so groß wie N_2 zugänglich; es existiert keine Obergrenze für die Größe der Poren. ... Für die Art des Pillars oder der Methode der Einlagerung existieren keine Einschränkungen." Aufgrund dieser Definition stellen MOPS eine Untergruppe von Einlagerungsverbindungen dar, deren Mikroporosität im Zwischenschichtraum liegen muss. Beweise dafür sind eine rationale Serie der d_{001} Linien und Physisorptionsmessungen. Ladungshomogenität ist eine Grundvoraussetzung, ebenso wie die Homogenität der generierten Mikroporen. Die Größe und Form der Mikroporen ist neben der Schichtladung, abhängig von der Größe, Form und Ladung des Pillars.

Manche Anstrengungen, ein organisches oder metallorganisches Molekül, welches den Ansprüchen eines hochgeladenen und sphärisch geformten Moleküls entspricht, zu synthetisieren verliefen ins Leere. Die Synthese der Käfigverbindung **7** war nicht erfolgreich. Eine Zersetzung des Startmaterials **19** war die einzige Beobachtung die getätigt werden konnte. Das kationische Halbaminale war höchstwahrscheinlich zu instabil um isoliert zu werden. Der Pillar **6** konnte erfolgreich synthetisiert werden, unglücklicherweise war die

Synthese trotz identischer Reaktionsbedingungen nicht reproduzierbar. Weitere Versuche endeten jeweils in einer Mischung des Mono- und Dikations, welche wir nicht im Stande waren zu trennen. Die Synthese der metallorganischen Pillars **5** und **6** schlugen ebenfalls fehl. Eine mögliche Erklärung dafür liegt in der fehlenden Elektronendichte am zentralen Cobaltion des Sandwichkomplexes. Dadurch konnten die wichtigen Intermediate **37** und **47**, zwei Sandwichkomplexe mit jeweils einer Aldehydfunktion an einem Ring, nicht synthetisiert werden. Trotz aller Enttäuschungen konnte pseudo-meta-Bis(5,12-(N,N,N-trimethylmethylenaminium))-[2.2]paracyclophanbromid neben einer Serie anderer Moleküle dieser Klasse von Pillars erfolgreich synthetisiert werden. Ausgehend des Aldehyds **51**, wurde **53** mittels Reduktion und darauffolgender nukleophilen Substitution synthetisiert. Mit **53** im Vorrat konnten eine Serie von Molekülen, durch eine einfache Substitution in einer Übernachtreaktion und der Verwendung unterschiedlicher tertiärer Amine, synthetisiert werden.



Schemata 19: Syntheseroute für Pillar **10**, **55a** und **55b**.

Diese Art von Pillar ist weiteres ideales Beispiel für die Modularität des kompletten Systems. Die Ladungsdichte eines Schichtsilikats kann durch die Schichtladungsreduzierung eingestellt werden, indem man sich in einer Kationenaustauschreaktion den Hofmann-Klemen-Effekt zu Hilfe nimmt. Dadurch kann die Größe der Mikroporen auf molekularer Ebene eingestellt werden. Der verwendete Pillar kann ebenfalls durch simplen Austausch des tertiären Amins verändert werden. Auf diese Weise ist ein fast unendlicher Pool an Variationen möglich.

Nach Einlagerung von Pillar **10** in einen Hektorit wurden jedoch keine Mikroporen generiert, wie durch Physisorptionsmessungen festgestellt wurde. Nichtsdestotrotz zeigte das neue Material in der Adsorption zweier sehr ähnlicher Alkohole, But-3-yn-2-ol und 2-Methyl-but-2-yn-2-ol, ein interessantes Adsorptionsverhalten. Ausgehend von einer molaren 48.7:51.3 Mischung wurde But-3-yn-2-ol mit einem Verhältnis von 72.0:28.0 besser adsorbiert als der größere Alkohol, was bemerkenswert für eine einzelne Adsorption im Gasequilibrium ist. Die

Adsorption und Auftrennung können durch keilförmige Poren erklärt werden, die sich ausbilden, wenn sich Mikrostrukturen formen. Unglücklicherweise kann das neue Material nur als Einlagerungsverbindung betrachtet werden und nicht als mikroporös organisch gepillartes Silikat. Mit den neu generierten MOPS konnten größenselektive und sogar zum ersten Mal enantioselektive Adsorptionen durchgeführt werden. Benutzt wurden dafür die gleichen Mischungen wie für den mit Pillar **10** gepillarten Hektorit.

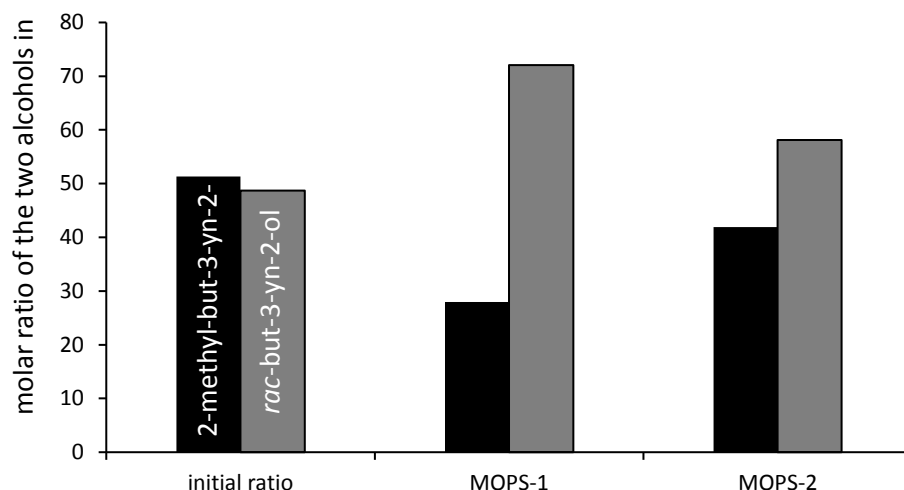


Abbildung 18: Größenselektive Adsorption einer ungefähr equimolaren Mischung von But-3-yn-2-ol und 2-Methyl-but-3-yn-2-ol.

Im Vergleich dazu konnten durch Einlagerung des chiralen metallorganischen Komplexes $\text{Co}(\text{sep})^{3+}$ in einen Stevensit Mikroporen generiert werden, wie durch Röntgenstreuung und Physisorptionsmessungen bestätigt wurde. Bei der größenselektiven Adsorption konnte ein molares Verhältnis von 74.5 zu 25.5 von But-3-yn-2-ol zu 2-Methyl-but-3-yn-2-ol erreicht werden. Bei der enantioselektiven Adsorption einer racemischen Mischung von R und S But-3-yn-2-ol wurde ein maximaler ee von 8.2% in einer einzelnen Adsorption im Gasequilibrium erreicht werden. Dabei wurde R-But-3-yn-2-ol bevorzugt von (+)-Co(sep) adsorbiert wohingegen (-)-Co(sep) das andere Enantiomer preferierte. Dieser Wert wurde für das mit Pillar 9 gepillarte Silikat ohne Schichtladungsreduktion erreicht. Je dichter der Pillar im

Zwischenschichtraum gepackt ist, desto stärker scheint die sterische Induktion zu sein.

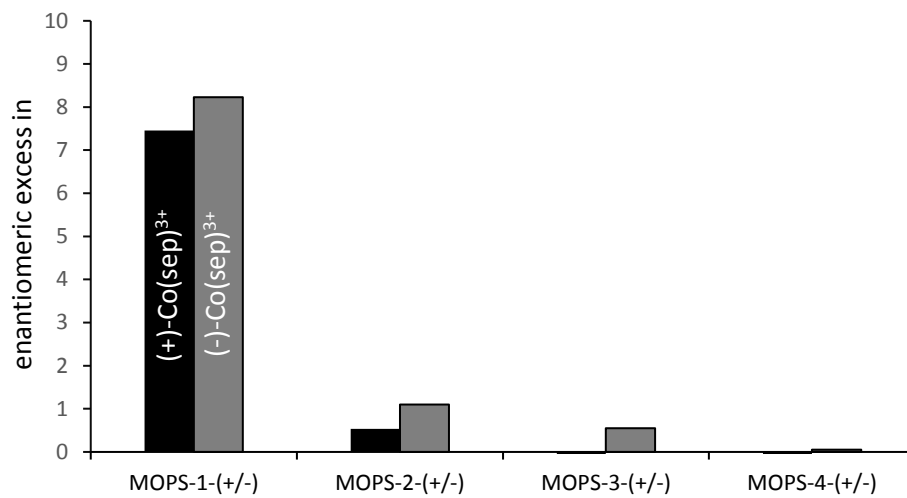


Abbildung 16: Enantioselektive Adsorption einer racemischen Mischung von R und S But-3-yn-2-ol.

Das gesamte Konzept ist sehr vielversprechend. Dennoch müssen viele Anstrengungen für deren Ausarbeitung unternommen werden. Bei zukünftigen Arbeiten muss unbedingt auf eine mit mindestens 3+ ausreichend große Ladung des organischen Kations geachtet werden um eine möglichst kleine äquivalente Fläche des Pillars zu erreichen.

D Experimental

1 General Information

NMR spectra were recorded on a Bruker DRX 500 - spectrometer (500 MHz ^1H -NMR, 126 MHz ^{13}C -NMR) or Bruker DRX 300 - spectrometer (300 MHz ^1H -NMR, 75,5 MHz ^{13}C -NMR). Chemical shifts were reported as δ in parts per million [ppm] relative to the signal of the appropriate solvent.⁶⁵ Spectra were evaluated in 1st order and coupling constants J are reported in Hertz [Hz]. Splitting patterns for the spin multiplicity are described in abbreviations: s = singlet, d = doublet, t = triplet, q = quartet, dd = doublet of doublet, ddd = doublet of doublet of doublet, dt = doublet of triplet, pt = pseudo triplet, m = multiplet.

Gas chromatography: Gas chromatograms were recorded on a Shimadzu GC-2010 using a chiral Lipodex E column (25 m) column under the following conditions: 0.5 μL injection volume, split 1:100, T_{inj} 250 $^{\circ}\text{C}$, constant flow of hydrogen carrier gas (1.2 mL/min = 40 cm/s), T_{det} 250 $^{\circ}\text{C}$; column temperature initially 40 $^{\circ}\text{C}$ (3 min) then raised to 120 $^{\circ}\text{C}$ (10 $^{\circ}\text{C}/\text{min}$). Quantities of but-3-yn-2-ol in the individual samples were determined by external calibration.

Column chromatography was performed using silica gel MN Kieselgel 60 (63 – 20 μm) from Macherey-Nagel. Solvents used as a mobile phase are announced specifically.

Thin liquid chromatography was performed using DC-Aluminiumplatten 60 F254 from Merck. Detection resulted from UV-irradiation at a wavelength of 254 nm or by using a KMnO_4 -solution as dyeing reagent (KMnO_4 (1 g); Na_2CO_3 (2 g); H_2O (100 mL)).

IR-spectra were recorded on a Spectrum One FT-IR-spectrometer from Perkin Elmer. Adsorptions are announced in wave numbers [cm^{-1}].

Ultrasound irradiation was performed in a SONOREX SUPER RK 106 from Bandelin.

Mass spectra were recorded on a Finnigan MAT 8500 using the MAT SS 300 data system with an ionization energy of 70 eV. The probes were measured with direct injection or by

pretreatment with a Hewlett-Packard 5890 Series II GC-unit. Relative intensities are announced in % based on the basis peak (100%).

High resolution mass spectra were recorded on a UPLC/Orbitrap MS Systems from Thermo Fisher Scientific (ESI).

Optical rotation measurements were performed on a Perkin Elmer Polarimeter 343 ($\lambda = 589$ nm).

Melting points were measured on a Büchi Melting Point M-565.

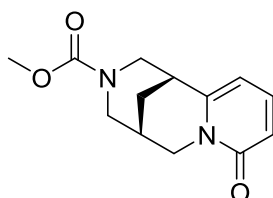
Chemicals: The solvents methanol, ethanol, 1-propanol, *iso*-propanol, ethyl acetate, *n*-hexane, diethyl ether, methyl *tert*-butylether, acetone, dichloromethane, tetrahydrofurane were purified by single distillation. All other solvents were used as received. Dry solvents were produced by the common methods according to literature.

All other reagents were used as received. If a further purification was necessary, it has been announced specifically

2 Synthesis of the organic compounds

For new compounds a full set of analytical data is given. The analytical data from compounds that are already known are compiled with literature and only a $^1\text{H-NMR}$ is given.

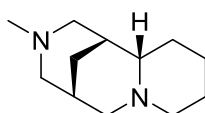
2.1 Synthesis of (-)-Methyl-(1R,9R)-6-oxo-7,11-diazatricyclo[7.3.1.0]tridecane [22]⁶



In a flame dried schlenk flask, cytosine and triethylamine were added to 80 mL of dry dichloromethane. The solution was immersed in an ice bath and methyl chloroformate was added dropwise over a period of 10 min. After additional stirring for an hour at 0°C and 3 hours at room temperature, the solvent was evaporated under reduced pressure. The residue was collected by ethylacetate and filtered over Celite to remove any solids. The filter cake was washed with ethylacetate and the solvent was then evaporated under reduced pressure. The product was purified by column chromatography over silica (DCM/MeOH 9/1) and received as colorless oil. (79 %)

$^1\text{H-NMR}$ (500 MHz, CDCl_3): δ = 1.90-2.05 (m, 2 H), 2.47 (br s, 1 H), 3.00 (m, 3 H), 3.45-3.63 (m, 3 H), 3.88 (dd, 1 H, J = 15.6, 6.3 Hz), 4.13 (d, 1 H, J = 15.3 Hz), 4.03-4.37 (m, 2 H), 6.06 (m, 1 H), 6.45 (dd, 1 H, J = 9.1, 1.2 Hz), 7.28 (dd, 1 H, J = 9.1, 6.9 Hz).

2.2 Synthesis of (+)-(1R,2S,9S)-11-Methyl-7,11-diazatricyclo[7..3.1.0]tridecane [24]⁶



A flame dried schlenk flask was charged with cytosine methylcarbamate, platinum(IV)-oxide and MeOH. The resulting stirred suspension was carefully refilled with argon 3 times before it

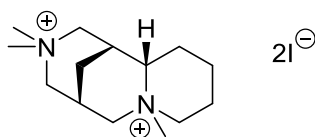
was backfilled with hydrogen via a hydrogen balloon attached to a septum. The black mixture was stirred vigorously for several hours. The completion of the reaction was determined via TLC (DCM/MeOH, 9/1). The solids were removed by filtration through Celite and the filter cake was washed 2 times with a mixture of dichloromethane and methanol (9/1). The Solvent was removed under reduced pressure to give the crude hydrogenation product as an off-white solid. (90 %)

$^1\text{H-NMR}$ (500 MHz, CDCl_3): δ = 4.76 (m, 1 H), 4.61 (d, 0.85 H, J = 14.0 Hz), 4.36 (d, 0.15 H, J = 14.0 Hz), 4.28 (d, 0.15 H, J = 13.0 Hz), 4.19 (d, 0.85 H, J = 13.0 Hz), 3.66 (s, 0.5 H), 3.60 (s, 2.5 H), 3.48–3.42 (m, 1 H), 3.06 (d, 0.85 H, J = 13.4 Hz), 3.00 (d, 0.15 H, J = 13.4 Hz), 2.94 (d, 0.15 H, J = 13.8), 2.86 (dd, 0.85 H, J = 13.8, 1.8 Hz), 2.79 (d, 1 H, J = 13.5 Hz), 2.46 – 2.30 (m, 2 H), 2.22 – 2.09 (m, 14H), 2.22 – 2.09 (m, 1 H), 2.02 – 1.72 (m, 5 H), 1.69–1.54 (m, 2 H).

A flame dried schlenk flask was charged with tetrahydrofurane und lithium aluminiumhydride. The resulting solution was immersed in an ice bath and a solution of crude hydrogenation product in tetrahydrofurane was added dropwise over 10 min at 0 °C. The suspension was warmed to room temperature and then refluxed for 16 h. After cooling the mixture again to 0 °C, ethyl ether was added. The rest of lithium aluminiumhydride was then quenched very slowly with $\text{NaSO}_4 \cdot 10\text{H}_2\text{O}$, which caused enormous evolution of hydrogen gas. The mixture was stirred furthermore until no evolution of hydrogen gas could be observed. The suspension was then filtered through Celite to remove any solids. After evaporation of the solvent under reduced pressure, the crude product was purified by Kugelrohr distillation at 150-160 °C and received as a colorless oil. (71 %)

$^1\text{H-NMR}$ (500 MHz, CDCl_3): δ = 1.20-1.33 (m, 2 H), 1.42-1.60 (m, 5 H), 1.62-1.77 (m, 3 H), 1.78-1.83 (m, 1 H), 1.87 (d, 1 H, J = 11.0 Hz), 1.94 (dd, 1 H, J = 11.3, 3.0 Hz), 2.12 (s, 3 H), 2.12-2.17 (m, 1 H), 2.21 (d, 1 H, J = 11.3 Hz), 2.79-2.90 (m, 2 H), 2.92-3.01 (m, 2 H).

2.3 Synthesis of (+)-(1R,2S,9S)-11-Methyl-7,11-diazatricyclo[7.3.1.0]tridecane-(1R,5S,11aS)-3,3,7-trimethyldodecahydro-1,5-methanopyrido[1,2-a][1,5]diazocine-3,7-dium [6]

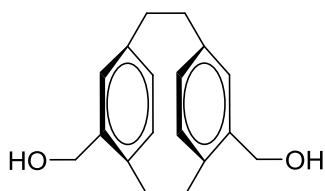


A flame dried bomb tube was charged with **24** (58 mg, 0.3 mmol, 1.0 eq), methyl iodide (0.16 mL, 2.5 mmol, 8.0 eq) and methanol (6 mL). The mixture was heated at 90 °C for 24 h. Then it was cooled to room temperature and the solvent was removed under reduced pressure. The yellow brown residue was recrystallized in 5 mL chloroform and half of a pipette of methanol to give a yellow-brown solid (43 %).

¹H-NMR (500 MHz, D₂O): δ = 1.51-1.64 (m, 2 H), 1.73-1.99 (m, 5 H), 2.47-2.55 (m, 1 H), 2.66 (d, 1 H, J = 10.5 Hz), 2.81 (d, 1 H, J = 9.7 Hz), 3.12 (td, 1 H, J = 24.5, 12.3, 3.5), 3.20 (dd, 1 H, J = 13.2, 2.9 Hz), 3.28 (s, 3 H), 3.33 (s, 3 H), 3.35 (s, 3 H), 3.36-3.46 (m, 4 H), 3.50 (d, 1 H, J = 14.9 Hz), 3.92 (m, 1 H), 4.00 (m, 1 H).

¹³C-NMR (500 MHz, D₂O) δ = 21.4, 21.9, 22.4, 24.5, 27.0, 28.5, 48.8, 56.4, 58.3, 58.5, 58.8, 59.3, 62.4, 67.9.

2.4 Synthesis of 4,13-Hydroxymethylen-[2.2]paracyclophan [52]⁶¹

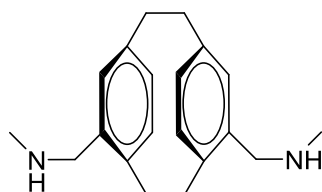


A flame dried schlenk flask was charged with 4,13-Formyl-[2.2]paracyclophan (1.0 g, 3.8 mmol, 1.0 eq), provided by the group of *Greiner*, and 60 mL of dry tetrahydrofurane. The solution was immersed in an ice bath and cooled to 0 °C. LiAlH₄ (3.18 g, 8.4 mmol, 2.2 eq) was slowly added in portions. The reaction mixture was then stirred for 3 h at room temperature.

The excessive LiAlH_4 was quenched with saturated solution of NH_4Cl until no more gas evolution was observed. The product was then extracted 3 times with ethyl acetate. The organic phases were combined and dried over MgSO_4 . The solvent was removed under reduced pressure and the residue was purified by column chromatography (n-hexane/ethyl acetate, 1/1) to the product as a white solid (715 mg, 70 %).

$^1\text{H-NMR}$ (500 MHz, CDCl_3): δ = 1.58 (s, 2 H), 2.84-2.91 (m, 2 H), 2.96-3.03 (m, 2 H), 3.04-3.12 (m, 2 H), 3.35-3.43 (m, 2 H), 4.39 (dd, 2 H, J = 12.9, 4.5 Hz), 4.70 (dd, 2 H, J = 12.9, 5.1 Hz), 6.40 (dd, 2 H, J = 7.7, 1.7 Hz), 6.47 (m, 2 H), 6.59 (d, 2 H, J = 7.7 Hz).

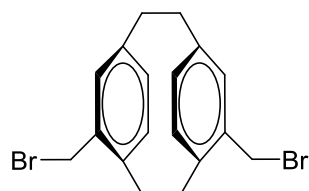
2.5 Synthesis of pseudo-meta-bis(5,12-(N-Methylaminomethylen))-[2.2]paracyclophan [54]⁶⁶



A 50 mL round-bottom flask was charged with 5 mL methanol, 5,12-Formyl-[2.2]paracyclophan (528 mg, 2.0 mmol, 1.0 eq) and methylamine (aq 40 %, 570 μL , 8.0 mmol 4.0 eq). The Solution was stirred for 30 hours at room temperature. Then the solution was cooled down to 0 °C and NaBH_4 (151 mg, 4.0 mmol, 2.0 eq) were added carefully. The reaction was allowed to warm to room temperature and was stirred for another three hours. The solvent was evaporated and 5 mL of dichloromethane and water were added. The product was extracted into the organic phase, which was then washed saturated solutions of NaCl and Na_2CO_3 . The organic phase was dried over Na_2SO_4 and the solvent was removed in vacuo. Purification followed via column chromatography over silica ($\text{CHCl}_3/(\text{MeOH}/\text{NH}_3)$, 9/1(3/1)). The product was obtained as a white solid.

$^1\text{H-NMR}$ (500 MHz, CDCl_3): $\delta = 1.35$ (s, 2 H), 2.40 (s, 6 H), 2.76-2.88 (m, 2 H), 2.92-3.08 (m, 4 H), 3.31-3.41 (m, 2 H), 3.41 (d, 2 H, $J = 13.1$ Hz), 3.75 (d, 2 H, $J = 13.1$ Hz), 6.30 (d, 2 H, $J = 1.7$ Hz), 6.35 (d, 2 H, $J = 7.7$), 6.57 (dd, 2 H, $J = 7.7, 1.7$ Hz).

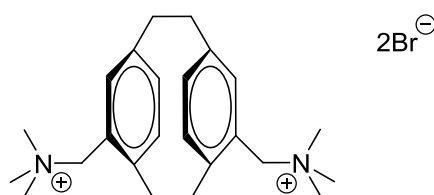
2.6 Synthesis of pseudo-*meta*-bis(5,12-brommetylen)-[2.2]paracyclophan [53]^{61,67}



A flame dried schlenk flask was charged with 5,12-Hydroxymethylen-[2.2]paracyclophan (715 mg, 2.7 mol, 1.0 eq) and 25 mL of tetrahydrofurane. The reaction mixture was immersed in an ice bath, while adding PBr_3 (1.58 g, 5.9 mmol, 2.2 eq) dropwise. The mixture was allowed to warm to room temperature and was stirred for another 12 h. The completion of the reaction was determined via TLC. The excessive PBr_3 was quenched with water and the solution was extracted 4 times with 200 mL of ethyl acetate. After drying the solvent over MgSO_4 , it was removed under reduced pressure and purified by column chromatography (n-hexane/chloroform, 3/1) to give the product as a white solid (640 mg, 60 %).

$^1\text{H-NMR}$ (500 MHz, CDCl_3): $\delta = 2.93$ -3.01 (m, 2 H), 3.02-3.09 (m, 2 H), 3.40-3.52 (m, 4 H), 4.21 (d, 2 H, $J = 10.4$ Hz), 4.48 (d, 2 H, $J = 10.4$ Hz), 6.38-6.42 (m, 4 H), 6.56 (d, 2 H, $J = 7.7$ Hz).

2.7 Synthesis of pseudo-*meta*-bis(5,12-(*N,N,N*-trimethylmethylenaminium))- [2.2]paracyclophan dibromide [10]⁶¹



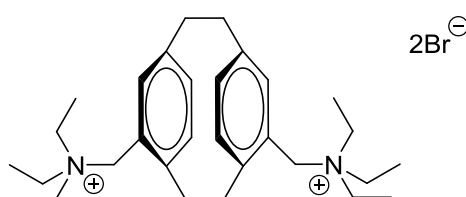
In a 100 mL flask 5,12-Brommethylen-[2.2]paracyclophan (700 mg, 1.78 mmol, 1 eq) was dissolved in 20 mL of acetone. After adding 9 mL of an aqueous solution (50 %) of Trimethylamine, the reaction was stirred for 24 h at room temperature. A white solvent precipitated. The solvent was removed under reduced pressure and resolved in hot methanol which was then cooled to room temperature and overlaid with chloroform. The solvent was removed carefully and the solid was dried under reduced pressure. This crystallization method was repeated three times to receive the pure product as a white solid. (456 mg, 68 %)

$^1\text{H-NMR}$ (500 MHz, D_2O): δ = 2.90 (s, 18 H), 3.05 (m, 8 H), 3.46 (m, 2 H), 4.25 (d, 2 H, J = 13.0 Hz), 4.45 (d, 2 H, J = 13.0 Hz), 6.53 (m, 6 H).

$^{13}\text{C-NMR}$ (500 MHz, D_2O) δ = 32.6, 33.6, 51.8, 51.8, 51.8, 66.9, 126.6, 133.5, 134.9, 140.1, 141.3, 141.4.

ESI-MS $[\text{M-H}^+]$ $\text{C}_{24}\text{H}_{36}\text{N}_2^{2+}$: 352.3

2.8 Synthesis of pseudo-meta-bis(5,12-(N,N,N-Triethylmethylenaminium)) [2.2]paracyclophan dibromide [55a]⁶¹



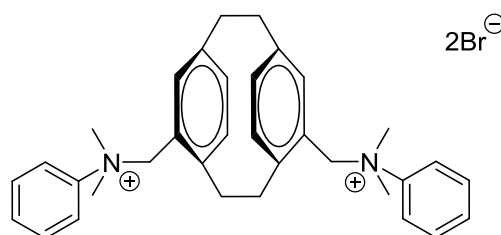
In a 100 mL flask 5,12-Brommethylen-[2.2]paracyclophan (200 mg, 0.5 mmol, 1 eq) was dissolved in 20 mL of acetone. After adding 2.25 mL of triethylamine, the reaction was stirred for 24 h at room temperature. A white solvent precipitated. The solvent was decanted carefully and the solid was dried under vacuum. The product was purified by crystallization in methanol and chloroform, and received as a white solid. (292 mg, 96 %)

$^1\text{H-NMR}$ (500 MHz, D_2O): $\delta = 1.31$ (t, 18 H, $J = 7.3$ Hz), 3.05-3.24 (m, 18 H), 3.51 (m, 2 H), 4.33 (s, 4 H), 6.67-6.78 (m, 6 H).

$^{13}\text{C-NMR}$ (500 MHz, D_2O) $\delta = 7.24, 33.26, 33.60, 52.47, 58.67, 126.13, 133.75, 134.69, 138.66, 141.31, 141.40$.

ESI-MS [M-H^+] $\text{C}_{30}\text{H}_{48}\text{N}_2^{2+}$: 433.3

2.9 Synthesis of pseudo-meta-bis(5,12-(*N,N,N*-dimethylphenylmethylenaminium))- [2.2]paracyclophan dibromide [55b]⁶¹



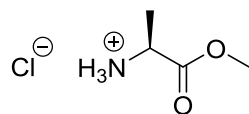
In a 100 mL flask 5,12-Brommetylen-[2.2]paracyclophan (200 mg, 0.5 mmol, 1 eq) was dissolved in 10 mL of acetone. After adding Me_2NPh (642 μL , 5.07 mmol, 10.0 eq) the reaction was stirred for 24 h at room temperature. A white solvent precipitated. The solvent was decanted carefully and the solid was washed with 10 ml of acetone. The product was purified by crystallization in methanol and chloroform, and received as a white solid. (258 mg, 80 %)

$^1\text{H-NMR}$ (500 MHz, DMSO-d_6): $\delta = 2.65 - 2.75$ (m, 4 H), 2.87-3.10 (m, 4 H), 3.46 (s, 6 H), 3.49 (s, 6 H), 4.81 (m, 4 H), 6.06 (s, 2 H), 6.36 (d, 2 H, $J = 7.5$ Hz), 6.43 (d, 2 H, $J = 7.5$ Hz), 7.40-7.67 (m, 10H).

$^{13}\text{C-NMR}$ (500 MHz, D_2O) $\delta = 32.20, 33.38, 51.84, 52.89, 71.57, 120.93, 126.41, 129.79, 130.34, 133.22, 134.83, 139.49, 140.84, 141.59, 143.44$.

ESI-MS [M-H⁺] C₃₄H₄₀N₂²⁺: 475.4

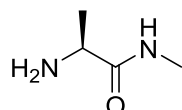
2.10 Synthesis of (L)-alanine methylester hydrochloride [30]⁴⁶



A 1 L round flask was charged with 600 mL methanol and L-alanine (10.0 g, 114 mmol, 1.0 eq) and was cooled to 0 °C. While stirring the solution SOCl₂ (32.9 mL, 454 mmol, 4.0 eq) was added carefully and dropwise. The ice bath was removed and the solution stirred for another 18 h. Then the solvent was removed under vacuum. The raw product was washed several times with 100 mL of diethylether. Further purification of the white solid was not needed. (15.7 g, >99%)

¹H-NMR (500 MHz, D₂O): δ = 1.53 (d, 3 H, J = 7.3 Hz), 3.81 (s, 3 H), 4.17 (q, 1 H, J = 7.3).

2.11 Synthesis of (L)-alanine methylamide [31]⁴⁶



In a 500 mL round flask (S)-alanine methylester hydrochloride was dissolved in a solution of methylamine (30%, 77.4 mL, 627 mmol) in ethanol. The solution was stirred overnight and the solvent was subsequently removed under vacuum. The raw product was washed several times with diethyl ether to remove the remaining methylamine. The remaining white solid was dried under vacuum recrystallized in a mixture of ethanol and hexane. (12.4 g, 89.9 mmol, 99%).

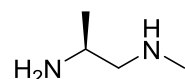
¹H-NMR (500 MHz, D₂O): δ = 1.47 (d, 3 H, J = 7.0 Hz), 2.75 (s, 3 H), 4.01 (q, 1 H, J = 7.0).

The crude product was dissolved in 25 mL of ethanol. Then Na₂CO₃ (21.0 g, 198 mmol, 2.2 eq) was added and the solution was heated under reflux for 2-3 h. The suspension was filtered

and the solvent of the filtrate was removed. The pure product was received as white solid. (5.2 g, 51 mmol, 56 %)

$^1\text{H-NMR}$ (500 MHz, D_2O): $\delta = 1.33$ (dd, 3 H, $J = 7.0, 1.5$ Hz), 1.42 (s, 2 H), 2.81 (d, 3 H, $J = 5.0$ Hz), 3.49 (q, 1 H, $J = 7.0$).

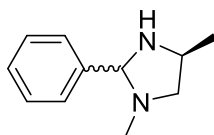
2.12 Synthesis of (S)- N^1 -methylpropane-1,2-diamine [32]⁴⁶



A flame dried 250 mL schlenk flask was charged with 100 mL THF and LiAlH_4 (4.82 g, 127 mmol, 2.5 eq). The suspension was immersed in an ice bath. While stirring, a solution of the amide 31 (5.18 g, 50.7 mmol, 1 eq) in 10 mL THF was added dropwise. Subsequently the reaction mixture was stirred and heated under reflux for 18 h. Then the reaction was slowly cooled to room temperature. 50 mL of diethylether were added to dilute the mixture and $\text{Na}_2\text{SO}_4 \cdot 10\text{H}_2\text{O}$ were added portionwise until no gas evolution could be observed, controlled by a bubble counter. The Reaction mixture was filtered over celite and the filter cake was washed 3 times with ca. 20 mL THF. Then the solvent was removed under vacuum and furthermore the crude product was purified by column chromatography ($\text{CH}_2\text{Cl}_2/(\text{MeOH}:\text{NH}_3)$, 7/1(9:1)). The product was received as colorless oil. (2.41 g, 54 %)

$^1\text{H-NMR}$ (500 MHz, CDCl_3): $\delta = 1.06$ (d, 3 H, $J = 6.4$ Hz), 2.35 (dd, 1 H, $J = 11.7, 8.4$ Hz), 2.43 (s, 3 H), 2.53 (d, 1 H, $J = 11.7, 4.2$ Hz), 2.98 (m, 1 H).

2.13 Synthesis of (4S)-1,4-dimethyl-2-phenylimidazolidine [57]



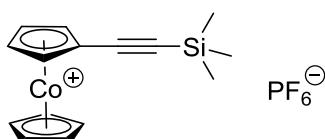
In a 100 mL round-bottom flask the diamine **32** (1.0 g, 11.3 mmol, 1.0 eq) and benzaldehyde (1.15 mL, 11.3 mmol, 1.0 eq) were dissolved in 40 mL of ethanol. After stirring the reaction mixture for 20 h at room temperature, the solvent was removed under vacuum. The crude product was purified by Kugelrohrdestillation at 50 °C under high vacuum and received as a colorless oil. (633 mg, 32%)

$^1\text{H-NMR}$ (500 MHz, CDCl_3): δ = 1.19 (d, 1.5 H, J = 6.4 Hz), 1.29 (d, 1.5 H, J = 6.4 Hz), 1.93 (s, 1 H), 2.08 (t, 0.5, J = 8.7 Hz), 2.19 (s, 3 H), 2.61 (t, 0.5 H, J = 8.7 Hz), 2.97 (dd, 0.5 H, J = 9.0, 3.7 Hz), 3.46 (m, 1 H), 3.61-3.70 (m, 0.5 H), 3.97 (s, 1 H), 7.28-7.38 (m, 3 H), 7.47 (dd, 2 H, J = 9.5, 7.8 Hz).

$^{13}\text{C-NMR}$ (500 MHz, CDCl_3): δ = 21.54, 22.05, 38.57, 38.78, 51.59, 52.05, 62.35, 64.05, 84.23, 85.80, 127.57, 127.61, 128.39, 128.43, 128.56, 140.15, 140.70.

ESI-MS $[\text{M-H}^+]$ $\text{C}_{11}\text{H}_{16}\text{N}_2$: 175.12292.

2.14 Synthesis of (n5-Cyclopentadienyl)[n4-(exo)-1,3-cyclopentadiene]cobalt(I) and ((Trimethylsilyl) ethynyl)-cobaltocenium Hexafluorophosphate [**35**]⁵⁰



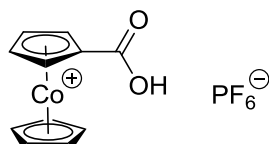
A flame dried Schlenk flask was charged 80 mL dry THF and (trimethylsilyl)acetylene (970 μL , 6.8 mmol, 1.14 eq). The solution was cooled down to -15 °C and a $n\text{BuLi}$ solution (2.52 mL, 2.5 M, 6.3 mmol, 1.05 eq) was added carefully. After stirring for 45 min, Cobaltocenium Hexafluorophosphate (2.0 g, 5.98 mmol, 1 eq) was added portionwise. While stirring the mixture for 30 min, the cooling bath was removed and the reaction temperature slowly raised

to room temperature. The color of the solution changed from yellow over orange to red due to the nucleophilic addition. The reaction mixture was then sonicated for another 15 min at room temperature, giving a homogeneous dark red solution. Subsequently, the solvent was removed in vacuo, followed by a solid-phase extraction over several cycles using 120 mL dry hexane under argon. The hexane was then removed in vacuo and stored for further workup process from the final product. After removing the volatiles the intermediate was obtained as a dark red solid (95%, 1.63 g, 5.68 mmol). The intermediate can be used without further purification.

A flame dried Schlenk flask equipped with a reflux condenser was charged, under argon at room temperature and excluding light, with 60 mL of dry dichloromethane, the intermediate (1.63 g, 5.68 mmol, 1.0 eq) and triphenylcarbenium hexafluorophosphate. The reaction mixture was stirred for 10 min at room temperature and the previously collected 120 mL of hexane were added to the yellow brown mixture. The product precipitated during the next 20 min while stirring was continued. Subsequently, the precipitate was filtered off using a Büchner funnel and then washed with three portions of diethyl ether, two portions of cold water and again with three portions of diethyl ether. The product was received as an amber powder after drying in vacuo. (69 %, 1.68 g, 3.9 mmol).

$^1\text{H-NMR}$ (500 MHz, CD_3CN): δ = 0.27 (s, 9 H), 5.64-5.68 (m, 7 H), 5.84 (pt, 2 H, J = 1.9 Hz).

2.15 Synthesis of Cobaltocenium carboxylic acid hexafluorophosphate [36]⁵⁰

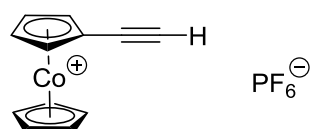


A 100 mL round-bottom flask was charged with 35 (1.0 g, 2.32 mmol, 1 eq), 18 mL of acetonitrile and sodium fluoride (99.5 mg, 2.37 mmol, 1.02 eq). Then 35 mL of an aqueous solution of potassium permanganate (991.6 mg, 6.28 mmol, 2.7 eq) were added to the amber solution. While vigorous stirring the solution was refluxed for 2 h. After cooling the mixture to room temperature it was filtered through a paper filter resulting in a yellow filtrate and

manganese dioxide. The precipitate was washed two times, once with hot water and once with hot acetonitrile using ultra sound. The collected aqueous solutions were concentrated to 10 mL approximately. Subsequently, hexafluorophosphoric acid (485 μ L, 55 % aq, 3.0 mmol, 1.3 eq) was added to the concentrated solution and the product crystallized in a refrigerator overnight. The yellow product was filtered off over a Büchner funnel and washed two times with ice water and two times with diethyl ether. The product was dried in vacuo to receive a yellow solid. (753 mg, 1.99 mmol, 85 %)

$^1\text{H-NMR}$ (500 MHz, CD_3CN): δ = 5.75 (s, 5 H), 5.79 (pt, 2 H, J = 2.1 Hz), 6.09 (pt, 2 H, J = 2.1 Hz).

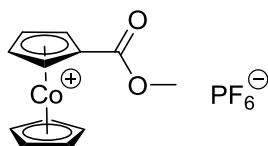
2.16 Synthesis of Ethynylcobaltocenium Hexafluorophosphate [39]⁵⁰



A 100 mL round-bottom flask was charged with 35 (815 mg, 1.89 mmol, 1.0 eq), 25 mL of an acetonitrile/water mixture (3/2, v/v) and sodium fluoride (86.4 mg, 2.1 mmol, 1.1 eq). The solution was stirred and refluxed for 2 h, and furthermore stirred overnight at room temperature. The solution was filtered to remove the dark solid byproduct, which was washed with acetonitrile several times. The collected aqueous phases were concentrated under vacuo until all of the acetonitrile has been removed. Thereby, the product started to precipitate. The solution was further concentrated until the total volume of it was approximately 5 mL. Hot acetonitrile was added dropwise to the mixture until all of the product has been redissolved. Then hexafluorophosphoric acid (331 μ L, 55 % aq, 2.06 mmol, 1.09 eq) was added and the acetonitrile was evaporated again. The product slowly started to crystallize. Crystallisation was completed by immersing the mixture in an ice bath for several hours. The product was filtered off over a Büchner funnel, washed several times with diethyl ether and dried in vacuo. The product was received as a yellow-brown powder. (673 mg, 1.56 mmol, 82 %)

$^1\text{H-NMR}$ (500 MHz, CD_3CN): δ = 3.72 (s, 1 H), 5.69 (pt, 2 H, J = 2.1 Hz), 5.70 (s, 5 H), 5.91 (pt, 2 H, J = 2.1 Hz).

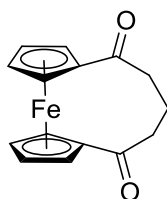
2.17 Synthesis of Cobaltocenium carboxylic acid methyl ester hexafluorophosphate [37]⁶⁸



A 50 mL round-bottom flask was charged with cobaltocenium carboxylic acid hexafluorophosphate (300 mg, 0.8 mmol, 1 eq) and 10 mL of methanol. While stirring, SOCl_2 (350 μL , 4.8 mmol, 6 eq) was slowly added dropwise. After adding the reagent the solution was stirred at room temperature overnight. Then the solvent was removed in vacuo. The crude product was purified by column chromatography over alumina using a acetonitrile/diethyl ether mixture (3/1). The product was then eluted with water. After concentrating the combined aqueous phases, an equimolar amount of hexafluorophosphoric acid (w 55 %) was added dropwise to precipitate the product. It was then filtered off over a Büchner funnel and dried in vacuo. The product was obtained as a yellow powder. (245 mg, 0.63 mmol, 78 %)

$^1\text{H-NMR}$ (500 MHz, CD_3CN): δ = 3.90 (s, 3 H), 5.74 (s, 5 H), 5.80 (pt, 2 H, J = 2.0 Hz), 6.10 (pt, 2 H, J = 2.0 Hz).

2.18 Synthesis of 1,5-(Ferrocen-1,10-diyl)pentan-1,5-dione [58]^{43e}



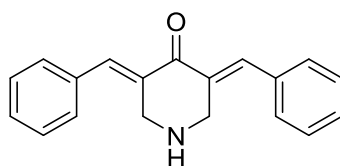
A flame dried 500 mL Schlenk flask was charged with 150 mL anhydrous dichloromethane and acetylferrocene (10.0 g, 43.8 mmol, 1.0 eq). Then a solution of chlorpropionyl chlorid (8.60 g, 65.7 mmol, 1.5 eq) was added. The mixture was cooled down to 0 °C and AlCl₃ (17.5 g, 131 mmol, 3.0 eq) was slowly added portionwise over a period of one hour. While stirring the reaction mixture for 1.5 h the temperature was kept at 0 °C. Completion of the reaction was determined via TLC. The suspension was then drained onto ~300 g of crushed ice. When the ice was completely melted, the phases were separated and the aqueous phase was extracted with dichloromethane three times. The collected organic phases were first washed four times with 10 % aq NaOH, then two times with water and dried over Na₂SO₄. The solvent was evaporated to receive the crude product 1-acetyl-1'-(3-chloropropionyl)ferrocene (13.7 g, 98 %). The product was used in the next step without any further purification.

¹H-NMR (500 MHz, CDCl₃): δ = 2.32 (s, 3 H), 3.09 (t, 2 H, J = 6.4 Hz), 3.87 (t, 2 H, J = 6.4 Hz), 4.51 (t, 2 H, J = 1.9 Hz), 4.52 (t, 2 H, J = 1.9 Hz), 4.76 (t, 2 H, J = 1.9 Hz), 4.78 (t, 2 H, J = 1.9 Hz).

A 500 mL round-bottom flask was charged with 150 mL of methanol and the crude product from the first step (13.7 g, 42.8 mmol). 10 % aq NaOH (70 mL, 174 mmol) was added to the solution. The reaction as refluxed for 30 min. Afterwards the reaction mixture was cooled down to 0 °C. The precipitate was filtered off, washed with water and dried in vacuo. The diketone was received as orange-red crystals. (11.2 g, 39.7 mmol, 93 %)

¹H-NMR (500 MHz, CDCl₃): δ = 2.40-2.58 (m, 6 H), 4.54 (t, 4 H, J = 2.0 Hz), 4.80 (t, 4 H, J = 2.0 Hz).

2.19 Synthesis of (3E,3E)-3,5-dibenzylidenpiperidin-4-on [16]³⁷

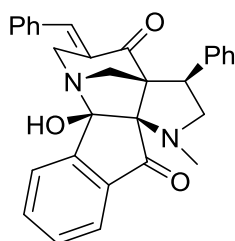


A 100 mL round-bottom flask was charged with 4 mL of pure acetic acid and piperidin-4-on (135 mg, 0.88 mmol, 1.0 eq). While stirring, HBr was added carefully dropwise until all of the

starting material was dissolved. Afterwards, benzylic aldehyde (0.2 mL, 1.75 mmol, 2.0 eq) were dropped into the solution. After stirring for 24 h a yellow suspension was formed. The mixture was filtered over a Büchner funnel and the precipitate was washed once with ethanol and once with diethyl ether. After drying in vacuo, the product was obtained as yellow solid. (220 mg, 0.8 mmol, 91 %)

$^1\text{H-NMR}$ (500 MHz, $\text{DMSO-}d_6$): δ = 4.52 (s, 4 H), 7.47-7.57 (m, 10 H), 7.90 (s, 2 H), 9.21 (s, 1 H, D_2O exchangeable).

2.20 Synthesis of 2-Hydroxy-11-methyl-13-phenyl-16-[(E)-phenyl-methylidene]-1,11-diazapentacyclo[12.3.1.0^{2,10}.0^{3,8}.0^{10,14}]octadeca-3(8),4,6-triene-9,15-dione [19]³⁷



A flame dried 100 mL Schlenk flask was charged with 10 mL Methanol, sarcosine (204 mg, 2.27 mmol, 1.0 eq), ninhydrin (404 mg, 2.27 mmol, 1.0 eq) and dibenzylidenpiperidinon (626 mg, 2.27 mmol, 1.0 eq). The reaction mixture was stirred and refluxed for one hour. The progress of the reaction was determined via TLC. After cooling the reaction to room temperature, the brown-red solution was poured into water. The suspension was filtered over a Büchner funnel and washed two times with water. Purification from the crude product followed via crystallization in ethyl acetate to obtain a yellow solid. (688 mg, 1.5 mmol, 67 %)

$^1\text{H-NMR}$ (500 MHz, CDCl_3): δ = 2.26 (s, 3 H), 2.70 (d, 1 H, J = 12.7 Hz), 3.43 (d, 1 H, J = 17.4 Hz), 3.74 (dd, 1 H, J = 17.4, 2.5 Hz), 3.81 (t, 1 H, J = 10.3 Hz), 3.93-3.99 (m, 2 H), 4.87 (dd, 1 H, J = 10.1, 5.4 Hz), 6.79 (d, 2 H, J = 7.0 Hz), 7.10 (s, 1 H), 7.14-2-26 (m, 5 H), 7.32 (t, 2 H, J = 7.5 Hz), 7.40-7-46 (m, 3 H), 7.52 (d, 1 H, J = 7.7 Hz), 7.67 (d, 1 H, J = 7.7 Hz).

3 Adsorption experiments

3.1 Synthesis of the MOPS

The stevensite $[\text{Na}_{0.47(3)}]^{inter}[\text{Mg}_{2.59(5)}\text{Li}_{0.17(3)}]^{oct}[\text{Si}_4]^{tet}\text{O}_{10}\text{F}_2$ used was synthesized via melt synthesis.⁷⁰ For pillaring, the hectorites (100 mg) were treated hydrothermally four times for 12 h at 60 °C with 18 mg of cobalt sepulchrate trichloride, (-)-Co(sep)Cl₃ or (+)Co(sep)Cl₃ (sep = C₁₂H₃₀N₈ = 1,3,6,8,10,13,16,19-octaazabicyclo[6.6.6]-eicosane)⁶⁹ in 5 mL H₂O.

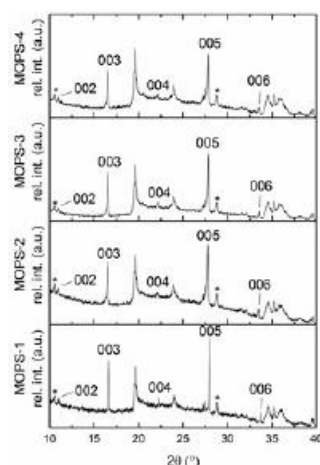


Figure 17: Powder X-ray diffraction pattern of MOPS-1 to MOPS-4 from 10-40° 2 θ ; asterisks mark a protoamphibole impurity phase.

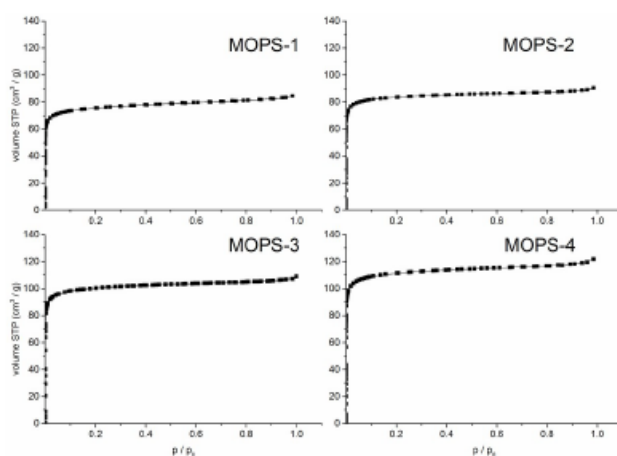


Figure 18: Physisorption isotherms Ar/Ar(I) at 87.35 K for MOPS-1 to MOPS-4 (linear scale).

For pillaring, the hectorites (100 mg) were treated hydrothermally four times for 12 h at 60 °C with 20 mg of pseudo-meta-bis(5,12-(N,N,N-trimethylmethylenaminium))- [2.2]paracyclophan dibromide in 5 mL H₂O.

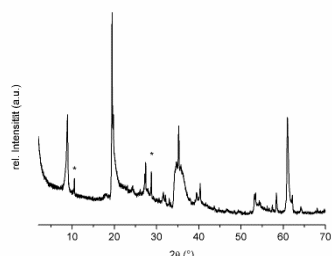


Figure 19: Powder X-ray diffraction pattern of MOPS from 10-40° 2 θ ; asterisks mark a protoamphibole impurity phase.

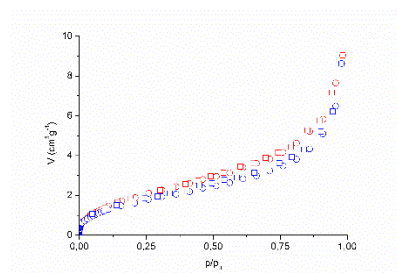


Figure 20: Physisorption isotherms Ar/Ar(I) at 87.35 K for MOPS (linear scale).

3.2 Adsorption of a mixture of 2-methyl-but-3-yn-2-ol and *rac*-but-3-yn-2-ol

The MOPSS pillared with (+)-Co(sep)³⁺⁷⁰ and pseudo-meta-bis(5,12-(N,N,N-trimethylmethylenaminium))- [2.2]paracyclophan were heated at 100 °C under high vacuum (10⁻⁹ bar) for 24 h, cooled and transferred to an argon glove box. There, three 10 mg samples of each MOPSS were weighed into open Eppendorf plastic vials (1.5 mL) which were placed in a horizontally adjusted 50 mL Schlenk tube together with an open glass weighing tube containing 300 μ L of a mixture of 153 μ L 2-methyl-but-3-yn-2-ol and 147 μ L *rac*-but-3-yn-2-ol to secure a saturated atmosphere with a molar ratio of 51.3:48.7. The Schlenk tube was stoppered and kept at 4 °C for 48 h. Then it was connected to an argon line and after removal of the 2-methyl-but-3-yn-2-ol / but-3-yn-2-ol source the sample vials were each treated with

500 μL of dry acetone p.a.. The vials were sealed, vortexed for 1 min, treated with a cooled ultrasonic bath for 30 min to desorb the alcohols from the inorganic material, and centrifuged. The acetone extracts were analysed by GC-FID on a Shimadzu GC-2010 equipped with a chiral Lipodex E column (25 m) under the following conditions: 0.5 μL injection volume, split 1:100, T_{inj} 250 $^{\circ}\text{C}$, constant flow of hydrogen carrier gas (1.2 mL/min = 40 cm/s), T_{det} 250 $^{\circ}\text{C}$; column temperature initially 40 $^{\circ}\text{C}$ (3 min) then raised to 120 $^{\circ}\text{C}$ (10 $^{\circ}\text{C}/\text{min}$). Quantities of but-3-yn-2-ol in the individual samples were determined by external calibration. All experiments were repeated three times and the standard deviation was calculated.

	<i>(rac)</i> -but-3-yn-2-ol (μL / 10 mg CMOPS)	2-methyl-but-3-yn-2-ol (μL / 10 mg CMOPS)	Molar Ratio <i>(rac)</i> -but-3-yn-2-ol / 2-methyl-but-3-yn-2-ol (%)
I- CMOPS	1.242 \pm 0.048	0.552 \pm 0.057	73.7 \pm 0.5 / 26.3 \pm 0.5
II- CMOPS	1.550 \pm 0.026	0.891 \pm 0.025	68.4 \pm 0.2 / 31.6 \pm 0.2
III-CMOPS	1.497 \pm 0.022	0.932 \pm 0.037	66.7 \pm 0.3 / 33.3 \pm 0.3
IV- CMOPS	1.382 \pm 0.015	0.986 \pm 0.032	63.5 \pm 0.4 / 36.5 \pm 0.4
Initial ratio			48.7 \pm 1.1 / 51.3 \pm 3.1

Table 4: Measured values for Figure 15: Uptake of (\pm)-but-3-yn-2-ol and 2-methyl-but-3-yn-2-ol by CMOPS-1 to CMOPS-4.

	<i>(rac)</i> -but-3-yn-2-ol (μL / 10 mg CMOPS)	2-methyl-but-3-yn-2-ol (μL / 10 mg CMOPS)	Molar Ratio <i>(rac)</i> -but-3-yn-2-ol / 2-methyl-but-3-yn-2-ol (%)
MOPS-1	0.135 \pm 0.028	0.069 \pm 0.026	72.0 \pm 1.8 / 28.0 \pm 1.8
MOPS-2	0.266 \pm 0.077	0.247 \pm 0.087	58.1 \pm 1.5 / 41.9 \pm 1.5
Initial ratio			48.7 \pm 1.1 / 51.3 \pm 3.1

Table 5: Measured values for Figure 18: Uptake of (\pm)-but-3-yn-2-ol and 2-methyl-but-3-yn-2-ol by MOPS-1 and 2.

3.3 Adsorption of *rac*-but-3-yn-2-ol

The MOPSs pillared with (+)-Co(sep)³⁺ and (-)-Co(sep)³⁺ and pseudo-meta-bis(5,12-(N,N,N-trimethylmethylenaminium))-[2.2]paracyclophan were heated at 100 $^{\circ}\text{C}$ under high vacuum (10^{-9} bar) for 24 h, cooled and transferred to an argon glove box. Three 10 mg samples of each

MOPS were weighed into open Eppendorf plastic vials (1.5 mL) which were placed in a horizontally adjusted 50 mL Schlenk tube together with an open glass weighing tube containing 300 μ L of *rac*-but-3-yn-2-ol to secure a saturated atmosphere. The Schlenk tube was stoppered and kept at 4 °C for 48 h. Then it was connected to an argon line and after removal of the but-3-yn-2-ol source the sample vials were each treated with 500 μ L of dry acetone p.a.. The vials were sealed, vortexed for 1 min, treated with a cooled ultrasonic bath for 30 min to desorb the but-3-yn-2-ol from the inorganic material, and centrifuged.

The acetone extracts were analyzed as described before whereby enantiomers were identified and assigned by chromatographic comparison with authentic pure (+)- and (-)-but-3-yn-2-ol. All experiments were repeated three times and the standard deviation was calculated.

	<i>(rac)</i> - but-3-yn-2-ol (μ L / 10 mg CMOPS)	<i>(S)</i> - but-3-yn-2-ol (μ L / 10 mg CMOPS)	<i>(R)</i> - but-3-yn-2-ol (μ L / 10 mg CMOPS)	Enantiomeric excess (%)
I- CMOPS	1.733 \pm 0.014	0.797 \pm 0.012	0.937 \pm 0.017	7.45 \pm 0.45
II- CMOPS	2.243 \pm 0.019	1.109 \pm 0.020	1.134 \pm 0.018	0.54 \pm 0.31
III-CMOPS	2.459 \pm 0.049	1.223 \pm 0.050	1.236 \pm 0.048	-0.05 \pm 0.43
IV- CMOPS	2.362 \pm 0.019	1.178 \pm 0.019	1.185 \pm 0.019	-0.31 \pm 0.31

Table 6: Measured values for Figure 16: Uptake of (\pm)-but-3-yn-2-ol and by MOPS-1 to -4 pillared with (+)-Co(sep).

	<i>(rac)</i> - but-3-yn-2-ol (μ L / 10 mg CMOPS)	<i>(S)</i> - but-3-yn-2-ol (μ L / 10 mg CMOPS)	<i>(R)</i> - but-3-yn-2-ol (μ L / 10 mg CMOPS)	Enantiomeric excess (%)
I- CMOPS	1.689 \pm 0.044	0.919 \pm 0.046	0.770 \pm 0.041	8.24 \pm 0.48
II- CMOPS	2.088 \pm 0.016	1.062 \pm 0.015	1.026 \pm 0.017	1.10 \pm 0.44
III-CMOPS	2.279 \pm 0.044	1.152 \pm 0.044	1.126 \pm 0.044	0.55 \pm 0.37
IV- CMOPS	2.272 \pm 0.046	1.143 \pm 0.046	1.128 \pm 0.047	0.05 \pm 0.38

Table 7: Measured values for Figure 16: Uptake of (\pm)-but-3-yn-2-ol and by MOPS-1 to -4 pillared with (-)-Co(sep).

4 References

- ⁶⁵ G. R. Fulmer, A. J. M. Miller, N. H. Sherden, H. E. Gottlieb, A. Nudelman, B. M. Stoltz, J. E. Bercaw, K. I. Goldberg, *Organometallics* **2010**, *29*, 2176-2179.
- ⁶⁶ A. E. Mourad, A. M. Nour-el-Din, R. A. Mekhamer, *J. Chem. Eng. Data* **1986**, *31*, 367-369.
- ⁶⁷ E. A. Tuesdale, D. J. Cram, *J. Org. Chem.* **1980**, *45*, 3974-3981.
- ⁶⁸ N. El Murr, E. Laviron, *Tetrahedron Letters* **1975**, *16*, 875-878.
- ⁶⁹ I. I. Creaser, R. J. Geue, J. M. Harrowfield, A. J. Herlt, A. M. Sargeson, M. R. Snow, J. Springborg, *J. Am. Chem. Soc.* **1982**, *104*, 6016-6025.
- ⁷⁰ M. M. Herling, U. Lacher, M. Rieß, S. Seibt, M. Schwedes, H. Kalo, R. Schobert, J. Breu, *Chem. Commun.* **2017**, *53*, 1072-1075.

E Acknowledgment

Mein erster Dank geht an Herrn Professor Dr. Rainer Schobert für die nette Aufnahme in seinen Arbeitskreis, die interessante Themenstellung, die intensive Betreuung und die Bereitstellung der erforderlichen Mittel.

Des Weiteren möchte ich mich bei Herrn Dr. Thomas Schmalz für die fachlichen sowie persönlichen Gespräche bedanken, aber auch für die praktische Unterstützung.

Der analytischen Abteilung der Fakultät danke ich für die Einweisung in die erforderlichen Messinstrumente, sowie für die Durchführung einiger Messungen.

Bei meinen Kollegen vom Arbeitskreis Schobert bedanke ich mich für die tolle Zeit die wir miteinander verbracht haben. Besonders herausheben möchte ich dabei meine beiden Kollegen aus dem Malle-Lab, René Schmidt und David Linder. Ohne euch wäre die Zeit nicht einmal annähernd so geil gewesen. Unsere Feierabendbiere, Balkongespräche, Musikpartys und sonstigen Unternehmungen werde ich echt vermissen und ich hoffe wir bleiben für immer Freunde.

Bei Professor Dr. Josef Brey, Markus Herling und Martin Rieß aus der Anorganischen Chemie I möchte ich mich für die gute Zusammenarbeit bedanken.

Der größte Dank von allen geht an meine Familie, an meine Eltern Marion und Thomas Schwedes, meine Geschwister Stephan, Anne und Timm, auch an meinen Schwager Basti und meine Schwägerin Katha, meine Neffen Lenny, Finn, Anton und Noah. Ohne die finanzielle Unterstützung meiner Eltern wäre das ganze Studium nicht möglich gewesen. Ohne die aufmunternden, ermutigenden, freundlichen Worte meiner gesamten Familie, die unglaublich schöne Zeit die ich in meiner Freizeit mit ihnen hatte haben mir Kraft und Inspiration in schweren Zeiten gespendet das Ganze durchzuziehen. Ich liebe euch alle!!!

(Eidesstattliche) Versicherungen und Erklärungen

(§ 8 Satz 2 Nr. 3 PromO Fakultät)

Hiermit versichere ich eidesstattlich, dass ich die Arbeit selbstständig verfasst und keine anderen als die von mir angegebenen Quellen und Hilfsmittel benutzt habe (vgl. Art. 64 Abs. 1 Satz 6 BayHSchG).

(§ 8 Satz 2 Nr. 3 PromO Fakultät)

Hiermit erkläre ich, dass ich die Dissertation nicht bereits zur Erlangung eines akademischen Grades eingereicht habe und dass ich nicht bereits diese oder eine gleichartige Doktorprüfung endgültig nicht bestanden habe.

(§ 8 Satz 2 Nr. 4 PromO Fakultät)

Hiermit erkläre ich, dass ich Hilfe von gewerblichen Promotionsberatern bzw. –vermittlern oder ähnlichen Dienstleistern weder bisher in Anspruch genommen habe noch künftig in Anspruch nehmen werde.

(§ 8 Satz 2 Nr. 7 PromO Fakultät)

Hiermit erkläre ich mein Einverständnis, dass die elektronische Fassung der Dissertation unter Wahrung meiner Urheberrechte und des Datenschutzes einer gesonderten Überprüfung unterzogen werden kann.

(§ 8 Satz 2 Nr. 8 PromO Fakultät)

Hiermit erkläre ich mein Einverständnis, dass bei Verdacht wissenschaftlichen Fehlverhaltens Ermittlungen durch universitätsinterne Organe der wissenschaftlichen Selbstkontrolle stattfinden können.

Niedertaufkirchen, 24.09.2019,

Ort, Datum, Unterschrift